

PROJECT FINAL REPORT

(Publishable Version)

Grant Agreement number: 224042

Project acronym: MIRSURG

Project title: Mid-Infrared Solid-State Laser Systems for Minimally Invasive Surgery

Funding Scheme: STREP

Period covered: from 01 June 2008 to 30 November 2011

Name of the scientific representative of the project's co-ordinator:

Dr. Valentin PETROV

Max-Born-Str. 2A

12489 Berlin

Germany

Tel: 0049-30-63921272

Fax: 0049-30-63921289

E-mail: petrov@mbi-berlin.de

Project website address: www.mirsurg.eu

1. Final publishable summary report

1.1 Executive summary

The goal of this project was to develop advanced table-top solid-state photonic sources for a specific wavelength in the mid-IR spectral range, as a practical, reliable and cost-effective alternative to large-scale free-electron lasers (FELs), for an important application in biomedicine (health): minimally invasive surgery (MIS). Previous experiments had verified that the use of mid-IR FEL at wavelengths near 6.45 μm , with a focused beam penetration depth comparable to the cell size and coupled both into the spectral wing of the water bending mode and the amide-II vibrational mode, results in tissue ablation with minimal collateral damage and very effective ablation rate. This finding was extremely important as a useful tool for minimally invasive human surgery. However, the clinical use of FEL is ultimately not viable due to large size, high cost, operational complexity and restricted access at a few multi-million-dollar accelerator-based facilities worldwide. Several attempts to develop non-FEL alternatives had largely failed to meet the necessary requirements in terms of pulse energy and repetition rate. The main strategy in this project was to exploit nonlinear optical techniques (optical parametric oscillators, OPOs) in combination with novel near-IR laser pump sources (near 1 and 2 μm) and new materials (e.g. orientation patterned GaAs) to obtain an unprecedented mid-IR pulse energy level near 6.45 μm with beam quality sufficient to exceed the ablation threshold in terms of energy density (fluence). Efficient MIS will require also relatively high repetition rate, however, it was known from previous experiments that >5 kHz repetition rates are not compatible with desired ablation effect. Thus, having in mind realistic limits on the conversion efficiency and the expected minimum required pulse energy, the overall objective could be summarized as an average power of about 1 W at 6.45 μm with millijoule single pulse energy and pulse duration not exceeding few microseconds (μs). This major requirement could be satisfied with energies starting from ~ 1 mJ (at <1 kHz) up to 10 mJ (at ~ 100 Hz). Two basic OPO approaches, differing in the time structure, and two different pump wavelength ranges (1 and 2 μm), were investigated in the project for generation of 6.45 μm radiation with less than few μs (macro-) pulse duration at sufficiently high conversion efficiency. The project encompassed four distinct elements: (1) Material research (nonlinear crystals); (2) Pump laser development (near 1 and 2 μm); (3) OPO development (frequency conversion to 6.45 μm); and (4) Validation in tissue ablation experiments. The partners, 4 companies and 5 institutes from 7 member states, with proven track record, extensive expertise, and complementary skills provided the critical mass and strong cohesion to achieve the goals of the project in the most successful, effective and timely manner. The primary goal of the MIRSURG project has been achieved: a table top laser system (much smaller and cheaper than a FEL) has been developed that can effectively ablate biological tissue at a wavelength of 6.45 μm with a pulse length in the ns range. The targeted average power of >1 W at 6.45 μm has been achieved at 200 Hz and the >5 mJ pulse energy available at 200 Hz and lower repetition rates is more than sufficient for the tissue ablation itself whose threshold was determined to be ~ 1 J/cm². The actual repetition rate (200 Hz, 100 Hz or less) can be chosen in future real applications depending on the speed necessary to achieve the required effect.

1.2 Description of project context and objectives

Lasers have tremendous potential as high-precision surgical tools, owing to the ability to focus the beam to a small spot size and select wavelengths which are either strongly or selectively absorbed in the target tissue. The goal of laser ablation is to remove a defined volume of unwanted tissue while leaving the adjacent tissue biologically viable. Tissue ablation in eloquent structures of the body, such as brain and eye, requires maximum precision in ablation of the target tissue while minimizing collateral damage to adjacent tissue structures. The viability of the remaining tissue is of great importance in assessing the effectiveness of ablation.

Both ultraviolet (UV) and infrared (IR) lasers offer the potential for performing precise ablation of biological tissues due to the strong absorption at these wavelengths. Excimer lasers, which operate in the UV have proven to be particularly adept at carrying out effective tissue ablation in corneal stroma. However, concerns regarding the potential mutagenic effects of UV radiation have limited applications to other tissues. In addition, from an ultimately practical point of view, the UV radiation cannot be delivered via optical fibers. As a result of this concern over mutagenic effects, mid-infrared (mid-IR) wavelengths have been investigated, with the goal of achieving precise removal of tissue while maintaining peripheral tissue free from chemical, thermal, and mechanical damage.

Traditionally, the investigations of IR tissue ablation have been centered at 2.1 μm (Ho:YAG), 2.94 μm (Er:YAG), and 10.6 μm (CO_2) because these wavelengths are somewhat more readily attainable through conventional laser technology. Thermal damage associated with these lasers, especially in the free running mode (typically associated with pulse durations of several hundred μs), has been significant. In the case of the Er:YAG and the continuous wave (cw) CO_2 laser, the conditions of thermal confinement are not met, whereas in the case of the Ho:YAG the optical penetration depth is too large. While Q-switching the Er:YAG leads to thermal confinement, the penetration depth at 2.94 μm is extremely shallow (1 μm), which leads to excessively high temperatures in the ablation zone with a relatively low material removal per pulse. For cw CO_2 lasers, thermal damage can be on the order of 0.2-1 mm. When operated in a rapid scanning or a pulsed mode with pulses as short as 180 ns, thermal damage can be reduced to 70-160 μm and about 50 μm , respectively. However, due to the deeper penetration depth (~ 12 μm) at 10.6 μm , it is not possible to achieve the reduced thermal damage observed at other IR wavelengths. Due to these important shortcomings of Er:YAG and CO_2 lasers, the quest for alternative laser sources to provide precise tissue ablation goes on. Diode-pumped Tm-lasers for instance operate at slightly shorter wavelengths compared to Ho-lasers at which the penetration depth is smaller.

A series of important experiments in USA have demonstrated that targeting a mid-IR Mark-III Free-Electron Laser (FEL) to wavelengths near 6.45 μm results in tissue ablation with minimal collateral damage and a substantial ablation rate, useful for human surgery. The penetration depth at this wavelength amounts to several μm which is comparable to the cell size, i.e. close to the optimum value. Larger penetration depths will increase the number of damaged cells, while shorter penetration would result in lower material removal per pulse. Wavelengths near 6.45 μm couple into the spectral wing of the bending mode of water centered at 6.1 μm as well as the amide-II vibrational mode centered at 6.45 μm . The reduction in collateral damage at this wavelength is due to the differential absorption, which causes compromised tissue integrity by laser heating of the non-aqueous components prior to explosive vaporization. The amide bond helps link the amide groups in collagen to one another in a highly ordered matrix. Thus, targeting the wavelength to this molecular bond will effectively reduce tissue integrity, resulting in lower amount of energy required for ablation.

While the Mark-III FEL (in the meanwhile shut down for economic reasons) has been successfully used in eight initial trials in human neurosurgery and ophthalmic surgery, it is unlikely that such a

laser would ever offer any potential for widespread clinical use due to its high expense, complex implementation and many logistic issues. Indeed, the FEL is a multi-million accelerator-based light source that requires a large radiation-shielded facility, and a technically sophisticated operating staff. Therefore, it was important to develop new technologies to replace the FEL for practical clinical applications in human surgery. Several different non-FEL sources attracted attention in the past as potential alternatives to the FEL, but no such sources have been developed for clinical use due to the technological and engineering challenges. However, if the promising results obtained with the mid-IR FEL could be reproduced or even improved using lasers based on more practical alternative technologies, then the engineering effort to develop compact, inexpensive, table-top laser systems suitable for clinical use would have been well justified. Progress in the development of solid-state lasers and mid-IR nonlinear optical crystals indicated that alternative sources based on nonlinear frequency conversion could be feasible as viable replacements for the FEL. The design and realization of such solid-state laser systems operating near 6.45 μm with temporal structure suitable for minimally invasive surgery (MIS) was main objective of the project MIRSURG.

Understanding of the effect of the pulse duration and structure on the process of ablation is essential for the transition from a FEL to a non-FEL laser source because any conventional laser system will clearly produce drastically different duration/structure. FELs are broadly tunable, pulsed sources providing both high average and high peak power. As an example, the Mark-III mid-IR FEL at Vanderbilt was continuously tunable from 2 to 9 μm . It had a complex pulse structure where each macro-pulse, with duration of 4-5 μs , was a burst of ps micropulses, with a micropulse repetition frequency of 2.85 GHz (~15000 micropulses per macro-pulse). The macro-pulse repetition rate could be adjusted between 1 and 30 Hz with macro-pulse energies up to 100 mJ. Since a single 6.45 μm macro-pulse at a given energy focused to a several hundred μm diameter spot consistently ablated soft tissue, the macro-pulse repetition rate is not the most critical parameter but determines the ablation efficiency. The structure of the FEL pulse train could be manipulated by pulse stretching, increasing the duration of the micropulse from ~1 ps to ~200 ps, keeping the micropulse frequency, macro-pulse duration, and pulse energy unchanged. Such studies of the ablation threshold and efficiency for water, gelatine and mouse dermis showed insignificant difference. Hence, nonlinear effects are not important in the ablation of soft tissue and the picosecond micropulse structure of the FEL is not a crucial parameter that needs to be reproduced. One would expect that a <5 μs long pulse would be just as effective but the role of the pulse or macro-pulse duration with respect to efficient tissue ablation and minimal collateral damage has in fact never been studied.

The wavelength of 6.45 μm is accessible by strontium vapour lasers. Such gas-discharge custom-made lasers delivered up to 2.4 W of average power at 5-20 kHz. Despite a poor spatial beam profile, this laser could ablate both water and soft tissue. However, its pulse energy (<185 μJ) was insufficient for single pulse ablation even when focused to the smallest possible spot size (130 μm). Instead, the high pulse repetition rate caused the ablation to occur in a quasi-cw manner. The dynamics of ablation showed micro-explosions but at a rate well below the pulse repetition frequency, with significant collateral thermal damage, consistent with the high pulse frequency, thermal superposition and heat diffusion. Thus, the average power of such gas lasers is sufficient for efficient soft tissue ablation but the repetition rate is too high and the single pulse energy is too low.

At the beginning of MIRSURG, no laser system, including solid-state lasers, capable of generating coherent radiation near 6.45 μm with the desired parameters existed. The task could be accomplished, however, by optical frequency conversion based on second-order nonlinear processes in acentric crystals. These processes can take a variety of forms, including second-harmonic generation (SHG), sum- and difference-frequency generation (SFG and DFG), and optical parametric process. The most important process in the context of 6.45 μm generation is the parametric process, since this wavelength does not correspond to a harmonic of any available laser sources in the mid-IR

(including the CO₂ laser) and all existing solid-state laser systems are at shorter wavelengths in the 1-3 μm range. Such parametric devices of interest operate in different temporal regimes: from cw down to extremely short (fs) pulse durations. The temporal regime (pulse duration, profile, and repetition rate) is determined by the available laser pump source and greatly affects other characteristics such as power, energy, efficiency, spectral properties and output stability. Having in mind the FEL ablation experiments, it was clear that cw laser sources or free running pulsed laser sources with durations of several hundred μs in conjunction with optical parametric oscillators (OPOs) are not suitable for MIS. The same is also true for the synchronously pumped OPOs (SPOPOs), in which ultrashort (ps or fs) pulses are generated at high (typically ~100 MHz) repetition rates by matching the OPO cavity length to that of the mode-locked pump laser. From the point of view of efficient frequency conversion in the nonlinear crystal, all such schemes would be inefficient because of the low peak powers or there will be limitations from the available average power. Similar arguments and also the complexity ruled out DFG as another possible nonlinear frequency conversion scheme.

While 5 μs could be considered as an upper limit for the pulse duration of the (macro-) pulse, there should be a lower limit on the pulse duration set by the peak intensity. Single pulses of fs or ps duration, at pulse energy on the mJ level would obviously cause detrimental nonlinear effects not only in the conversion but also in the interaction process with the tissue and in the delivery system (e.g. IR transmitting optical fibers). Hence, travelling-wave type optical parametric generators (OPGs) and amplifiers (OPAs) (cavity free) had also to be ruled out for this specific application.

Thus, only two types of parametric devices were identified as possible replacement of the FEL: ns OPOs pumped by Q-switched lasers and SPOPOs pumped by a limited train (<5 μs) of ultrashort pulses, i.e. by macro-pulses. The challenge with the Q-switched pump lasers was related to the fact that the envisaged repetition rate is too high for flash-lamp pumping and simultaneously too low for cw diode-pumped Q-switched lasers to achieve the necessary average pump power. Shorter ns pump pulses with higher intensity ensure lower OPO threshold which helps to avoid damage to the nonlinear crystal. Macro-pulse SPOPOs are pumped primarily by Q-switched and mode-locked oscillators followed by laser amplifier stages. They operate also at ~100 Hz macro-pulse repetition rates and sufficiently high average powers are available from Nd-based mode-locked solid-state lasers with pulse durations of 10-100 ps. The micropulses (typically ~100) follow at a repetition rate of ~100 MHz. Thus, the macro-pulse duration is of the order of 1 μs (100/100 MHz) and so both macro-pulse length and repetition rate resemble the characteristics of the FEL.

Having identified the potential schemes of parametric devices for generation of the 6.45 μm radiation with the required time structure it was important to decide which nonlinear materials and pump laser sources could be used. These two issues were closely related, because the nonlinear material imposes constraints on the pump wavelength related to two-photon or residual absorption. Unfortunately the well established oxide crystals which have mature growth technology and exhibit low residual absorption and scattering losses cannot be used for generation of 6.45 μm because they are already absorbing at this wavelength. Only very few non-oxide (chalcogenide) nonlinear crystals with sufficient birefringence for phase-matching exist, that could be considered for 6.45 μm generation. ZnGeP₂ (ZGP) requires a pump wavelength of at least 2 μm because of residual absorption. Similarly, AgGaSe₂ (AGSe) and AgGaS₂ (AGS) would require pump wavelengths exceeding 1.5 and 1 μm, respectively, to avoid two-photon absorption (TPA). ZGP is obviously one of the most promising materials for generation of 6.45 μm radiation because it has the highest nonlinearity for any commercially available nonlinear crystal ($d_{36}=75$ pm/V). Moreover, ZGP exhibits also high thermal conductivity (35 W/mK) which facilitates high average powers. Residual losses near 2 μm can be as low as 3%/cm. Maximum average power of 30 W at >50% conversion efficiency had been demonstrated with a degenerate 10 ns ZGP OPO operating near 4 μm, pumped at 10 kHz by a Q-switched Ho-laser. However, mJ pulse energies near 6.45 μm had never been achieved with such a

ZGP based OPO. At slightly lower wavelengths, ZGP can be also pumped by Tm-lasers, at slightly increased pump loss. Tm-lasers have the advantage that can be easily diode pumped near 800 nm, by the same AlGaAs diodes used for Nd-lasers. ZGP OPOs can be pumped with higher quantum efficiency for generation of 6.45 μm also with Er-lasers near 3 μm . However, such lasers are far less developed than Ho- or Tm-lasers, especially in the Q-switched mode of operation.

AGSe and AGS (with nonlinear coefficients and thermal conductivity lower than ZGP) are only interesting for pumping at wavelengths shorter than 2 μm , especially in the 1 μm range (AGS) where the most powerful, commercially available Nd- (and more recently Yb-) based laser sources operate. Although the quantum efficiency for pumping near 1 μm sets a relatively low limit on the achievable conversion efficiency, the study of such schemes deserved attention, because these are the most developed, reliable, and commercially available pump sources. At wavelength near 1 μm , several more sophisticated nonlinear materials such as HgGa_2S_4 and LiInSe_2 exhibit certain advantages over AGS in terms of higher nonlinear coefficients, damage threshold, and thermal conductivity, as well as lower anisotropic thermal expansion. The availability, reliability and power scalability of the 1 μm pump sources are attractive features not only for direct down-conversion to 6.45 μm but also for cascaded OPO schemes, which were also widely studied in the project, for example using KTiOPO_4 (KTP) in a 1 μm pumped OPO, to pump a second OPO stage based on ZGP.

Besides birefringent nonlinear materials, however, one can use quasi-phase-matching in isotropic but acentric crystals. Unfortunately, such mid-IR crystals are not ferroelectric, precluding patterned electric field poling. Nevertheless, one of the promising trends in this field is the growth of orientation patterned GaAs (OP-GaAs), a semiconductor with mature technology, combining high nonlinearity ($d_{14}=83 \text{ pm/V}$), low absorption losses ($<2\%/ \text{cm}$), and high thermal conductivity (46 W/mK). GaAs requires wavelengths above 1.8 μm to avoid TPA. Promising OPO results with this material existed in the beginning of the project in terms of average power and conversion efficiency, however, at high (e.g. 20 kHz) repetition rates, i.e. at low single pulse energies.

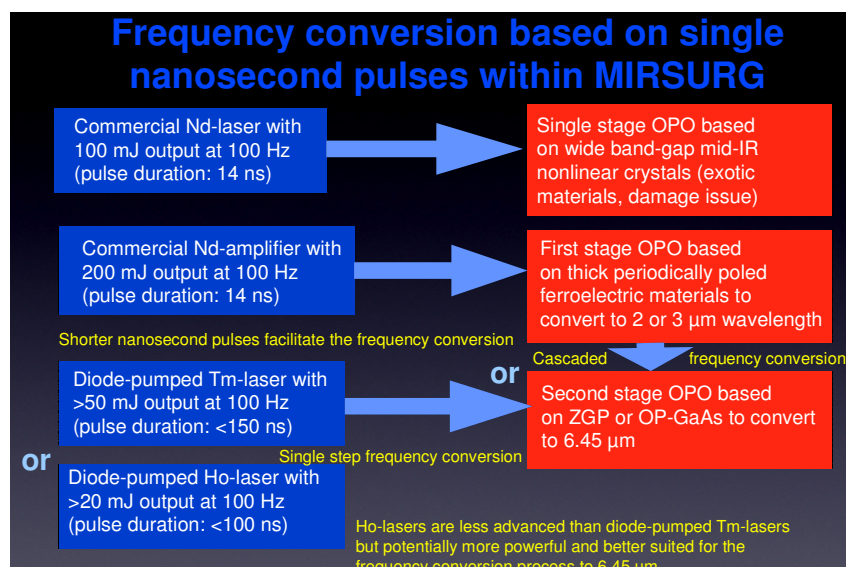
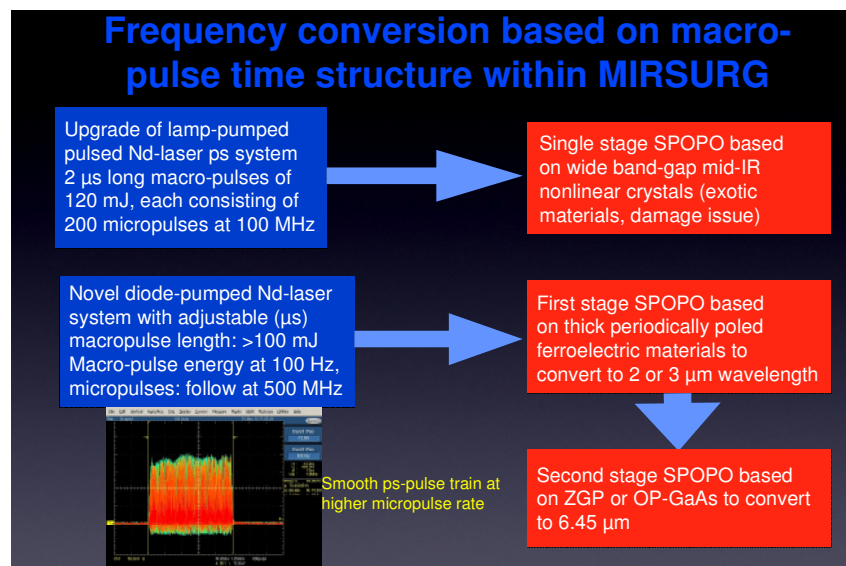
Since steady-state mode-locking of Er, Ho, or Tm lasers is still problematic such sources could not be employed for pumping SPOPOs. Thus, this alternative macro-pulse approach was only considered for Nd- or Yb-doped solid-state pump lasers at $\sim 1 \mu\text{m}$ and wide band-gap crystals of the AGS type or for cascaded SPOPOs with ZGP or GaAs crystals in their second stage.

Two experimental investigations described in 2007, just before the start of MIRSURG, aimed at comparing different non-FEL sources with FEL for soft tissue ablation at 6.45 μm . The first system was an Er:YAG Q-switched laser pumped ZGP OPO, generating 100 ns pulses with a maximum energy of 0.25 mJ per pulse at 6.45 μm . The repetition rate was 1-5 Hz. Ablation craters in porcine cornea produced by 50 pulses indicated a very similar damage zone of 7.2 μm both with the OPO and the FEL sources. The second system, starting from a 1 μm oscillator, was based on DFG and Raman shifters and characterized by high complexity. It delivered up to 2 mJ energy at 6.45 μm in a 3 ns pulse but at a repetition rate of only 0.5 Hz. This laser system successfully ablated rat brain tissue, where both the collateral damage and the ablation rate compared favorably with that previously observed with the Mark-III FEL. Nevertheless, it is important to emphasize that both systems and their operating parameters were far from simultaneously satisfying the requirements of pulse energy and repetition rate for human surgery, with the second system also having intrinsic limitation with regard to scalability. Thus, the first experiment was performed with an average power of only 1.25 mW (0.25 mJ \times 5 Hz) which was only sufficient to create craters but not for laser incision. The second experiment was at an even lower average power of 0.5 mW (1 mJ \times 0.5 Hz) and only partial incision was observed.

The first human neurosurgery with the Mark-III FEL was performed using 1500 macro-pulses of 6.45 μm radiation within 50 s (i.e. at 30 Hz). The energy applied was, however, 32 mJ/macro-pulse,

so that the average power was of the order of 1 W for a spot size of 310 μm . Having in mind the better focusability, the requirements for a dedicated 6.45 μm surgical solid-state laser system were set by the pioneers of the FEL experiment at about 0.5 W average power. Much lower average powers (20 mW corresponding to 2 mJ at 10 Hz) were sufficient for ophthalmic surgical procedures. Taking into account possible losses in the delivery system, *the goal of the MIRSURG project was set to the ambitious average power of 1 W at 6.45 μm , roughly 3 orders of magnitude above the level demonstrated at that time with alternative non-FEL systems.* The requirements, as derived from the unique experience with FEL and some very preliminary and mostly unsuccessful experiments with three alternative sources can be summarized as follows: (i) the pulse duration may vary from a few ns (single pulse version) to a μs (macro-pulse version); (ii) there is minimum pulse energy for efficient tissue ablation in the mJ range at 6.45 μm (iii) effective MIS will require a sufficiently high pulse repetition rate and hence an average power of ~ 1 W. Variable repetition rate will enable to study its influence in soft tissue ablation.

The main goal which had to be achieved within the MIRSURG project comprised nonlinear crystal development and characterization, laser system development (at different wavelengths and in different temporal regimes), and OPO and SPOPO development for frequency conversion, as well as validation and visualization studies in tissue ablation experiments performed with delivery optics.



1.3 Description of the main S&T results/foregrounds

An important part of the material research carried out within the MIRSURG project has been dedicated to Orientation-Patterned Gallium Arsenide (OP-GaAs). As expected, it has enabled to make significant progress in all the key aspects of its fabrication process.

OP-GaAs growth: The major design criteria to fabricate OP-GaAs crystals include the period of the orientation-patterning and its duty cycle, the propagation losses and the targeted dimensions of the samples. The state-of-the-art at the beginning of the project offered low loss materials with quasi-phase matching (QPM) properties suited to efficient wavelength conversion from pump lasers around 2 μm to the targeted mid-IR window, around 6.45 μm , but with a limited thickness. A key objective has thus been to push the limits of the state-of-the-art in OP-GaAs fabrication to obtain crystals with a thickness above 1 mm. A gradual increase had been planned, starting at 0.4 mm during the first year, further expecting 0.8 mm and finally targeting 1.2 mm towards the end of the project.

The Hydride Vapor Phase Epitaxial growth (HVPE) on periodically oriented templates formerly involved frequent growth interruptions, necessary to get rid of the parasitic nucleation in the tube of the HVPE machine, which strongly reduces the growth speed and the quality of the material. These characteristics were satisfactory during the first half of the project to improve the deposited thickness up to 0.8 mm and address several issues related to the thicker and heavier wafers such as unloading from the HVPE machine without cleavage and post processing of individual samples (see next paragraph). Nevertheless, the numerous corresponding cleaning cycles proved a significant drawback for both the user-friendliness of the process and the prospects for further thickness increase. Subsequent efforts were thus focused on this phenomenon. Thanks to a novel configuration of the sample holder, it was possible to strongly limit the parasitic nucleation. This now enables one to grow samples thicker than 1 mm in one or two cycles. Figure 1 shows a half wafer at the output of the HVPE step and some post-processed samples. Figure 2, taken after side polishing and chemical revelation of one of the latest samples, gives an example of the quality of the gratings that are obtained with the new growth conditions, meeting the expectations of the project.

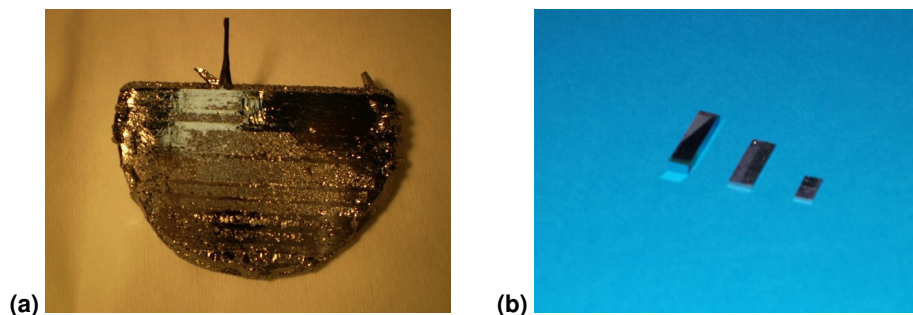


Figure 1: Half OP-GaAs wafer after thick HVPE growth (a) and processed samples of various thicknesses after dicing and facet polishing (b).

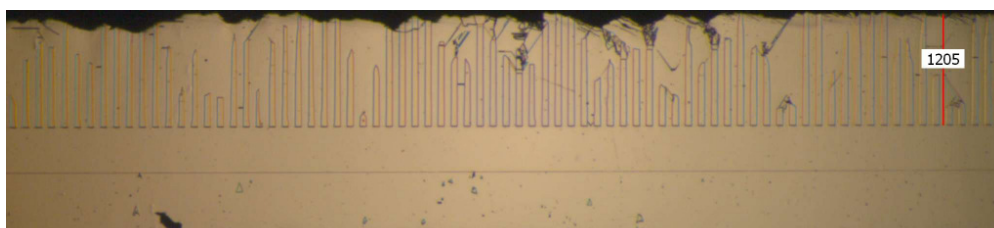


Figure 2: 1205 μm thick OP-GaAs sample. The grating period is around 150 μm .

Sample preparation: The post-growth processing procedures available at the beginning of the project were suited to sample preparation up to 0.5 mm. To address the fabrication of thicker OP-GaAs samples, significant modifications have been studied and implemented for the three main sample preparation steps.

Post-growth wafer handling: Parasitic deposition occurring on the bottom side of the wafers has been identified as a major drawback of thick HVPE growth runs. After the HVPE growth, the thickness of this parasitic GaAs material on the bottom side can be measured thanks to a mechanical sensor using the center of the wafer as a reference: it sometimes reaches up to 600 μm near the edge for a 0.8 mm growth run. Nevertheless, it proved possible to design a special handling procedure to lap them with the proper control and to obtain satisfactory reference planes.

Referencing and dicing: Because of a similar uncontrolled deposition blurring the top side of the wafers in some thick growth runs, it can become difficult to know where to dice the samples. Handmade marks have been used to date to solve this problem, but two other solutions have more recently been implemented. The first one, i.e. top face polishing and etching, was validated. The second one, suited to the fabrication of more apparent reference marks, involves more complicated technological steps and will be further improved in the future.

Final sample polishing: Two alternative methods (polishing saw blades and deep ICP-RIE etching) have been tested to try to avoid individual polishing of the two laser facets of each sample, but neither of them gave a satisfactory surface roughness. The polishing procedure based on a single polishing die fixed to the sample and used to date for 0.5 mm thick OP-GaAs samples was thus implemented and proved appropriate for thicker samples. It has been further improved thanks to the use of a second polishing die.

Sample characterization: The objectives of this task were twofold. On the one hand, it is necessary to carry out all the standard characterization steps involved in the OP-GaAs fabrication process and in the post-growth preparation of optical grade QPM samples. On the other hand, the specific challenges of the MIRSURG project in terms of crystal thickness required additional efforts to link the measured parameters to the growth conditions and make progress in the way very thick gratings can be fabricated. The motivations behind the various macroscopic, microscopic and laser characterizations listed at the beginning of the MIRSURG project have proven to be adequate to enable significant progress in OP-GaAs fabrication. Thus, the comparison of full wafer pictures taken at various points of the process helps to select and post-process the most promising samples. The microscopic observations have provided useful assessments of local defects and discrepancies in the average growth rate between opposite sides of the wafers.

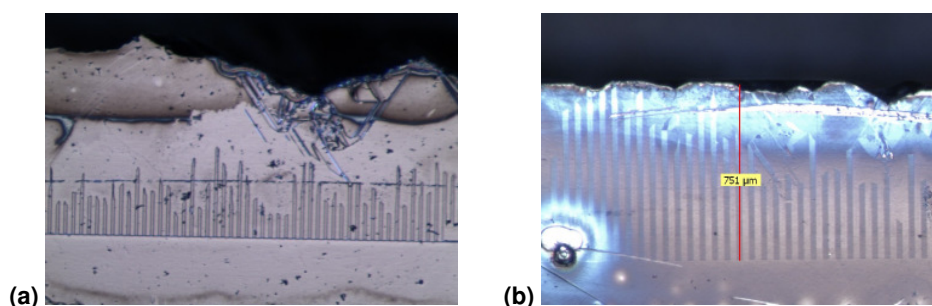


Figure 3: Side views of thick OP-GaAs samples (periods: $\sim 30 \mu\text{m}$ (a) and $\sim 60 \mu\text{m}$ (b)).

The efforts carried out in parallel to model the growth conditions indicated that suitable growth parameters can be found, with the range of values for the available HVPE reactor, to obtain a lasting vertical growth on the periodically orientation-patterned templates. Figure 3 helps to link the results

of growth modeling with the characterization of real samples. The following points can thus be stressed: (i) Local defects can lead to unexpected morphological growth conflicts and therefore locally alter the grating quality; (ii) External factors influencing the growth parameters, such as parasitic nucleation possibly modifying the flux or defect incorporation at domain boundaries, can also change morphological growth conflicts and therefore alter the grating quality over large areas. Note that those factors may also depend on the grating period.

Nevertheless, the model developed indicates that suitable growth parameters can be found to obtain a lasting vertical growth on the periodically orientation-patterned templates. It has been validated up to a 0.8 mm thickness for grating periods around 60 μm and above 1.2 mm for periods around 150 μm .

Last but not least, the laser experiments demonstrated that the process improvements turned into a valuable increase in the damage threshold, reaching values superior to 1 J/cm^2 .

Table 1 lists the OP-GaAs crystals fabricated during the MIRSURG project:

Table 1: List of fabricated OP-GaAs samples.

Project period	Sample #	Period [μm]	Length [mm]	Thickness [μm]
1	broken	72.6	15	400
1	1	72.6	15	740
1	2	63.6, 64.8, 66	19	770
Objectives			15	400
2	3	72.6	15	740
2	4	64.8 and 66	23	770
Objectives			20	800
3	5	57.2 and 63.6	23	1260
3	6	140 and 146	23	1200
3	7	63.0 and 63.8	20	1500
3	8	63.0	30	1400
3	9	140 and 146	30	1500
3	10	63.0	23	1500
Objectives			30	1200

The development of periodically-poled ferroelectrics was essential material research for realization of the first stage of 1064 nm pumped high-energy mid-IR optical parametric devices based on cascaded frequency conversion. In addition to the structuring of crystals from several families with unprecedented thicknesses including multiple-grating designs, the MIRSURG project enabled to develop additional processing techniques such as short pulse poling for QPM crystal fabrication, and to investigate optical damage issues in QPM and wide band-gap nonlinear materials.

Criteria for crystal selection: The semiconducting nonlinear crystals such as OP-GaAs and ZnGeP_2 (ZGP) which are still the best choice for generating 6.45 μm radiation owing to their high nonlinearity and good opto-mechanical properties, cannot be used with well established laser sources at $\sim 1 \mu\text{m}$ due to linear and two-photon absorption (TPA). Thus materials for frequency conversion to the 2-4 μm spectral range were developed within MIRSURG which can be used for pumping those semiconductor-based parametric conversion stages in a tandem configuration. Ferroelectric oxides, such as KTiOPO_4 (KTP) isomorphs, MgO-doped LiNbO_3 (MgLN), MgO-doped LiTaO_3 (MgLT), are the preferred choice as a gain media in 2-4 μm parametric devices since they can be electric-field-poled to produce QPM structures, exploiting the largest second-order nonlinearity and non-critical interactions. Owing to the high-peak power requirements that are rather common in mid-IR devices, the possibility to fabricate large-aperture QPM structures becomes an important consideration. Such

capability has been demonstrated in Mg:LT, KTP and KTiOAsO₄ (KTA) with a focus on these two last families due to their high optical damage threshold and extended range of transmission.

Periodic poling and characterization of KTA: In terms of electric field poling the important parameters to consider are the ionic conductivity, the homogeneity and the availability of large crystal wafers from commercial vendors. Although RbTiOAsO₄ (RTA) presents ionic conductivity 3 orders of magnitude lower than that of KTA, which simplifies the poling process, its use is severely limited by the lack of commercial suppliers of high-quality large single-domain crystals. On the other hand, KTA is readily available and widely used in birefringence phase-matched mid-IR parametric devices. Periodic poling of 0.5 mm thick KTA crystals was previously carried out at temperature below 170 K. This method not only adds complexity in instrumentation and processing but also limits the total aperture of the poled device since the coercive field of the material increases substantially at lower temperatures. Based on previous observations that poling with relatively short pulses prevents domain broadening in KTP, a room temperature poling process was developed for KTA using commercial, single domain *c*-cut, flux-grown KTA crystals of dimensions 11×6×1 mm³ in *x*-,*y*-,*z*- directions of the dielectric tensor, respectively. The conductivity of the crystals varied from 1.5×10⁻⁷ to 4×10⁻⁷ S/m. To fabricate the periodic domain structure, an aluminum grating with a period of 39.5 μm was deposited on the *c*-face of the crystals by standard photolithographic techniques and the photoresist was left as an electric insulator. Liquid electrodes were used to contact the crystal to the external electric circuit. The poled area had dimensions of 8×3 mm². Due to the large ionic conductivity of KTA, the switching current is not suitable to monitor the poling process since it is usually difficult to discriminate it from the ionic current. Therefore, the method based on the transverse electro-optic effect was used together with in-situ 9th order second-harmonic generation (SHG). The magnitude of the electric field was set between 2.3 and 2.6 kV/mm depending on the specific ionic conductivity of each sample while the number of pulses was adjusted to maximize the SHG output. Figure 4 shows the resulting domain structure at (a) the patterned face and (b) the non-patterned face of a sample. Similar results were obtained for all the samples.

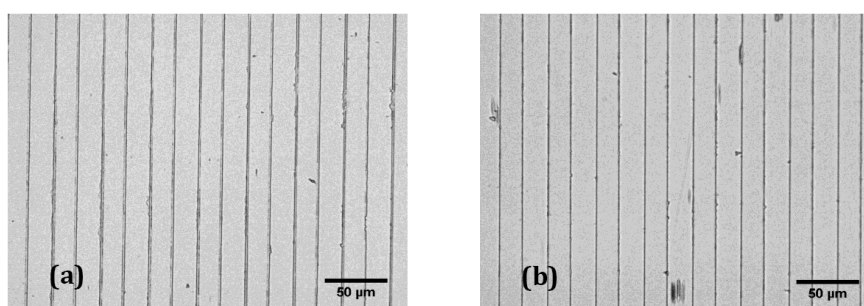


Figure 4: Microphotographs of selectively chemically-etched PPKTA: the originally lithographically patterned face (a), and the non-patterned face (b).

The uncoated PPKTA crystal was tested in a linear optical parametric oscillator (OPO) cavity to show the conversion of 1064 nm pump light to 1.538 and 3.452 μm signal and idler output, respectively. The pump source was a flash-lamp pumped Q-switched Nd:YAG laser producing pulses of 6.5 ns (FWHM) pulse length at a repetition rate of 20 Hz. The pump power was controlled by a wave plate - polarizer arrangement. The *z*-polarized pump light was launched along the *x*-axis of the crystal and focused by a 200 mm focal length lens to a beam waist of ~300 μm radius ($1/e^2$ intensity). The crystal temperature was stabilized by a Peltier element, normally to 25°C. Flat dielectric mirrors, both transmitting the pump light, were used as input and output couplers with the input coupler being highly reflective (HR, 99%) for the signal. The effective nonlinear coefficient d_{eff} of the PPKTA crystal was evaluated by measuring the threshold energy for different cavity lengths

while using a 90% reflectivity output coupler. In order to avoid parasitic oscillation, the crystal was rotated by about 5° and Fresnel reflections on the crystal surfaces were taken into account in the calculations. Figure 5 shows the measured threshold energies for cavity lengths of 30-50 mm together with calculated thresholds for different values of d_{eff} .

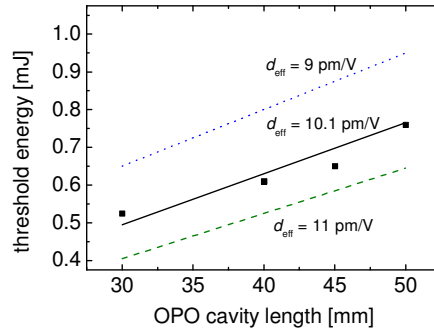


Figure 5: PPKTA OPO threshold dependence on cavity length and fitting experiment to numerical simulation.

Large aperture periodically poled KTP isomorphs: QPM structuring of thick crystals is not trivial due to the large domain aspect ratio and the large grating homogeneity along the whole crystal thickness that are needed. Intended for OPO experiments, QPM gratings in 3 mm-thick KTP crystals were successfully fabricated by electric field poling with short pulses. The poling period of $38.86 \mu\text{m}$ was designed for conversion from 1064 nm to the degeneracy point around 2128 nm with all waves polarized along the crystal c -direction. Uniform poling and homogeneous periodicity were achieved over the whole $9 \times 6 \times 3 \text{ mm}^3$ volume defined by the lithographic mask. A similar poling technique but with different pulse parameters was used to invert domains in up to 5-mm thick $\text{Rb}_x\text{K}_{1-x}\text{TiOPO}_4$ (Rb:KTP) solid solutions with very good results (Fig. 6). It was found, that due to two-orders of magnitude lower ionic conductivity in these solid solutions with $x \sim 0.01$, the domain duty cycle is transferred from the lithographic electrode pattern substantially more accurately than in flux-grown KTP. Measurements of nonlinear frequency conversion in cw and pulsed regimes reveal that the nonlinear coefficient value in solid solution crystals remains the same as that in undoped KTP. Table 2 lists the ferroelectric crystals fabricated during the MIRSURG project and dedicated to the first stage of 1064 nm pumped cascaded high-energy mid-IR optical parametric devices.

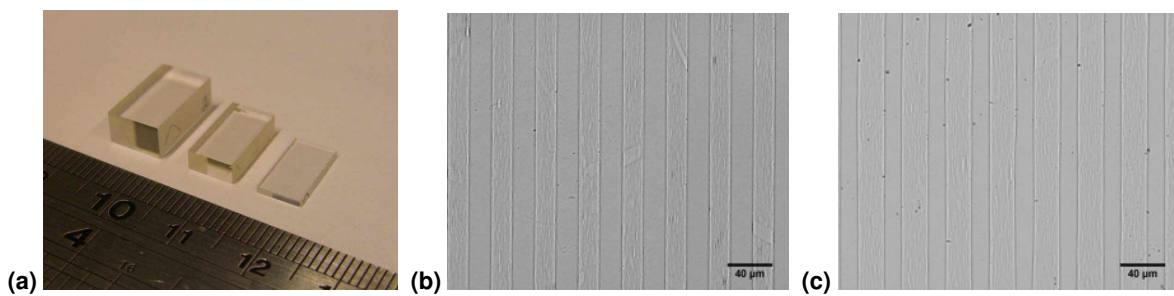


Figure 6: Fabricated PPRb:KTP crystals (a). Microscope pictures of selectively etched polar faces of a sample (patterned (b) and unpatterned (c)). The poling period is $38.8 \mu\text{m}$.

Table 2: Fabricated periodically structured ferroelectrics.

Material	Poling period [μm]	Designed pump wavelength [nm]	Designed signal wavelength [nm]	Designed idler wavelength [nm]	Thickness [mm]	Length [mm]
KTP	38.88	1064	2128	2128	3	11
KTA	39.50	1064	1537	3452	1	11
Rb:KTP	38.86	1064	2128	2128	5	11
Mg:LT	31.25	1064	1605	3157	1	11

Nonlinear optical materials obtained from external collaborators were characterized within the project for use in direct frequency conversion by OPOs from 1064 nm to the 6.45 μm spectral range. Important properties, besides transparency, dispersion and second order nonlinear coefficients, are the damage threshold in the nanosecond regime and the TPA. The mid-IR crystals studied include CdSiP_2 (CSP), $\text{GaS}_x\text{Se}_{1-x}$, LiInSe_2 (LISE), LiGaS_2 (LGS), BaGa_4S_7 (BGS) and BaGa_4Se_7 (BGSe).

Criteria for crystal selection: Suitable nonlinear crystals should have a band-gap corresponding to ≤ 532 nm (2.33 eV), say ≥ 2 eV, and be able to phase-match an idler wavelength of 6.45 μm with an effective nonlinearity $d_{\text{eff}} > 1$ pm/V. AgGaS_2 (AGS) is the only commercially available crystal satisfying these requirements. Besides its modest nonlinearity, the low thermal conductivity and strongly anisotropic thermal expansion are limitations that justify the search for other alternatives.

LISE and LGS: The Li-compounds with wurtzite type structure (LiInS_2 , LiInSe_2 , LiGaS_2 and LiGaSe_2) exhibit the largest band-gaps and have better thermo-mechanical properties than AGS but their nonlinear coefficients are even lower. The one with the highest nonlinearity, LISe, and the one with largest band-gap and damage resistivity, LGS, were investigated. Both crystals are relatively well characterized. The only unknown important property was the damage resistivity of uncoated and AR-coated crystals. The laser source for the damage tests was a diode-pumped electro-optically Q-switched Nd:YAG laser (14 ns, 100 mJ) optimized for a repetition rate of 100 Hz (the same laser used subsequently for OPO pumping) with energy stability of $\pm 1\%$. Typically, the pump level was increased in small steps and the reported damage values are average of the fluence before and after damage occurred for exposure time of 1 min (6000 shots). No reproducible results were obtained with AR-coated LISe samples (single or multiple layers deposited) which was related to bad reproducibility of the coatings, though in some cases the resistivity was improved compared to uncoated material. Hence, for LISe, the reported damage level refers to uncoated material only, Table 3, see Fig. 7b. In the case of LGS, single layer AR-coating centered at 1250 nm was designed for the pump and signal (OPO resonated wave) only, in order to obtain higher resistivity. The material chosen (YF_3) ensures that there is no absorption loss at the idler wavelength. The main conclusion is that the surface damage threshold is ~ 5 times higher for LGS compared to LISe. The values for LGS show good reproducibility without systematic difference between uncoated and AR-coated surfaces. Since similar coatings were applied to LISe, the AR-coating problems in LISe seem related to the surface chemical stability and not necessarily with the coating itself. The cracks seen in LGS occurred in fact on the next day and developed from the damaged front surface.

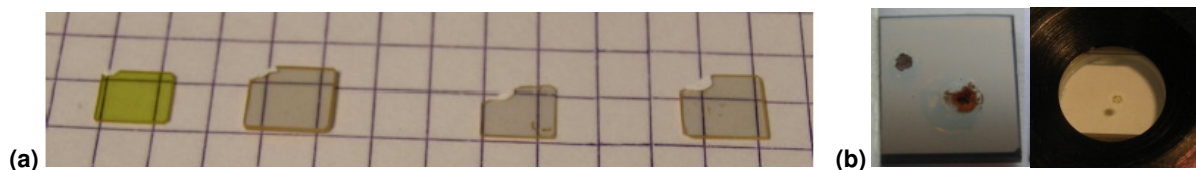


Figure 7: AGS (left) and 3 BGS samples used for determination of the nonlinear coefficients (a) and surface damage in uncoated LISe and LGS test plates (b).

$\text{GaS}_{0.4}\text{Se}_{0.6}$: Two essential advantages were expected from adding S to the well known nonlinear crystal GaSe (such crystals were grown especially for MIRSURG) - increase of the band-gap or the short wave cut-off limit and the hardness which is one of the basic limitations of GaSe. The band-gap of $\text{GaS}_{0.4}\text{Se}_{0.6}$ reached indeed ~ 2.3 eV (538 nm). Its long wave cut-off edge for clear transparency (at 0.1 cm^{-1} absorption) is at 10.2 μm but the transmission extends to $> 14 \mu\text{m}$. The index of refraction of $\text{GaS}_{0.4}\text{Se}_{0.6}$ was measured in the 0.633 – 10.0 μm spectral range using the auto-collimation technique on a prism (Fig. 8) and then fitted to Sellmeier equations (Table 4). The fit was tested by computing SHG phase-matching curves and comparing with experimental results. The nonlinear coefficient of the mixed compounds was measured by comparing the SHG conversion efficiency to that of pure

GaSe using fs pulses at 4.65 μm , see Table 5. The damage threshold of $\text{GaS}_{0.4}\text{Se}_{0.6}$ was estimated in the same way as for LISe and LGS, comparing to undoped GaSe (Table 3). The measured with 76 ps long pulses at 1064 nm TPA coefficient of $\text{GaS}_{0.4}\text{Se}_{0.6}$ is 3.5 lower in comparison with GaSe.

Table 3: Damage studies of uncoated and AR-coated nonlinear crystals with 14 ns pulses at 1064 nm.

Crystal	Damage threshold (axial) [J/cm^2]	Damage threshold (axial) [MW/cm^2]	Remarks on damage character, coatings, sample thickness, orientation and quality
LISe	0.5 / 0.78-0.92	36 / 56-66	white spots / crater and crack, uncoated, 1 mm, $\theta=90^\circ$, $\varphi=34^\circ$
LGS	3.33 / 4.70	238 / 336	turbidity / crack, uncoated, 1.25 mm, unoriented
LGS	3.44 / 3.71	246 / 265	turbidity / crater, single side YF_3 AR-layer, 1.25 mm, unoriented
LGS	3.84 / 4.45	274 / 318	turbidity / crack, double side YF_3 AR-layer, 1.25 mm, unoriented
LGS	3.52 / 3.61	251 / 258	turbidity / crater, uncoated, 3 mm, $\theta=90^\circ$, $\varphi=41^\circ$, old, low quality
BGS	3.7	264	crater rear side, uncoated, 2.2 mm, unoriented
BGSe	1.45	104	crater rear side, uncoated, 2.2 mm, $\theta=0^\circ$
BGSe	1.25	89	crater rear side, uncoated, 2.3 mm, $\theta=90^\circ$, $\varphi=90^\circ$
$\text{GaS}_{0.4}\text{Se}_{0.6}$	0.68	49	crater and crack, uncoated, 0.3-1 mm, $\theta=0^\circ$ (cleaved)
GaSe	0.48	34	crater and crack, uncoated, 0.3-1 mm, $\theta=0^\circ$ (cleaved)
CSP	0.18	13	darkening, uncoated, 2 mm, unoriented, low surface quality
CSP	0.25	18	crater, double side Al_2O_3 AR-layer, 2 mm, $\langle 112 \rangle$ -oriented
CSP	0.24	17	blackening, single side triple AR-multilayer, 2 mm, unoriented

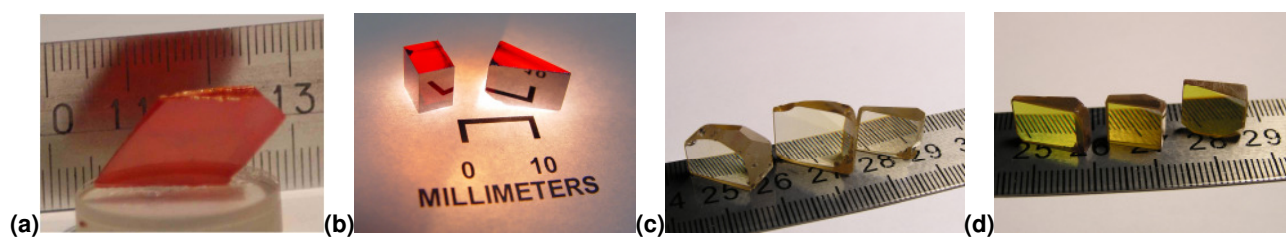


Figure 8: Prisms of the new $\text{GaS}_{0.4}\text{Se}_{0.6}$ (a), CSP (b), BGS (c), and BGSe (d) crystals for refractive index measurements (all photographs courtesy of the crystal growers).

CSP: CSP is a new and very promising nonlinear material, developed in USA after the start of the project. Nevertheless, it was clear that this material outperforms all other chalcogenide crystals suitable for 1064 nm pumping in many aspects, such as d_{eff} , hardness, or anisotropy of the thermal expansion, as well as the possibility of non-critical phase-matching with maximized d_{eff} . Its band-gap (2.2 - 2.45 eV) is just sufficient to avoid TPA at 1064 nm. A practical upper limit of 6.5 μm can be assumed for the transparency due to the onset of intrinsic multi-phonon absorption: This defines a range of 4 to 6.5 μm for important applications of CSP, one of them targeted in MIRSURG at 6.45 μm . CSP is an optically negative uniaxial chalcopyrite (tetragonal point group $\bar{4}2m$). Important physical properties had already been measured by the crystal growers and the existing Sellmeier equations were found reliable. The value of the d_{36} coefficient of CSP was estimated relative to ZGP by SHG near 4.6 μm , as described above for $\text{GaS}_{0.4}\text{Se}_{0.6}$. To confirm the reliability, also d_{36} of the defect chalcopyrite HgGa_2S_4 (HGS) was measured. Surprisingly CSP showed higher nonlinearity than ZGP though its band-gap is larger and this was confirmed later by other investigators. Damage tests of CSP were performed using 2-mm thick plates with and without AR-coating, Table 3. While AR-coatings seem to improve the resistivity, all values are rather low and further comparative studies near 2 μm (relative to ZGP) will have to figure out if the reason is related to multi-photon processes.

Relevant properties of BGS and BGSe: BGS and BGSe, discovered also after the start of the project, are similar to the Li-compounds. The as-grown by the Bridgman-Stockbarger method crystals are colorless (BGS) or light-yellow (BGSe), Fig. 8. The good transmission limits, estimated at an

absorption level of 0.3 cm^{-1} from unpolarized measurements, are $0.545\text{-}9.4 \text{ }\mu\text{m}$ (BGS) and $0.776\text{-}14.72 \text{ }\mu\text{m}$ (BGSe), see Fig. 9. The band-gaps correspond to $\sim 350 \text{ nm}$ (3.54 eV) for BGS and 469 nm (2.64 eV) for BGSe. Thus in both crystals no TPA should occur at 1064 nm . Both crystals are biaxial but while BGS is orthorhombic ($mm2$ point group) BGSe is monoclinic (m point group). The orientation of the dielectric frames (optical ellipsoids) was determined from conoscopic pictures using 633 nm light. The refractive indices, measured in the $0.42\text{-}9.5 \text{ }\mu\text{m}$ spectral range for BGS and in the $0.48\text{-}10.4 \text{ }\mu\text{m}$ for BGSe, were used to fit two-pole Sellmeier equations (Table 4).

Table 4: Sellmeier coefficients of $\text{GaS}_{0.4}\text{Se}_{0.6}$, BGS and BGSe: $n^2=A_1+A_3/(\lambda^2-A_2)+A_5/(\lambda^2-A_4)$ where λ is in μm .

Crystal	n	A_1	A_2	A_3	A_4	A_5
$\text{GaS}_{0.4}\text{Se}_{0.6}$ $0.633\text{-}10 \text{ }\mu\text{m}$	n_o	9.550489	0.054331	0.303723	1408.38	3738.138
	n_e	7.335355	0.037580	0.247335	1268.56	2580.856
BGS $0.42\text{-}9.5 \text{ }\mu\text{m}$	n_x	7.090307	0.019272	0.172059	858.223	1748.013
	n_y	7.812188	0.015907	0.182439	990.979	2653.548
	n_z	7.907286	0.015853	0.184081	981.884	2630.008
BGSe $0.48\text{-}10.4 \text{ }\mu\text{m}$	n_x	7.410040	0.051215	0.293340	1265.119	1896.441
	n_y	7.323096	0.052725	0.292889	1182.324	1573.474
	n_z	7.764197	0.069734	0.326812	1297.079	1975.857

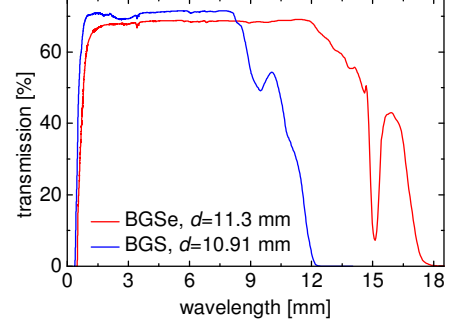


Figure 9: Unpolarized transmission of BGS and BGSe.

Table 5: Relative measurements of nonlinear coefficients. λ_F : fundamental wavelength for SHG.

Crystal	Nonlinear coefficient	Relative to	Measured at λ_F	Absolute values @ λ_F after rescaling applying Miller's rule
$\text{GaS}_{0.05}\text{Se}_{0.95}$	$d_{22}=0.89$	$d_{22}(\text{GaSe})$	$4.65 \text{ }\mu\text{m}$	$d_{22}=51.6 \text{ pm/V}$ @ $4.56 \text{ }\mu\text{m}$ with $d_{22}(\text{GaSe})=54 \text{ pm/V}$ @ $10.6 \text{ }\mu\text{m}$
$\text{GaS}_{0.1}\text{Se}_{0.9}$	$d_{22}=0.86$	$d_{22}(\text{GaSe})$	$4.65 \text{ }\mu\text{m}$	$d_{22}=49.9 \text{ pm/V}$ @ $4.56 \text{ }\mu\text{m}$ with $d_{22}(\text{GaSe})=54 \text{ pm/V}$ @ $10.6 \text{ }\mu\text{m}$
$\text{GaS}_{0.4}\text{Se}_{0.6}$	$d_{22}=0.76$	$d_{22}(\text{GaSe})$	$4.65 \text{ }\mu\text{m}$	$d_{22}=44.1 \text{ pm/V}$ @ $4.56 \text{ }\mu\text{m}$ with $d_{22}(\text{GaSe})=54 \text{ pm/V}$ @ $10.6 \text{ }\mu\text{m}$
CSP	$d_{36}=1.07$	$d_{36}(\text{ZGP})$	$4.56 \text{ }\mu\text{m}$	$d_{36}=84.5 \text{ pm/V}$ @ $4.56 \text{ }\mu\text{m}$ with $d_{36}(\text{ZGP})=75 \text{ pm/V}$ @ $9.6 \text{ }\mu\text{m}$
HGS	$d_{36}=0.328$	$d_{36}(\text{ZGP})$	$4.58 \text{ }\mu\text{m}$	$d_{36}=25.9 \text{ pm/V}$ @ $4.58 \text{ }\mu\text{m}$ with $d_{36}(\text{ZGP})=75 \text{ pm/V}$ @ $9.6 \text{ }\mu\text{m}$
BGS	$d_{31}=0.37$	$d_{36}(\text{AGS})$	$4.62 \text{ }\mu\text{m}$	$d_{31}=5.1 \text{ pm/V}$ @ $2.26 \text{ }\mu\text{m}$ with $d_{36}(\text{AGS})=13.9 \text{ pm/V}$ @ $2.26 \text{ }\mu\text{m}$
	$d_{32}=0.41$	$d_{36}(\text{AGS})$	$2.26 \text{ }\mu\text{m}$	$d_{32}=5.7 \text{ pm/V}$ @ $2.26 \text{ }\mu\text{m}$ with $d_{36}(\text{AGS})=13.9 \text{ pm/V}$ @ $2.26 \text{ }\mu\text{m}$

In order to determine in which principal planes phase-matched processes exhibit non-vanishing d_{eff} , the two-fold axis of BGS was identified as well as the correspondence between the dielectric (xyz) and crystallographic (abc) axes in both crystals. The calculated SHG phase-matching curves for BGS and BGSe were compared with experiment. Then all configurations for generation of $6.45 \text{ }\mu\text{m}$ radiation were analyzed. The d_{32} and d_{31} tensor components of BGS (the only two non-zero non-diagonal elements under Kleinman symmetry) were measured by SHG at 2260 and 4620 nm . The results are shown in Table 5 where $d_{31}/d_{32}>0$. Under Kleinman symmetry, there are four non-zero non-diagonal elements d_{i1} for the monoclinic BGSe. Only preliminary estimates were obtained from similar measurements which do not give the four coefficients of BGSe with proper relative signs. The surface damage thresholds measured for BGS and BGSe (Table 3) are rather high, the one for BGS is very similar to LGS which confirms the close relation of this property to the band-gap value.

A picosecond master-oscillator power-amplifier (MOPA) laser system at 1064 nm has been designed and developed as a pump source for synchronously pumped OPO (SPOPO) with macro-pulse format. All-diode-pumped solid-state (DPSS) laser technology has been implemented for all stages, including the high-energy amplifier. DPSS technology is more suitable for compact laser system to be used in clinical environments. This MOPA system was extensively characterized and later employed for pumping a mid-IR SPOPO. The output macro-pulse energy was limited to 50 mJ due to

the extremely high small-signal gain required for the amplification chain. The present limitations have been analyzed and possible improvements have been identified.

Two diode-pumped mode-locked picosecond lasers have been designed and developed, one at 450 MHz and another at 1 GHz. The relatively high repetition rate has been chosen in order to make the design more compact. Eventually, the 450-MHz 6-ps oscillator was realized with an optimized opto-mechanical design. The acousto-optic modulator (AOM) pulse-picker electronic control has been developed to enable selection of macro-pulse trains with length >100 ns, with typical energy of 100 nJ at 1 μ s duration. The overall system layout is shown in Fig. 10. The low-power high-gain preamplifier (2×200 W bars) increases the macro-pulse energy from ~ 45 nJ to ~ 1 mJ; the first high-energy Nd:YVO₄ amplifier module was configured for single-pass operation. Two resonant saturable-absorber mirrors (RSAMs) were added to suppress amplified spontaneous emission (ASE) and tendency to self-oscillation. Both RSAMs have small-signal reflectivity of few percent, and saturated reflectivity of $\sim 80\%$ at ~ 10 -ps pulses, with fast recovery of few tens of picoseconds. Five-pass side-pumped Nd:YAG bounce amplifiers were eventually employed, since additional passes did not add significant output energy.

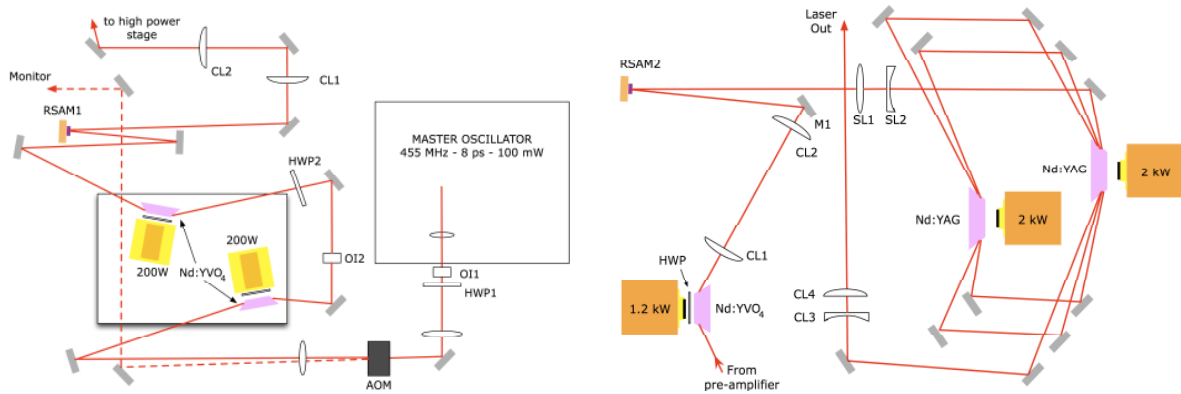


Figure 10: Layout of the MOPA laser system including the low-energy high-gain stage and the first high-energy module. AOM: pulse-picker allowing pre-compensation of amplifier distortions; OI: Faraday opto-isolators; CL: cylindrical lenses; SL: spherical lenses; HWP: half-wave plates.

The laser system was operated at a duty cycle of 1% settled by the high-power diode stacks, hence the repetition rate was limited to 50 Hz: The Nd:YVO₄ amplifiers were driven with 100- μ s pulses, and the Nd:YAG amplifiers were operated with 200- μ s pulses to take advantage of the longer fluorescence time allowing higher energy storage. Last-generation diode stacks can be run at higher duty cycle, allowing repetition rates of 100 Hz also with Nd:YAG amplifiers. The macro-pulse output energy was 50 mJ (starting from ~ 45 nJ after waveform pre-compensation). Both ASE contribution and the leakage of the cw train (static extinction ratio of the pulse picker $\sim 1:2000$) were effectively suppressed by the RSAMs.

Table 6: Saturation energy and small-signal gain for the three amplifier modules.

Amplifier		G_0 [dB]	E_{sat} [mJ]
Stage	Pump module diode array(s)		
I	2×200 W	49.0	0.60
II	1.2 kW	17.2	1.51
III	2×2 kW	22.6	19

Both the saturation energy E_{sat} and the small-signal gain G_0 for each module were measured by injecting an approximately flat-top input waveform $P_i(t)$ and recording the saturated output $P_o(t)$, repeating such procedure for each module (turning off the others). Hence a best-fit routine based on

Frantz-Nodvik equation, was run to extract both E_{sat} and G_0 for each module (a summary of results is presented in Table 6). The complete model of the amplifier chain including the RSAM nonlinear elements (according to specifications provided by the manufacturer) was used to predict the input waveform allowing a nearly flat-topped output envelope (Fig. 11). Here f_m is the modulation input function for the pulse-picker which defines the envelope shape for pre-compensation.

Input pulse shaping has only little effect on output energy (pre-compensation reduces the seed energy to $\sim 25\%$), while the overall efficiency is mostly influenced by the RSAMs, due to the high dynamics of the pre-compensated seed waveform. Indeed, while their saturated output would approach 80%, the pre-compensating input shape yields integrated reflectivity of 35-40% for the RSAMs (about 50% of the saturated reflectivity). A comparative analysis carried out with the Frantz-Nodvik model allows one to identify readily the sources of inefficiency in the system: (i) Output energy = 81 mJ with flat-top input and no RSAMs, (ii) Output energy = 75 mJ with pre-compensating input and no RSAMs, and (iii) Output energy = 50 mJ with pre-compensating input and with RSAMs.

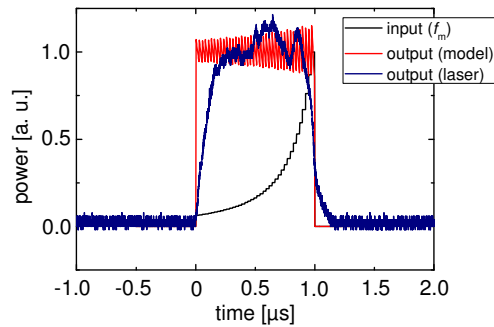


Figure 11: Input and output waveforms for the whole chain. Actual output macro-pulse is also shown.

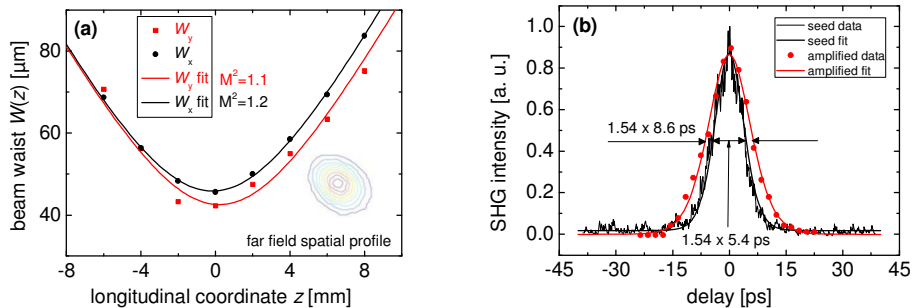


Figure 12: Beam quality measurement for the amplified macro-pulse (a) and output pulse autocorrelation (b).

Another important aspect for SPOPO pumping is the output beam quality as well as the spectral quality, which proved to be nearly diffraction- and Fourier-limited, respectively (Fig. 12).

It turns out that a straightforward but expensive upgrade would be the replacement of the low-power oscillator, acousto-optic pulse-picker and a 20-dB pre-amplifier with a high-power ~ 10 -W ps fiber laser and large-aperture, high-voltage fast electro-optical switch for waveform compensation. Otherwise, the present architecture could be preserved, with the addition of further (one or two) 2-kW pump diode stacks, ensuring larger beam cross section (thus energy extraction) without changing the overall small-signal gain (hence without increasing tendency to self-oscillation). However, it is worth noting that besides its uniqueness, the present realization of the macro-pulse ps laser system yields an overall optical-to-optical efficiency $\sim 6\%$ approaching that of most efficient (~ 8 - 10%) ns diode-pumped amplifiers reported to date, although these were not subjected to severe constraints such as envelope shaping and operation at very high gain.

Another part of the pump laser development within the project was devoted to ns pump sources in the 2- μm spectral range for single stage mid-IR OPOs. Novel cavity geometries for the Tm^{3+} :YAG laser have been developed and tested, based on the Total-Internal-Reflection (TIR) concept. Using two 120-W fiber-coupled laser modules at 804 nm, up to 7 W of average output power in free-running operation was achieved at 100 Hz (4-ms pump pulses). Output energy of 13.6 mJ with 400-ns pulse width was achieved at 100 Hz until optical damage occurred on the rod ends. With more pump power, the average output power in the free-running mode was scaled up to 12 W.

After some preliminary experiments and considerations, a resonator pumped by two 120-W fiber-coupled laser diodes at 804 nm (one from each end) was designed and investigated extensively (Fig. 13). It was possible to create large beam radius on all critical components and to increase the output coupler transmission up to 50%.

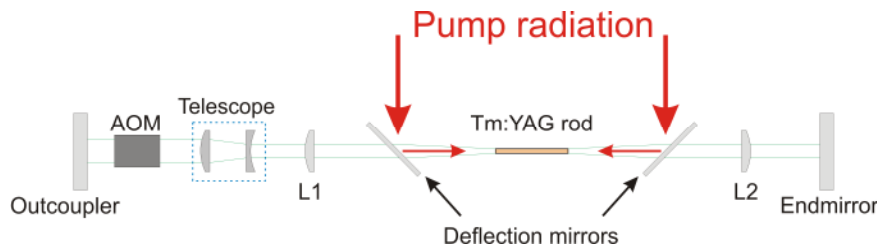


Figure 13: Set-up of the Tm:YAG laser with intra-cavity telescope for beam transformation.

This design proved to be excellent for generating diffraction-limited beams, which of course are most suitable for pumping OPOs efficiently. Figure 14a shows the performance of the Tm:YAG laser in free-running regime with two different output couplers. As much as 7 W of average output power was achieved at 100 Hz with 40% duty cycle (4-ms pump pulse).

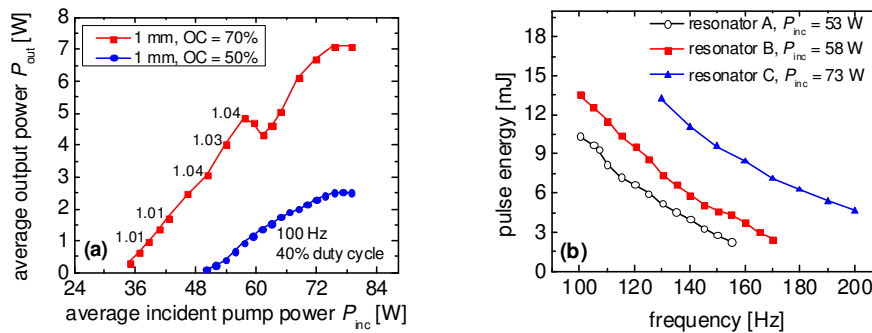


Figure 14: Input-output characteristics of the free-running Tm:YAG laser for different output coupler reflectivity (OC) and 1 mm pump focus diameter (a). The numbers along the curve are the measured M^2 values. Measured pulse energy vs. repetition rate of the Q-switched Tm:YAG laser at a pump duty cycle of 40% for different average pump powers P_{inc} (b).

Before Q-switching, a beam transforming telescope was inserted into the cavity in order to increase the beam radius on the AOM to avoid damage on it (see Fig. 13). The beam profile of the cavity was compared with and without the telescope. The mode radius in the AOM section of the cavity was quite large so that an aperture effect in the AOM occurred. Without the expansion of the beam by this telescope the beam profile was a very good fundamental mode. In order to avoid this aperture effect and after validating the damage threshold of the AOM AR-coating the telescope has been dismantled, and a telescope-free cavity was further used. Figure 14b shows the pulse energies achieved in Q-switched operation. Resonator configurations A and B refer to ones with an intracavity telescope while configuration C corresponds to an optimized set-up without telescope. Maximum

pulse energy at 100 Hz of 13.6 mJ with a pulse FWHM of 400 ns was achieved. The shortest pulse width of 300 ns at 130 Hz and pulse energy of 13.2 mJ were obtained with resonator C.

Due to the strong thermal lens of YAG the end facets of the rod were the limitation for the output energy in the Q-switched regime although the mode radius on the other intracavity optical elements was large enough to permit higher pulse energies before optical damage occurs. With the fixed rod dimensions of $\varnothing 3 \times 90$ mm, only a slight increase in pulse energy could be obtained by optimizing the coatings and output coupling rates for Q-switched operation at $M^2 < 1.1$. There are some additional possibilities to increase this energy limit. One important point is the change of the pulse operation mode from Q-switched to cavity dumped and the use of a special cavity design allowing one to precisely control the pulse width. From the measured pulse energy in the Q-switched regime this should allow one to scale up the laser output energy to several tens of mJ. To realize this, more pump power was necessary. Therefore, two 300 W fiber-coupled pump diodes emitting at ~ 804 nm at room temperature were employed. This also allows one to increase the pump spot diameter and decrease the pump duty cycle to reduce the thermal lens of the rod still having enough pump energy for high output pulse energies. Operating the high-power pump diodes at lower temperature permits pumping the Tm^{3+} :YAG rod at 798 nm, giving rise to a more optimum pump absorption. At the same average power therefore it is possible to decrease the duty cycle to enhance the pump efficiency. Scaling of the average output power up to 12 W was obtained in the free-running mode (Fig. 15a).

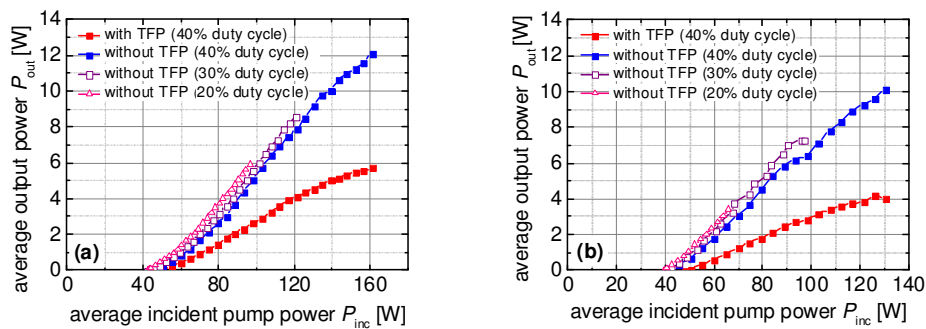


Figure 15: Average output power of the free-running Tm :YAG laser at 100 Hz with 1 mm pump focus diameter in front (a) and 2 mm focus diameter inside (b) the rod versus average incident pump power.

At the higher pump power the thermal lens turns out to be very strong even with a duty cycle of 40%. To reduce this effect slightly the pump area in the rod was increased by setting the 1 mm pump focus in front of the laser rod, thus pumping the whole volume much more uniformly due to the TIR of the divergent pump light inside the rod. Unfortunately, as can be seen in Fig. 15a, the thermal lens effect at such high powers was still strong, which causes severe depolarization effects in the crystal. Therefore, not restricting the laser polarization, i.e. without a thin-film polarizer (TFP) in the cavity, the unpolarized laser emission yielded two times higher output power than the emission with a TFP inside the cavity. When the duty cycle is decreased the pump efficiency increases. However, due to the lower pump pulse energy, the maximum extractable laser power is reduced, even at an output coupler reflectivity of 80%. This can be seen in Fig. 15a. Pumping the whole rod from both sides without a collimated beam or top hat-like intensity distribution like in Fig. 15a was unfortunately not efficient enough to reach the goal. By focusing the pump beam to a 2 mm pump spot diameter inside the rod the output power with the same output coupling is shown in Fig. 15b. Comparing the emitted power with and without a polarizer, the depolarization losses are found to be stronger compared to the 1 mm case shown in Fig. 15a.

It was impossible to pulse this system in cavity-dumped operation during the time of the project but the research on this Tm^{3+} :YAG laser will be continued in the future as the idea of cavity dumping is considered to be a good alternative for directly diode-pumped high pulse energy $2 \mu\text{m}$ pump sources.

As OPO pump sources near 2 μm , Ho-lasers have the advantage of longer wavelength to avoid absorption in the nonlinear crystal and longer storage time for Q-switching in comparison to their Tm counterparts. A novel 2.1 μm pump source was developed based on direct diode pumping of Ho:YAG which enabled efficient laser operation both in cw and Q-switched regime and set new standards. Slope efficiencies as high as 62 % and output powers of 55 W were achieved. In Q-switched regime, pulse energy >30 mJ was extracted from the oscillator at 100 Hz repetition rate.

One important aspect that had to be studied before the actual laser experiments was the absorption efficiency of the diode pumped Ho:YAG rods. For that purpose the diode stack emission spectra had to be characterized. Figure 16 shows the output spectra of the GaSb-based laser diode stack at 15°C which delivered 160 W of output power. The shift of the central wavelength from threshold to the maximum output power is ~45 nm and the FWHM is ~ 25 nm. Thus, several absorption peaks of Ho:YAG are addressed. This results in a variable absorption efficiency which was experimentally and theoretically investigated. The single pass transmitted pump power was measured and compared to the effective absorption coefficients on the basis of the diode spectrum and absorption spectrum of Ho:YAG. These studies dictated the optimum length and doping of the Ho:YAG rods. Depending on the operation mode two different rod types were used either for high power or high energy operation.

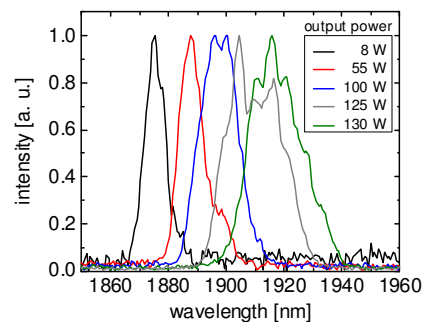


Figure 16: Emission spectra of the GaSb-based laser diode stack for different output powers at 15°C

High-power operation: For high power Ho:YAG laser operation a compact plano-plano resonator was chosen, see Fig. 17. The Ho(1%):YAG rod was 52 mm in length and 3 mm in diameter. It was barrel polished to enable pump light guiding via TIR and AR-coated on both facets for pump and laser wavelengths. The rod was actively water cooled to 18°C. The pump spot diameter on the incoupling facet of the rod was 2 mm. The mirror M1 was AR-coated for the pump wavelength and HR-coated for the laser wavelength. It was located as close as possible to the facet of the Ho:YAG rod. Five different output coupling rates (M2) were investigated (5%, 7%, 10%, 18%, and 33%).

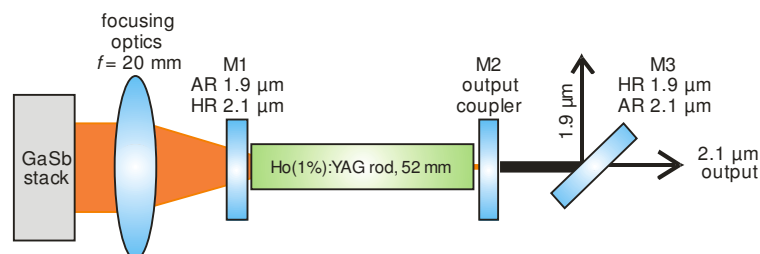


Figure 17: Compact linear Ho:YAG laser resonator formed by plane mirrors M1 and M2.

The transmitted pump light was deflected by the dichroic mirror M3. Figure 18 shows the input output curves. With 5% transmission output coupler a maximum output power of 55 W and a slope efficiency of 62% were achieved which are the highest values reported for diode-pumped Ho-lasers. In Q-switched operation few mJ of pulse energy were extracted limited by damage of the coatings.

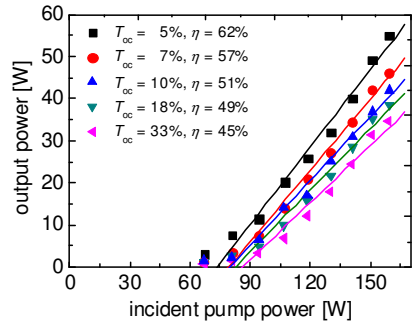


Figure 18: CW laser performance of the Ho(1%):YAG laser at room-temperature.

High-energy operation: For high-energy Q-switched operation the laser resonator had to be modified in order to maximize the laser mode radius and thus avoid damage. Two different routes for Q-switching were investigated: via AOM and via electro-optical modulator (EOM).

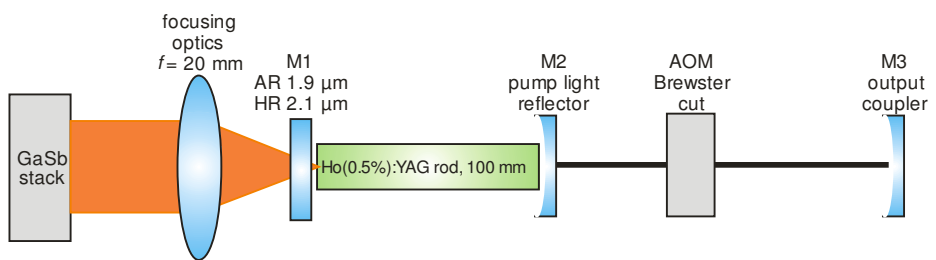


Figure 19: Experimental set-up of the Ho:YAG laser resonator designed for Q-switching.

The experimental set-up is shown in Fig. 19. A relatively long (100 mm) Ho(0.5 %):YAG rod was chosen to achieve a maximum gain length. The diameter was 3 mm and the rod was water cooled to 15°C. It was also barrel polished to ensure guiding of the pump light by TIR. The total resonator length was ~90 cm. The curved pump light mirror M2 reflected back the transmitted pump light for a second pass and additionally to maximize the laser mode. The output coupler M3 was partially reflecting for the laser wavelength (50%) and had a radius of curvature of 500 mm. A fused silica Brewster cut AOM was used for Q-switched operation and for linear polarisation of the laser.

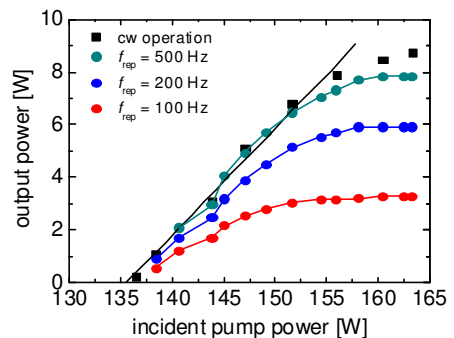


Figure 20: Average output power of the AOM Q-switched Ho:YAG laser for different pulse repetition rates.

Figure 20 shows the measured average output power in cw and AOM Q-switched operation. At the maximum pump power, damage-free operation with pulse energy of 15.7, 29.5, and 33 mJ was achieved at pulse repetition rate of 500, 200, and 100 Hz, respectively. The corresponding pulse durations were 200, 125, and 100 ns. These pulse energies are the highest values ever achieved with a diode-pumped Ho-laser. Nevertheless, the pulse energy is still scalable with one single amplifier stage. From comparison with Tm-fiber laser pumped systems, also the pulse energy from the master oscillator could be in principle doubled.

For EOM Q-switching a Pockels cell based on RTP was used in combination with a Brewster plate to enforce linear polarization. In that configuration 7.8 mJ of pulse energy and pulse duration of 200 ns were achieved. The current limit is pre-lasing for pump powers of ~148 W. Thus, the extinction ratio is too low to achieve high-energy laser pulses. Also, depolarization effects of the Ho:YAG rod decrease the extinction ratio. A possible solution is to use multiple Brewster plates or Glan laser polarizers which will be tried after the end of the project.

The only system operating at 6.45 μm in the beginning of the project was a macro-pulse format SPOPO based on flashlamp pump technology, employing a crystal of AGS for direct frequency conversion in a single step from 1064 nm. After upgrading the pump system, CSP was employed for the first time in a 90°-phase-matched SPOPO pumped at 1064 nm and 2- μs long idler macro-pulses near 6.4 μm with energy as high as 1.4 mJ and average power of 35 mW were achieved: each consisting of 200 micropulses of 12.6 ps duration. Maximum conversion efficiency exceeded 40%.

Pump source upgrade: The first prerequisite for increase of the output power of the macro-pulse SPOPO which can be in principle tuned to the desired wavelength of 6.45 μm was to upgrade the pump source and increase the pump energy at 1064 nm. The pump source contains a mode-locked Nd:YAG laser oscillator built around one Nd:YAG rod (110 mm long and 6 mm in diameter) that is pumped with a flashlamp at a repetition rate of 25 Hz. The oscillator cavity length of about 1.5 m is adjusted to the 100 MHz frequency of the acousto-optic mode-locker (AOML). Mode-locking is achieved using frequency doubling nonlinear mirror (FDNLM) constituted by a SHG crystal (BBO) and a dichroic mirror which provides a positive feedback on the peak intensity of the pulse circulating in the cavity. The FDNLM effect is balanced by the negative feedback provided by the nonlinear absorption in a GaAs semiconductor platelet. These two antagonist actions result in the stabilization of the pulse energy and duration. The pulse duration at the oscillator output is between 15 and 20 ps. An extracavity AOM suppresses the initial, non-stationary part of the train, and the resulting, almost steady-state macro-pulse consists of about 200 micropulses with 10 ns separation. The oscillator is protected by an optical isolator. A novel 3 pass amplification scheme was adopted, built around an identical Nd:YAG laser rod (110 mm long and 6 mm in diameter) which is pumped by two flashlamps. The beam diameter in the Nd:YAG rod is 3 mm for the first and second passes, and 5 mm for the third pass, in order to optimize the energy extraction. Maximum output pump power of about 3 W, e.g. $3/25=0.12$ J per bunch (macro-pulse) is achieved. The macro-pulse duration is 2 μs . The maximum picosecond micropulse energy is thus $120 \text{ mJ}/200=0.6$ mJ.

A telescope adapts the pump beam spot diameter to the aperture of the SPOPO nonlinear crystal. The non-collinear pump beam makes an angle of $\sim 2^\circ$ with the SPOPO cavity axis meaning that the signal beam oscillates in the cavity while the idler beam is emitted out of the cavity. Synchronous pumping requires the optical length of the cavity to be adjusted to that of the Nd:YAG oscillator (1.5 m).

CSP based SPOPO: With the present pump system, the first non-critical SPOPO based CSP pumped at 1064 nm was realized. The 9.5-mm long sample used was cut at $\theta=90^\circ$, $\phi=45^\circ$. Its aperture was 6 mm (along the c -axis) \times 6.75 mm. The residual losses measured for the relevant polarizations (e for the pump and o for the signal and idler) were 0.185 cm^{-1} at 1064 nm, 0.114 cm^{-1} at 1.3 μm , and 0.014 cm^{-1} at 6.4 μm . Both faces were AR-coated for pump, signal, and idler with an 8-layer coating.

The idler energy from the CSP SPOPO was measured both from the pump depletion and using a calibrated pyroelectric detector. The threshold corresponded to an average pump power of 15 mW or a single (micro)pulse energy of 3 μJ . The depletion together with the simultaneously measured transmission of the crystal is shown in Fig. 21a. The incident pump power was limited to slightly above 300 mW because strong pump depletion, reaching typically $\sim 40\%$, was observed starting from

about 100 mW of pump power. The actual crystal transmission at the pump wavelength, when the SPOPO cavity was blocked, was lower than expected. No signs of TPA are seen in Fig. 21a.

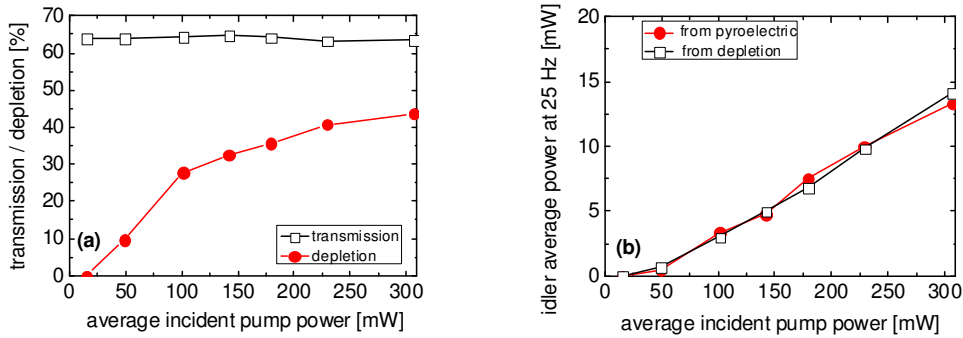


Figure 21: Pump depletion and crystal transmission at 1064 nm vs. pump power (a) and idler power vs. pump power (b).

Figure 21b shows the input-output characteristics. The directly measured idler power was in good agreement with estimations from the pump depletion. The maximum idler power of 14 mW corresponds to a single (micro)pulse energy of 2.8 μJ . Only normal incidence was studied but the slightly non-collinear interaction resulted in ~ 200 nm longer idler wavelengths. From the measured signal wavelength of 1276.55 nm, one arrives at an idler wavelength of 6397.5 nm, this was confirmed by calculations which predicted the same idler wavelength for an internal angle of 0.67° between the signal and the pump waves.

The signal spectrum was measured from a cavity leakage at a pump level of 200 mW, with 0.4 nm spectral resolution, Fig. 22a. Its bandwidth corresponds to 8 cm^{-1} or 240 GHz. The duration of the idler pulses was measured using non-collinear SHG in a 2-mm-thick type-I HGS crystal cut at $\varphi=45^\circ$, $\theta=40^\circ$. A ZnSe plate served as a beam splitter and second harmonic was detected by a PbS resistor. Figure 22b shows the result of averaging 4 traces. The Lorentzian fit gives a FWHM ~ 25 ps for the trace, which means a micropulse FWHM of 12.6 ps.

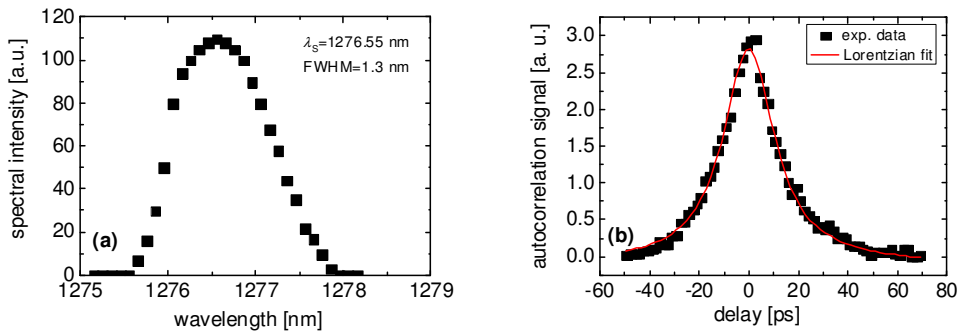


Figure 22: Signal spectrum (a) and idler autocorrelation (b) with experimental data (symbols) and Lorentzian fit (curve).

Finally, by using a hair dryer, slight heating of the crystal produced shorter (by ~ 2 nm) signal wavelength which translates into an idler wavelength in the targeted 6450 nm range - first indication of the possibility for practical tuning by temperature variation in the non-critical configuration.

When CSP was replaced by type-I AGS ($10 \times 10 \times 10\text{ mm}^3$), under the same experimental conditions, the parametric oscillation threshold increased to ~ 100 mW, i.e. about an order of magnitude. Moreover, the use of AGS was accompanied by gradual surface blackening. In this geometry, surface lifetime could be kept above ~ 400 h if only the pump average power did not exceed ~ 200 mW.

Power scaling and comparison with other crystals: While initially the CSP SPOPO was pumped up to ~ 300 mW, generating up to 14 mW at $\sim 6.4\ \mu\text{m}$ (corresponds to a micropulse energy of 2.8 μJ or a

macro-pulse energy of 0.56 mJ), subsequent work was aimed at scaling up the output power in order to utilize the much higher pump power available from the upgraded laser system. In addition, it was possible to compare the conversion efficiency of the SPOPO using 3 nonlinear crystals that enable phase-matching with the pump laser at 1064 nm without TPA: the CSP sample, AGS cut for type-II at $\theta=45^\circ$ and $\varphi=0^\circ$ ($10\times10\times10\text{ mm}^3$), and AGS cut for type-I phase-matching cut at $\theta=42^\circ$ and $\varphi=45^\circ$ ($10\times10\times10\text{ mm}^3$), both of them also AR-coated. As mentioned before this initial sample of CSP exhibited relatively high residual losses while for AGS these losses were negligible.

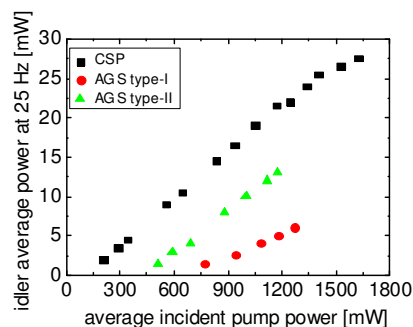


Figure 23: Average idler power of the SPOPO at 6.4 μm obtained with crystals of AGS type-I, AGS type-II, and CSP.

The conversion efficiency measurements for the idler at 6.4 μm are directly compared in Fig. 23. The maximum possible pump power incident on the SPOPO using the AGS crystals was limited by crystal damage to about 1.3 W at 1064 nm. The superiority of CSP is clearly seen both with respect to damage threshold, since the SPOPO could be pumped at least up to 1.8 W, and with respect to conversion efficiency and oscillation threshold. AGS type-II performs better than AGS type-I due to the higher effective nonlinearity. Pumping CSP with up to 2.5 W at 1064 nm, the SPOPO generated up to 35 mW at 6.4 μm (~2.5 times higher than in the initial experiment) resulting in macro-pulse energy of 1.4 mJ. Extrapolating the best conversion efficiency with the optimum performance of the pump laser means that this CSP SPOPO will be capable of generating an average power of about 100 mW at 6.4 μm (>4 mJ macro-pulse energy) with a better quality CSP sample.

The ultimate goal concerning macro-pulse SPOPO generation of 6.45 μm wavelength was to employ the developed within the project unique ps diode-pumped MOPA laser system at 1064 nm. In pursuing this objective, two parallel strategies were exploited, based on cascaded and direct schemes. Before the pump source became available, the early efforts were directed towards cw OPOs to establish some of the important operating benchmarks then extended to quasi-cw ps SPOPOs. The efforts finally culminated in the realization of an all-solid-state ps SPOPO providing >1.2 mJ of macro-pulse energy at 6.4 μm , in TEM_{00} spatial beam profile and with suitable time structure for MIS.

In the initial phase of the project, focused on cascaded two-step pumping, a compact, stable, high-power 1st-stage cw OPO for the near- and mid-IR based on MgO:PPLN pumped by a Yb-fiber laser at 1064 nm was developed, see Fig. 24a. Using a 50 mm long crystal and a signal output coupling scheme, 17.5 W of total power was generated for 28.6 W of pump at 61% extraction efficiency. The cw OPO generated 9.8 W of near-IR signal over 1594–1714 nm, simultaneously with 7.7 W of mid-IR idler over 3196–2803 nm, resulting in a total tuning of 513 nm, limited by the reflectivity of the OPO mirrors. Through careful control of thermal effects, a long-term peak-to-peak idler power stability of 5% was achieved over 14 h near room temperature, as shown in Fig. 24b, with both output beams exhibiting TEM_{00} spatial profile with $M^2 < 1.28$ for the idler and $M^2 < 1.37$ for the signal.

Following the successful development of the 1st-stage cw OPO, a high-power ps SPOPO based on the same MgO:PPLN crystal was realized, pumped by a compact, mode-locked Yb-fiber laser at 1064 nm, see Fig. 25a. The SPOPO delivered up to 7.4 W of near-IR signal and 4.9 W of mid-IR

idler, resulting in a maximum total average power of 12.3 W for 16 W of pump. Signal tuning across 1.43-1.63 μm and idler tuning over 4.16-3.06 μm was obtained, with a total power of ~ 11 W over most of the tuning range. Both signal and idler beams had TEM_{00} spatial profile with peak-to-peak power stability of 1.8% and 2.9% over 1 hour at the highest power, as shown Fig. 25b.

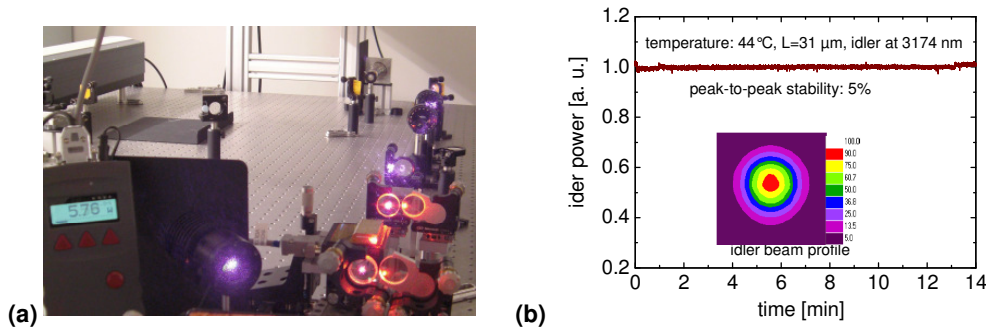


Figure 24: Photograph of high-power, 1st-stage cw OPO for the near- to mid-IR (a), and long-term power stability and far-field spatial profile of the idler beam (b).

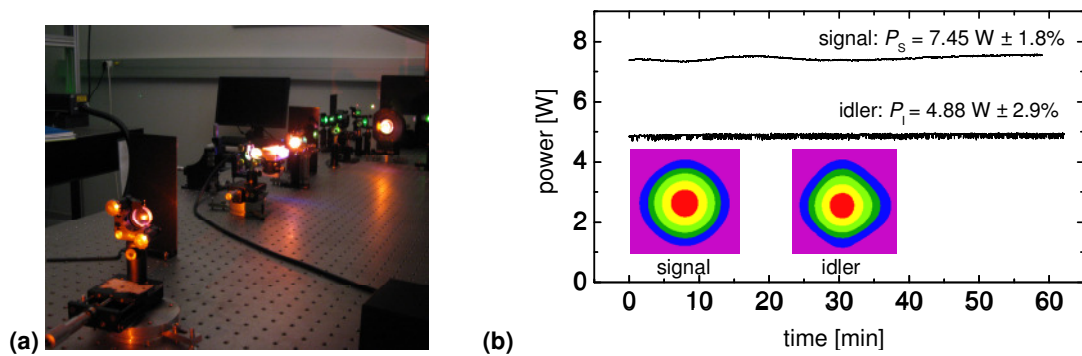


Figure 25: Photograph of the picosecond SPOPO pumped by a mode-locked Yb fiber laser at 1064 nm (a), and signal and idler stability over time and corresponding spatial beam profiles at maximum power.

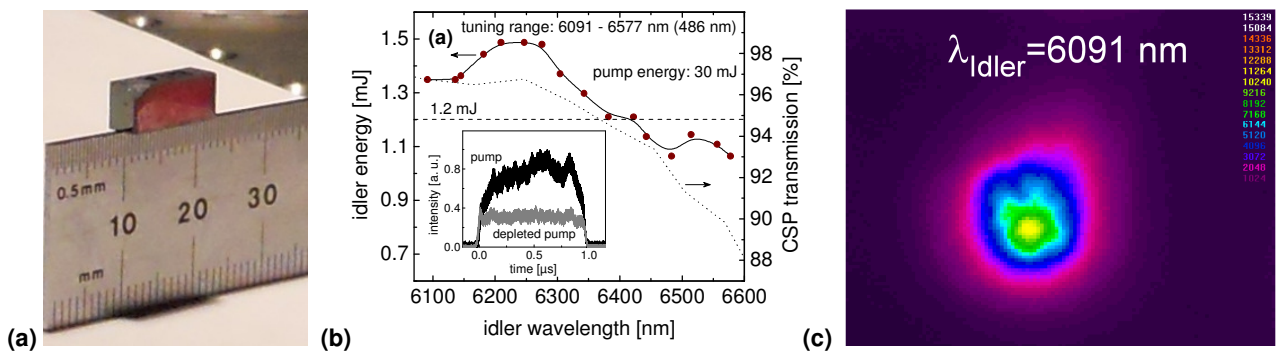


Figure 26: The 12.1-mm long CSP crystal (a), idler energy and CSP transmission across the tuning range (inset: macro-pulse envelope of the input pump and the depleted pump) (b), and idler spatial beam quality at 6091 nm (c), showing TEM_{00} mode profile.

Finally, using the table-top MOPA all-solid-state system with macro-pulse format developed within the project, a single-stage ps SPOPO for the mid-IR target wavelength of 6.4 μm was realized. With the 1064 nm pump source delivering up to 50 mJ of energy in 1- μs -long macro-pulses, with each macro-pulse containing 10 ps micropulses at 450 MHz, and deploying a compact (~ 30 cm) SPOPO cavity with a 12.1-mm-long sample of the new nonlinear material CSP, Fig. 26a, a macro-pulse energy >1.2 mJ at 6.4 μm was achieved for 30 mJ of input pump pulse energy, Fig. 26b, with tuning coverage of the 6-6.6 μm spectral range, in high beam quality with TEM_{00} spatial profile, Fig. 26c.

Few wide band-gap nonlinear crystals were employed in ns OPOs for direct frequency conversion from 1064 nm to the targeted 6.45 μm wavelength range. Using LISe idler tunability up to 8.7 μm was achieved at a repetition rate of 100 Hz. Under non-critical phase-matching CSP produced idler pulses near 6.2 μm with an energy as high as 0.47 mJ. Without a cavity, a 21.4-mm-long CSP, pumped by 8-ns pulses at 1064 nm in a double-pass configuration generated 0.523 mJ, 5.8-ns idler pulses at 6.125 μm . The average power of 52.3 mW at the repetition rate of 100 Hz is the highest ever achieved at such wavelengths with direct down-conversion from the 1- μm spectral range. A BGS OPO also produced pulse energies of 0.5 mJ in the 6- μm range with average power \sim 50 mW.

LISe OPO: The initial work on single stage OPO pumped at 1064 nm focused on the extension of the LISe tuning range to the mid-IR in order to cover the 6.45 μm spectral range, because experience with this material already existed at shorter wavelengths (limited tunability of 3.3-3.78 μm for the idler and average idler power $<$ 2.5 mW). Moreover, an important task was to scale up the average power by increasing the repetition rate to 100 Hz. The compact OPO cavity used is shown in Fig. 27. It consisted of two plane mirrors with a separation between 18.5 and 27.5 mm, depending on the LISe crystal used. The rear total reflector, TR, was an Ag-mirror. In the tuning ranges studied, the output coupler, OC, had a transmission of 18-22% at the signal and \sim 73-84% at the idler wavelength, hence, the OPO can be considered as singly resonant with double pass pumping. However, the signal was not totally reflected by the output coupler to avoid extreme intracavity fluence that could damage the crystals. The LISe crystals were pumped through the output mirror which had a transmission of 82% at 1064 nm. The beams were separated by the pump bending mirror, BM, which was HR for the pump and transmitted \sim 67% at the idler wavelength.

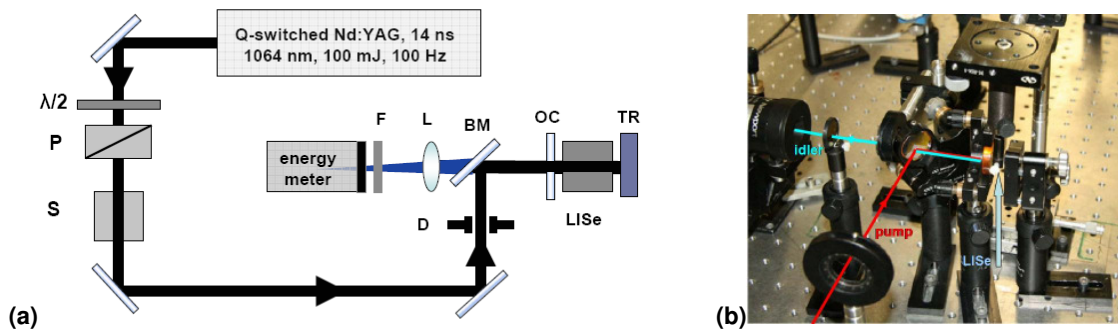


Figure 27: LISe OPO set-up (a). $\lambda/2$: half-wave plate, P: polarizer, S: mechanical shutter, F: 2.5 μm cut-on filter, L: 10 cm lens, D: diaphragm, BM: bending mirror, OC: output coupler, TR: total reflector. Photograph of the compact OPO (b).

The commercial pump laser generated 100 mJ, 14 ns pulses with an average power of 10 W. The energy stability was \pm 1%. A mechanical shutter (S) was employed to vary the repetition rate. A combination of a half-wave plate and a polarizer served to adjust the pump energy. The pump laser was protected by a Faraday isolator and the separation to the OPO was large enough to avoid feedback during the Q-switching process. The pump beam had a Gaussian waist radius of 1.9 mm in the position of the OPO. The output of the OPO, behind the bending mirror, BM, was detected by a calibrated pyroelectric energy meter positioned in front of the focus of a 10-cm MgF_2 lens, L. Only the idler was measured, the residual pump and the signal were blocked by a 2.5 μm cut-on filter, F.

Type-II e-oe phase-matching in the x - y plane was utilized. One LISe sample (A) was cut at $\phi=41.6^\circ$ for idler wavelength \sim 6.5 μm at normal incidence. It had an aperture of 5 mm (along z -axis) \times 6.5 mm and a length of 17.6 mm. This sample was AR-coated for pump and signal with a single layer of YF_3 . The losses (including scatter) were 0.16 cm^{-1} at 1064 nm and 0.07 cm^{-1} at 1600 nm. The second sample (B) was cut at $\phi=34^\circ$ for idler wavelength \sim 8.8 μm at normal incidence. It had an aperture of 5 mm (along z -axis) \times 7 mm and a length of 24.5 mm. This sample was AR-coated with the same single layer of YF_3 and exhibited similar loss coefficients.

The thresholds measured for minimum cavity length of 18.5 mm (sample A) and 25.5 mm (sample B) amounted to 6.8 and 7.9 mJ of incident energy, respectively. These values correspond to average fluence of 0.06 and 0.07 J/cm² or pump intensity of 4.3 and 5 MW/cm². Two times above the threshold the dependence of the output energy on the repetition rate was measured in the range 10-100 Hz. Fluctuations were within the experimental error and further measurements were performed at 100 Hz without the shutter, see Fig. 28a. Maximum energies of 282 μ J at 6.514 μ m and 116 μ J at 8.428 μ m were measured. These values correspond to external quantum conversion efficiencies of 10.3% and 4.3%, respectively. The maximum average power at 100 Hz reached 28 mW.

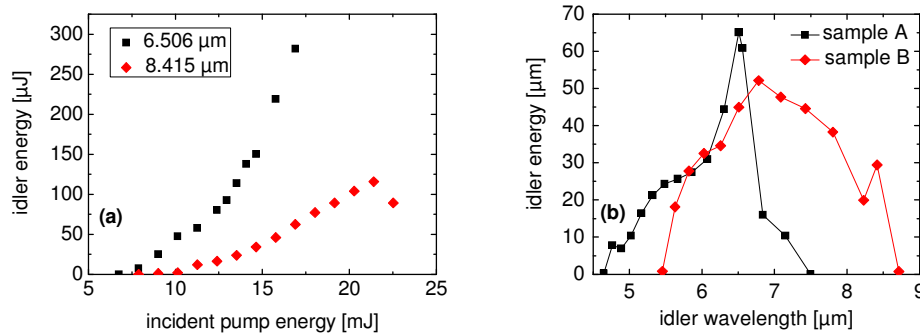


Figure 28: Output idler energy at normal incidence with LISe sample A (black squares) and sample B (red diamonds) vs. pump energy at 1064 nm (a). Last point for B denotes surface damage. OPO idler tuning at fixed pump energy (b).

The OPO linewidth measured at the signal wavelength of 1272 nm was \sim 58 GHz (\sim 1.9 cm⁻¹). The pulse-to-pulse stability for the idler pulses measured at maximum output level was \pm 5%. The pulse duration at the same signal wavelength measured with a fast (0.7 ns) InGaAs photodiode was 7 ns. The tuning curves (Fig. 28b) were recorded by lengthening the cavity to 20.5 mm (sample A) and 27.5 mm (sample B) and tilting the crystals in the critical plane. The pump energy was 11.8 mJ for sample A and 16.9 mJ for sample B. The upper limit of the tunability is determined by the LISe absorption which sets in from about 8 μ m. The point which deviates from the smooth dependence for sample B is near 8.428 μ m, corresponding to normal incidence, which can be explained by some enhancement of the feedback by the partial reflection of the crystal faces.

CSP OPO: This OPO active element (similar to the one used in the first SPOPO experiments) was cut at $\theta=90^\circ$, $\phi=45^\circ$ and had a length of 8 mm. Its aperture was 6 mm (along the *c*-axis) \times 6.75 mm. The residual losses measured for the relevant polarizations were 0.198 cm⁻¹ at 1064 nm, 0.114 cm⁻¹ near 1.3 μ m, and 0.014 cm⁻¹ near 6.2 μ m. Both faces were AR-coated for pump, signal, and idler with an 8-layer coating. The pump source was the same and the OPO cavity was similar to the one described previously about LISe, see Fig. 27, with a mirror separation of 9.5 mm. Only normal incidence was studied. In this non-critical scheme, the measured signal wavelength was 1.285 μ m, corresponding to an idler at 6.193 μ m.

The maximum idler energy measured at 10 Hz repetition rate was 0.47 mJ, at an incident pump energy of 21.4 mJ. This gives a conversion efficiency of 2.2% for the idler alone or a quantum conversion efficiency of \sim 12.8%. Only slightly lower output energies were observed at 20 Hz which can be attributed to the residual crystal absorption at the pump wavelength. The maximum average output power (idler only), reached in this case, was 9.1 mW. The measurements in Fig. 29a extend to an upper limit, where surface damage to the AR-coating of the input face was observed. Nevertheless, the output energy level achieved with this very first sample of CSP already exceeded the best result previously reported at such long wavelengths with \sim 1 μ m pumped OPOs, namely 372 μ J at 6 μ m using AGS. Moreover, the input/output characteristics in Fig. 29a show no saturation, in contrast to the AGS performance, which means that power scaling can be expected even without increasing the pump beam diameter.

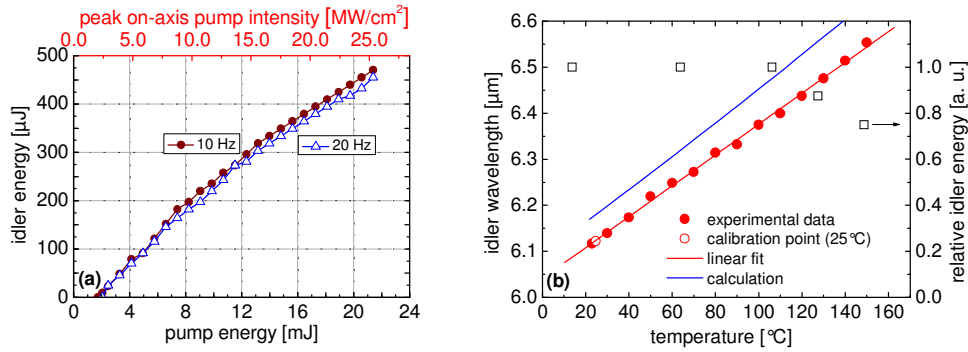


Figure 29: Idler output energy vs. incident pump energy on the OPO crystal for two repetition rates (a) and temperature tuning in the non-critical type-I configuration of CSP (b).

The OPO linewidth, measured at the signal wavelength, was ~ 52 GHz (~ 1.7 cm^{-1}). The duration of the signal pulse was 10 ns. The pulse-to-pulse stability for the idler pulses at 350 μJ output was $\pm 5\%$.

Using an analogous sample of CSP, 9.5 mm in length, and a very similar 11 mm long cavity it was possible to extend the above results to sub-ns idler pulse durations using a special 1 ns pump source at 1064 nm. Without going into details, since this OPO operated at 1 kHz, an essential result from this experiment was the temperature tuning achieved from room temperature to 150 $^{\circ}\text{C}$, see Fig. 29b. Tuning from 6.117 to 6.554 μm was obtained for the idler. Thus CSP possesses nice tuning capability under non-critical conditions which allows one to utilize its transparency up to the intrinsic limit set by multiphonon absorption. The deviations from calculations in Fig. 29b amount to 60...100 nm for the idler and in terms of temperature they are of the order of 20 K. However, at the signal wavelength, the discrepancy between experiment and calculation is only 3...3.5 nm. The output idler energy is almost constant, slightly decreasing above 6.4 μm , partially due to the idler absorption, to 75% of its maximum value, towards the longest idler wavelength, see Fig. 29b.

These results present first OPO demonstrations with CSP pumped at 1064 nm. As with the SPOPOs, future progress will depend essentially on the availability of samples with reduced residual loss and improved surface damage resistivity. New cavity designs for better extraction of the idler energy, and power scaling using crystals of larger aperture will be essential. Unfortunately experiments with a Rotated Image Singly-Resonant Twisted RectAngle (RISTRA) cavity (as used in 2- μm pumped OPOs described in the following, resulted in marginal improvement of the CSP OPO idler beam quality with only $\sim 50\%$ enhancement in the maximum achievable intensity compared to the linear cavity. Since the RISTRA concept has previously been proven to be useful under similar conditions with type-I interaction, the absence of angle birefringence in non-critical 90° phase-matching is considered to be the main reason for the marginal spatial quality improvement observed with CSP.

CSP OPG: Efficient parametric frequency down-conversion at low (such as 100 Hz) repetition rates relies normally on ns OPOs employing a resonant cavity but can be also achieved with optical parametric generators (OPGs) employing a single-pass traveling-wave scheme. Such OPGs could only reach threshold with the high peak power available from ultrafast (fs or ps, up to ~ 1 ns) amplified pump sources but ultrashort pulses would not be useful for the envisaged MIS application because at the targeted energies higher order nonlinear effects will occur. However, it can be expected that, for pulse durations between 1 and 10 ns, high-gain nonlinear materials can work also in OPG configurations. The advantage of OPGs is that seeding is much easier to apply for narrow-band single-frequency operation.

OPG operation at 100 Hz was realized using a CSP crystal of 21.4 mm length with an aperture of 4.1 (along c -axis) \times 6.1 mm^2 and cut for non-critical (90°) type-I (oo-e) interaction. Both faces were AR-coated with a single layer of Al_2O_3 for the pump and signal wavelengths. The pump beam from

the upgraded diode-pumped Q-switched Nd:YAG laser / amplifier system delivering up to 250 mJ pulses of 8-ns duration at 100 Hz, after spatial filtering and attenuation by a system of wave plate and polarizer, was expanded to a slightly elliptical shape with approximately Gaussian spatial distribution and diameter of ~ 10.4 and ~ 12.1 mm in the horizontal and vertical (along the crystal c -axis) directions, respectively. A nearly flat-top spatial profile was then obtained by a circular aperture which reduced the beam diameter to ~ 3.8 mm, matching the limited crystal aperture. The CSP crystal was pumped in double-pass using a 45° ZnSe bending mirror for the pump radiation which was highly transmitting (HT) at both, signal and idler wavelengths, and a Ag total reflector for a second pass, see Fig. 30a. All separations were kept as short as possible to avoid air absorption of the idler.

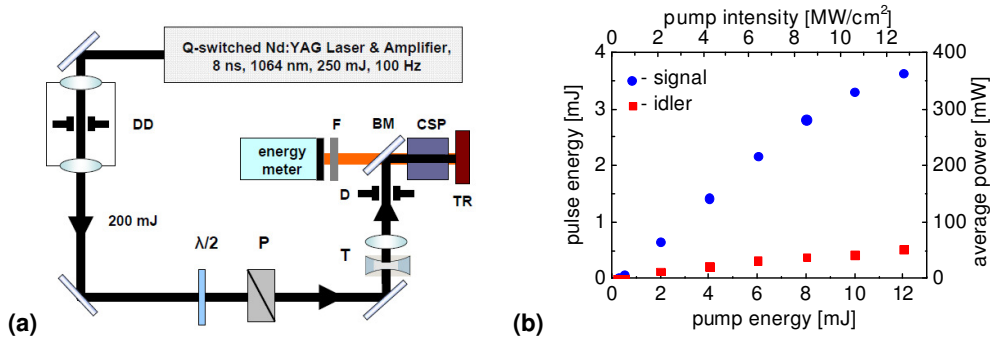


Figure 30: CSP OPG set-up (a). T: telescope, D: diaphragm, BM: bending mirror, TR: total reflector, F: exchangeable filters, P: polarizer, $\lambda/2$: half-wave plate, DD: diamond diaphragm for spatial profile cleaning. Signal (1288 nm) and idler ($6.125 \mu\text{m}$) output energy, and average power at 100 Hz versus incident pump energy at 1064 nm (b).

The OPG threshold was found at 213 μJ of incident pump energy ($\sim 0.23 \text{ MW/cm}^2$ peak on-axis intensity), see Fig. 30b. At the maximum applied pump energy of 12 mJ (12.7 MW/cm^2), the total output energy exceeded 4 mJ, from which ~ 3.64 mJ were at 1288 nm (signal) and ~ 0.52 mJ at $6.125 \mu\text{m}$ (idler). The fluctuations were $\pm 5\%$, measured for the idler. There was some trend of saturation of the idler energy – the ratio of the signal to idler energy increases with the pump level reaching ~ 7 at maximum level, while the theoretical value (without taking into account the different reflection of the crystal AR-coatings) should be ~ 4.8 . Obviously, residual reflections may contribute to an OPO feedback effect. This was checked by tilting the crystal in order to facilitate non-collinear interaction and the conclusion was that the surface reflections formed a low-finesse cavity for the idler. This could be expected since the AR-coating was not optimized for the idler wavelength. Thus, the present experiment corresponds more or less to quasi-OPG or weakly-resonant OPO operation.

As expected the signal and idler had shorter pulse durations of 4.4 and 5.8 ns, respectively, than the pump. Estimating the beam diameter with the knife-edge method gave M^2 values of 7.1 and 7.8 for the idler output beam in the horizontal and vertical directions, respectively.

Taking into account the maximum signal pulse energy obtained with the double-pass CSP-based OPG, a quantum conversion efficiency of 34.7% (or $\sim 25\%$ if the idler is considered which experiences some losses) is obtained. Before the onset of saturation, e.g. at a pump power of 6 mJ, these efficiencies amount to 41.4% and $\sim 31\%$, respectively. All these values are much higher than the CSP OPO quantum conversion efficiency reported above. Moreover, maximum pump pulse peak intensity was about two times higher in the OPO and so the risk of damage while the M^2 factor was inferior. Therefore, it can be concluded that the OPG concept is feasible in the temporal regime between 1 and 10 ns for achieving higher output energies and average powers with CSP. Only normal incidence was studied in the OPG configuration but as demonstrated above temperature tuning to $6.45 \mu\text{m}$ should not have a serious effect on the output energy level.

BGS OPO: Single stage OPO operation in the mid-IR was achieved also with BGS pumped at 1064 nm. The 14.05-mm long active element had an aperture of 9.8×9.5 mm². It was cut at $\theta=12^\circ$, $\phi=0^\circ$ for oo-e type-I phase-matching with the 9.8-mm edge parallel to the y-axis (vertical in the present case). Single layer Al₂O₃ AR-coating was applied for pump and signal and residual absorption did not exceed 0.01 cm⁻¹ at all three wavelengths. This OPO was pumped by the same upgraded 8-ns, 1064 nm pump source described before, delivering up to 250 mJ per pulse at 100 Hz and the OPO cavity was similar to the one used for LISe and CSP. A telescope was used to expand the pump diameter to ~5.5 and ~8.8 mm in the horizontal and vertical directions, respectively.

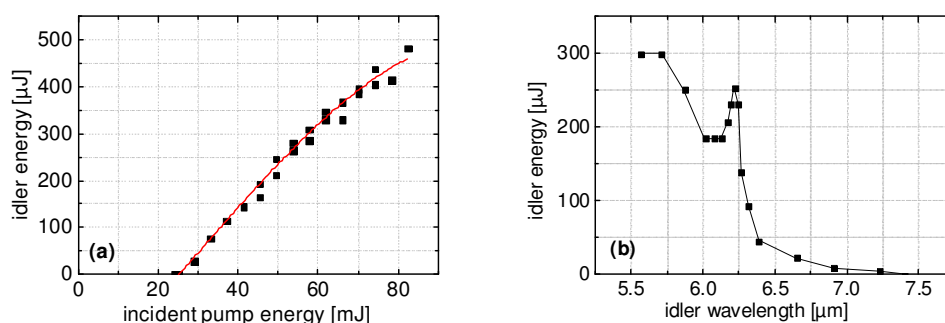


Figure 31: Input-output characteristics of the BGS OPO at normal incidence for a cavity length of 17 mm (a) and idler tuning characteristics for a cavity length of 20 mm recorded at an incident pump energy of 58 mJ at 1064 nm (b).

Figure 31a shows the input-output characteristics obtained at normal incidence for a minimum cavity length. The threshold of 25 mJ corresponds to an axial fluence of 0.134 J/cm² or a peak intensity of 16.7 MW/cm². The slope efficiency with respect to the idler output is ~1% in the initial stage but some saturation can be seen at higher powers. Nevertheless, an average idler power of ~50 mW was obtained at 100 Hz. The idler wavelength was 6.217 μm, in excellent agreement with calculations. The M² factor measured for the idler amounted to ~10. The OPO linewidth, measured at the signal wavelength was ~60 GHz (~2 cm⁻¹). In this experiment the limit was set at ~3 times the OPO threshold by damage of the Ag total reflector which occurred at >50 MW/cm² peak pump intensity.

Tuning was studied by tilting the crystal at slightly lengthened cavity (Fig. 31b). The idler wavelength range extended from 5.6 (non-critical interaction, $\theta=0^\circ$) to 7.3 μm with a pronounced enhancement at normal incidence due to the idler reflection by the crystal surfaces.

The obtained results prove that chalcogenide nonlinear crystals with relatively low nonlinearity but wide band-gap and high damage resistivity are also very attractive for OPOs pumped at 1064 nm for frequency conversion to the mid-IR above ~5 μm. In fact, comparing with previous experience with crystals of AGS and LISe, with the present BGS crystal it was possible to reach the highest ratio of pump power above threshold (~3) and the same level of idler pulse energy as with the highly nonlinear (more than 15 times higher nonlinearity) CSP for which the threshold in terms of pump energy was lower by about an order of magnitude. Since there were no thermal problems with BGS and no cumulative damage occurred, there was no problem to pump it also at a repetition rate of 100 Hz, achieving, similar to CSP, average power of ~50 mW in the 6-μm spectral range.

Nanosecond pulse laser radiation at 6.45 μm with higher energy level could be produced starting at 1064 nm with cascaded OPO. To push the state-of-the-art in such systems an all-diode-pumped system operating at the repetition rate of 100 Hz was designed and built taking advantage of a commercial pump laser and large aperture periodically structured nonlinear crystals in the 1st stage converting 1064 nm laser radiation to 2 μm narrowband pulses which, in turn were used to pump non-planar ring cavity ZGP OPO producing tunable output around 6.45 μm.

The first stage of the cascaded OPO system: The schematic layout of the cascaded source is shown in Fig. 32, where the first stage is enclosed in the blue box. The pump laser was a diode-pumped Q-switched single-frequency (seeded with a DFB fiber laser) Nd:YAG delivering 80 mJ, 10 ns - long linearly polarized pulses at 1064 nm with a repetition rate of 100 Hz. The laser output was split by a thin-film polarizer P1 into two channels, one powering the master PPKTP OPO, while the other was used to pump a PPRKTP optical parametric amplifier (OPA). The powers in both pump arms could be adjusted by half-wave plate and thin-film polarizer (P2, P3) arrangements. The splitting ratio was controlled by a half-wave plate in the pump laser assembly.

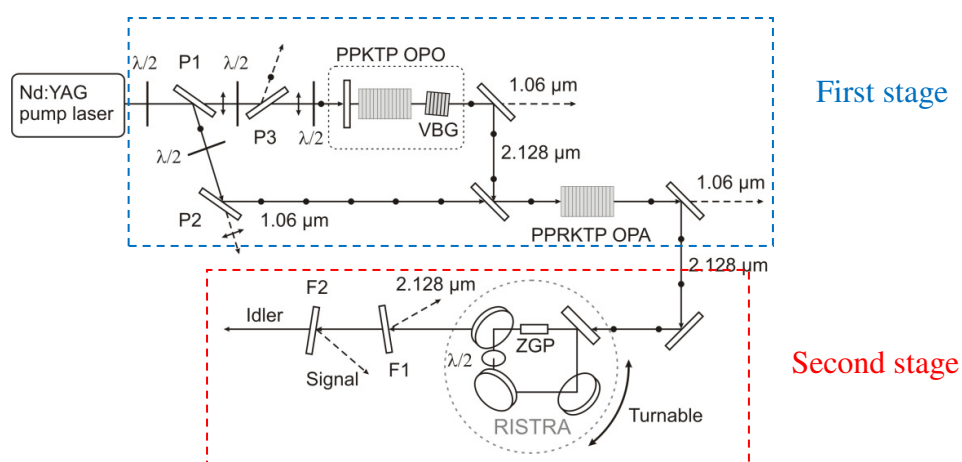


Figure 32: Cascaded optical parametric scheme pumped at 1.064 μm and generating 6.45 μm output.

An optical parametric MOPA configuration was employed for the first stage of the cascade. Such configuration is less efficient than a single-OPO stage, but enables better control over the beam quality and the spectral width of the output. This is especially important for relatively short and high-energy pulses where large Fresnel number OPO cavities have to be used. Due to the fact that the parametric gain bandwidth of degenerate type-I interaction in PPRKTP operating at 2.128 μm is very broad, of the order of 100 nm, the bandwidth narrowing in the first step of the cascade is mandatory. For narrowing the bandwidth at degeneracy, a volume Bragg grating (VBG) with a reflectivity of 50% and FWHM reflectivity bandwidth of 0.5 nm was used as an output coupler in the PPKTP master OPO. The OPO contained 10 mm-long PPKTP with an optical aperture of $3 \times 5 \text{ mm}^2$ and with a ferroelectric domain period of 38.86 μm and it was pumped through a plane-plane incoupling mirror which was HR at 2.128 μm while HT at the pump wavelength.

The PPKTP OPO pump power was determined by two, generally opposing, requirements, i.e., the requirement of high enough output energy in order to efficiently extract the pump energy in the OPA stage, which means running the OPA in saturation regime and, at the same time, limiting the master OPO pump level in order to maintain good beam quality. The beam quality can deteriorate quite drastically in a linear OPO cavity with large Fresnel number when the OPO is driven more than two-times above the oscillation threshold. For power amplification at 2.128 μm a single-pass OPA was employed, containing a 16 mm-long PPRKTP crystal with the same domain period as the one in the OPO but with the optical aperture of $5 \times 5 \text{ mm}^2$ in order to accommodate the pump beam with a diameter of about 3 mm. Both crystals in the OPO and in the OPA as well as the VBG were AR-coated for the pump and the parametric waves. The beam sizes of the OPA pump and the seed were matched using a telescope in the OPA pump arm. Both structured crystals used in the first stage were developed within the material research part of the project and represent current state-of-the-art in the periodic poling of KTP isomorphs. For seeding the OPA stage, 3.6 mJ pulse energy from the OPO was used, with the pulse length of about 8 ns. At the maximum available pump energy of 60 mJ the

OPA generated 26 mJ giving the amplification factor of 7.2 and the energy extraction efficiency of 43%. The output energy dependence on the pump pulse energy for the 2 μm MOPA is shown in Fig. 33. This energy extraction efficiency is very high indeed for a ns OPA, and is possible owing to high effective nonlinearity of the periodically structured crystals.

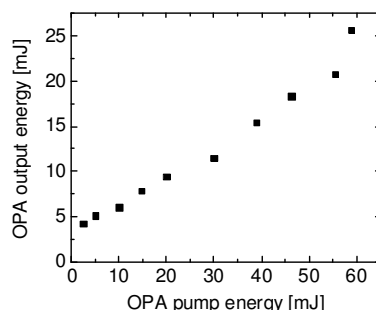


Figure 33: Output energy of the 2.128 μm MOPA versus pump energy.

The second stage of the cascaded OPO system: The output of the 2.128 μm MOPA was used for pumping the second frequency conversion stage which employed type-I ZGP nonlinear crystal cut at 52.5° for generation of 6.45 μm idler. Assuming that the output beams should have sufficient quality for efficient coupling into mid-IR delivery fibers inevitably places requirement of compensation of astigmatism and asymmetry in beam propagation factors arising from critical phase-matching.

A very promising technique to enhance the beam quality in the parametric process is based on the fact that the generated beam quality in critically phase-matched nonlinear interactions is much better in the direction of the Poynting vector walk-off than in the orthogonal direction. This fact was exploited in the so-called RISTRA compact ring cavity arrangement where the image is rotated 90° either with a dove-prism or a 3-dimensional mirror arrangement, while the polarization of the resonant signal is restored by an intracavity half-wave plate. Such an arrangement eliminates beam astigmatism, increases the beam quality and enables more efficient utilization of the nonlinear gain volume, determined by a circularly symmetric pump beam. This, in fact, reduces the RISTRA OPO threshold as compared to a linear cavity. Owing to these important advantages a tunable RISTRA ZGP OPO cavity was designed and built for the second step of the cascaded parametric source – the same construction used in the single stage OPO pumped at $\sim 2 \mu\text{m}$, which will be described later.

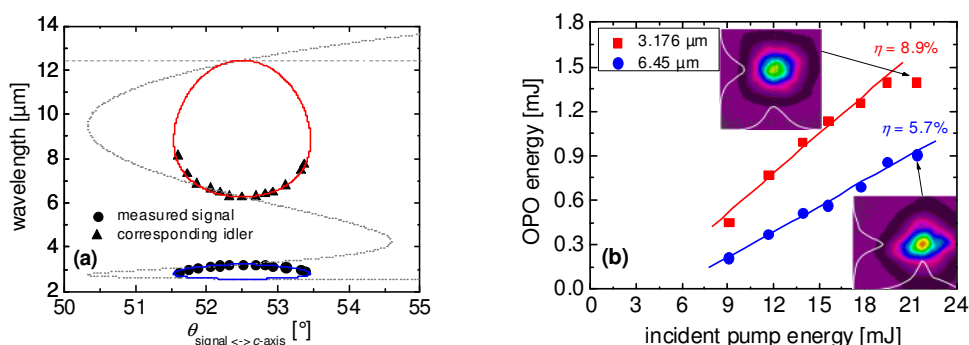


Figure 34: Signal and idler angle-tuning characteristics of the RISTRA ZGP OPO (a). Dotted line: collinear type-I phase-matching; data symbols: measured signal and idler wavelengths as function of RISTRA cavity rotation angle; solid lines: calculated non-collinear phase-matching; dashed line: ZGP upper wavelength transmission limit. Signal and idler energies for non-collinear RISTRA ZGP OPO (b). Insets: signal and idler spatial intensity profiles.

The RISTRA design enabled output wavelength tuning by simply rotating the cavity without any additional adjustments. For $\pm 1^\circ$ -rotation from the collinear position the idler tuned between 6.27 and

8.12 μm with the corresponding signal tuning between 3.22 and 2.88 μm as shown in Fig. 34a. The measured signal (3.176 μm) and idler (6.45 μm) output energies as a function of the 2.128 μm pump energy after the RISTRA incoupling mirror are shown in Fig. 34b. The maximum idler energy here was 0.91 mJ while the signal reached 1.4 mJ at the pump energy of 21.3 mJ. The insets in Fig. 34b show the RISTRA signal and idler beam intensity profiles measured at maximum pump energy at a distance of ~ 47 cm from the ZGP crystal. In both, the collinear and non-collinear phase-matching the beam profiles are smooth and largely symmetric. The RISTRA cavity and the idler beam path were in ambient air. The ZGP RISTRA OPO generated 5 ns-long output pulses, corresponding to the idler peak power of 193 kW and the signal peak power of 230 kW.

Tm- and Ho-lasers were used to pump ns OPOs near 2 μm to reach the target wavelength of 6.45 μm in a single frequency conversion step. With an OP-GaAs sample fabricated within the project and a linear OPO cavity, output power (pulse energy) of 8.4 mW (84 μJ) were obtained for the signal and idler (at 6.69 μm), at incident pump power of 68 mW (680 μJ). The RISTRA type ZGP OPO was pumped by a Ho^{3+} :LLF MOPA system, achieving up to 5.67 mJ at 6.45 μm at a repetition rate of 100 Hz with a beam quality of $M^2 < 2$, at an incident pump energy of 44 mJ and a pulse width of 38 ns. In the latest measurements, with shorter pump pulses of ~ 30 ns, a pulse energy of 6.4 mJ was obtained at 6.45 μm and 100 Hz. At 200 Hz, the average output power at 6.45 μm reached 1.09 W.

Tm^{3+} :YAG laser pumped OP-GaAs OPO: The first OPO experiments with an OP-GaAs crystal, manufactured within the material research part of the project showed very promising results at a repetition rate of 100 Hz pumping by a Q-switched Tm^{3+} :YAG laser, see Fig. 35. This Tm^{3+} :YAG laser was pumped by two 786 nm, 20 W diodes with a pump focus of 800 μm from two sides, through the end mirror M1 and through a 45°-mirror. The output coupler M2 had a reflectivity of 80% at 2 μm . Using an EOM for Q-switching at 100 Hz pulses of 2 mJ energy and 120 ns duration were obtained. The beam intensity profile of the Tm^{3+} :YAG laser is also shown in Fig. 35. The beam quality factor was measured to be $M^2 < 1.2$. The linewidth was 0.19 nm. The pump energy for the OPO was adjusted by a half-wave plate in front of a polarizer after the laser output coupler M2.

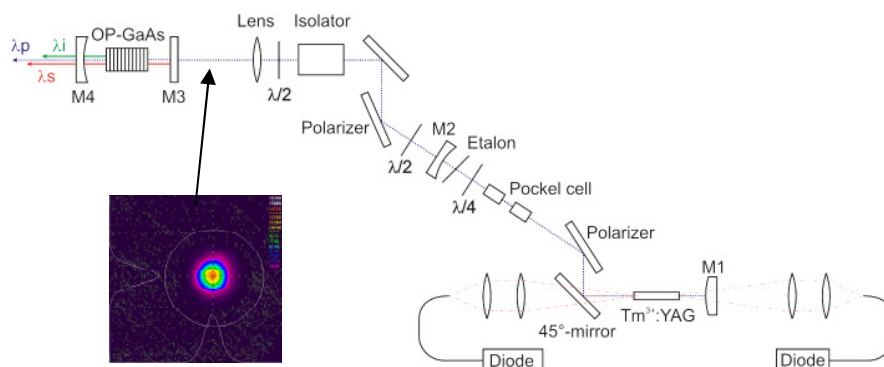


Figure 35: Schematic drawing of the Tm^{3+} :YAG pump set-up with the OP-GaAs OPO.

The AR-coated OP-GaAs crystal was 20 mm long with a thickness of 800 μm and possessed two grating periods (66 and 64.8 μm). After an optical isolator the created focal spot was 300 μm in diameter, well below the damage threshold. The OPO cavity consisted of a plane input coupler M3 which was HR for the signal and HT for the pump. The output coupler M4 was plane-concave and had a reflectivity of 85% for the signal and very low reflectivity for the idler. With the period of 64.8 μm the obtained idler wavelength was 6.69 μm (the signal wavelength was 2.88 μm). The measured OPO pulse energy is displayed in Fig. 36. At 68 mW (680 μJ) of incident pump power a total OPO output of 8.4 mW (84 μJ) was achieved for the signal and idler. The intensity profile of the OPO output at the maximum incident pump power is also shown in Fig. 36.

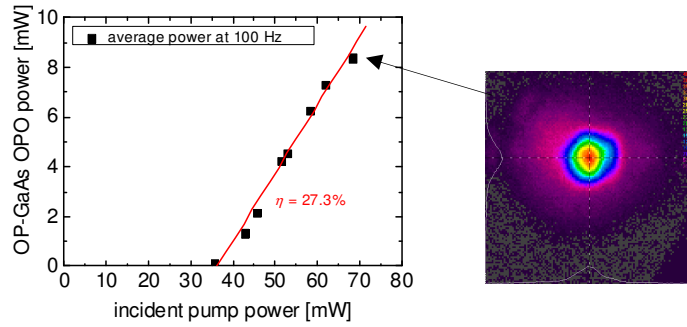


Figure 36: Experimental result with the Tm^{3+} :YAG pumped OP-GaAs OPO.

New OP-GaAs samples with a smaller period and better AR-coating were recently fabricated in which the effective region for high conversion efficiency is also larger but their testing had to be postponed due to instabilities and power fluctuations of the Tm^{3+} :YAG laser, making a new Tm^{3+} :YAG crystal and appropriate coating necessary. Nevertheless, such tests will be performed as soon as possible, and the results will be disseminated after the end of the MIRSURG project.

Ho^{3+} :LLF laser pumped ZGP OPO: A resonantly pumped Ho^{3+} :LLF laser with an additional amplifier stage was used to pump ZGP based OPOs. The Ho-laser was pumped by a Tm-fiber laser at 1938 nm and could deliver over 80 mJ of energy at 100 Hz with a pulse duration of 30 ns in true fundamental mode. An OPO ring cavity of the RISTRA type was designed and fabricated. A ZGP crystal with dimensions of $7 \times 7 \times 16 \text{ mm}^3$ was employed in this OPO. Its AR-coating was optimized for pump, signal and idler, and the absorption coefficient for the pump wavelength was measured to be 0.053 cm^{-1} . A schematic drawing of the set-up is shown in Fig. 37.

The linearly polarized laser emission from the Ho^{3+} :LLF laser can be attenuated by a half-wave plate and a polarizer at constant pulse width. The pump beam diameter measured on the OPO crystal was $\sim 3.8 \text{ mm}$. The residual pump was blocked by a filter mirror, HT for the signal and idler. The second mirror after the OPO reflected the signal radiation and transmitted only the idler.

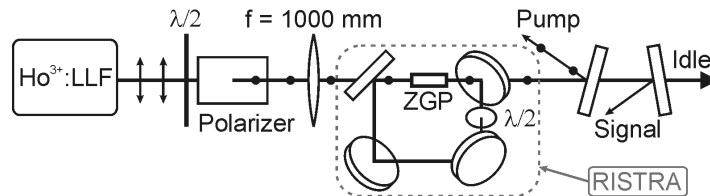


Figure 37: Pump laser and ZGP OPO set-up with filter mirrors to separate signal and idler wavelengths.

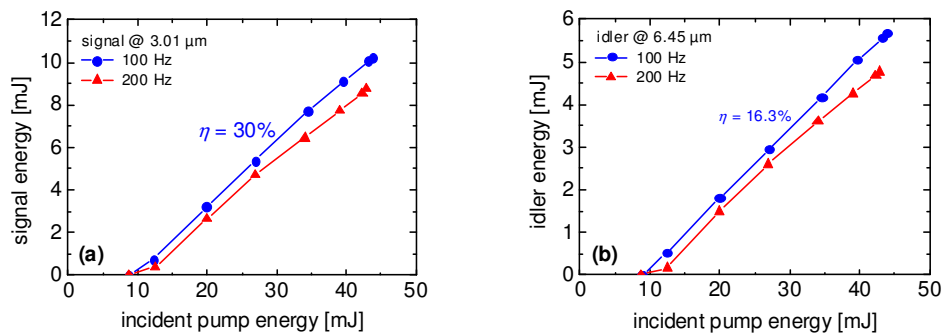


Figure 38: Output energy of the RISTRA type ZGP OPO for signal (a) and idler (b) at 100 Hz and 200 Hz.

The results obtained with the RISTRA type ZGP OPO are shown in Fig. 38 for the signal ($3.01 \mu\text{m}$) and idler ($6.45 \mu\text{m}$) wavelengths at 100 and 200 Hz. The temperature was 28°C and $rH = 40\%$. The

pump pulse duration was 38 ns. At 100 Hz, as much as 5.67 mJ of idler pulse energy were obtained at 6.45 μm and 10.25 mJ at 3.01 μm . The slope efficiency for the signal and idler was 30% and 16.3%, respectively. In this configuration several tissue interaction experiments were performed.

The repetition rate could be easily increased to 200 Hz because the $\text{Ho}^{3+}:\text{LLF}$ pump laser system can deliver quite the same output parameters. These OPO results are also shown in Fig. 38. At maximum pump energy an average idler power of 0.95 W was obtained which gives a pulse energy of 4.76 mJ at 6.45 μm . The curves for 200 Hz show a decreasing slope at higher pump energy. This could be the result of the heat load inside the nonlinear crystal producing a stronger thermal effect (thermal lens).

The spatial quality of the signal and idler beams was measured at maximum output energy and is displayed in Fig. 39. The M^2 values are well below the demands for good fiber coupling.

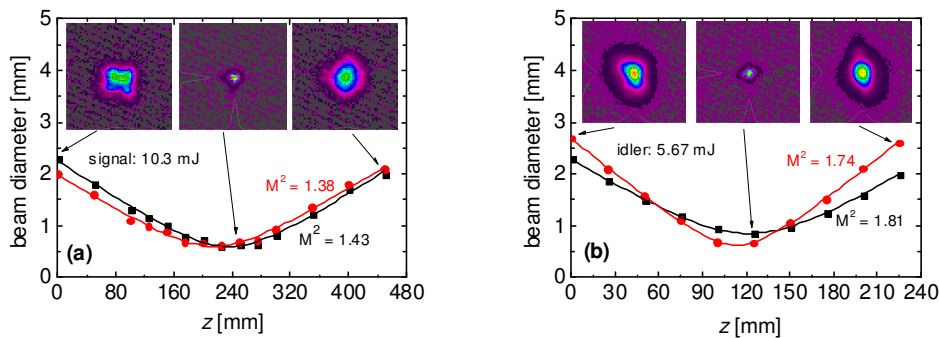


Figure 39: Measured beam diameter after focusing the signal at 3012 nm (a) and the idler at 6448 nm (b). The squares and red lines refer to the data and fits in the horizontal plane and the circles and black lines are for the vertical plane.

Figure 40 shows the measured idler spectrum at 6.45 μm for maximum pump level. The width of the measured spectrum is ~ 250 nm and the dips match very well the dips in the air transmission taken from data base (given here for a path length of 20 cm).

The influence of the humidity around the RISTRA OPO was investigated in Fig. 41. In Fig. 41a, the idler average power was measured with increasing distance and follows an exponential attenuation in air. The exponential fit gives an absorption coefficient of 0.0053 cm^{-1} at 28°C and $\text{rH} = 40\%$ for an idler wavelength of 6.45 μm , which implies a drop 5% in the measured pulse energy for every 10 cm propagation in air. Figure 41b corresponds to an operation point below the maximum where the idler power was measured during flushing the box around the OPO. When the measurement started at $\text{rH} = 50\%$ after opening the valve with dry air the power increased immediately and after ~ 6 minutes of flushing the difference was $\sim 8\%$. When flushing was stopped the power started to decrease going back to the original output value. The power stability in Fig. 41b is influenced by the flushing which creates more turbulences and the output was less stable due to several water absorption lines.

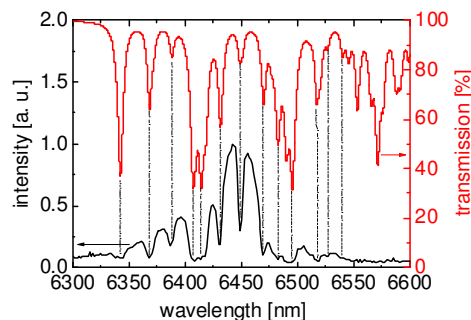


Figure 40: Spectrum of the idler at 28°C and $\text{rH} = 40\%$.

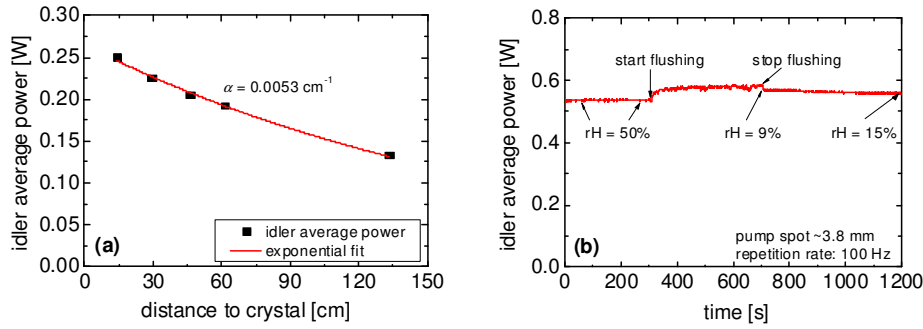


Figure 41: Attenuation of the idler propagating in air (a) and output power behavior during flushing with dry air (b).

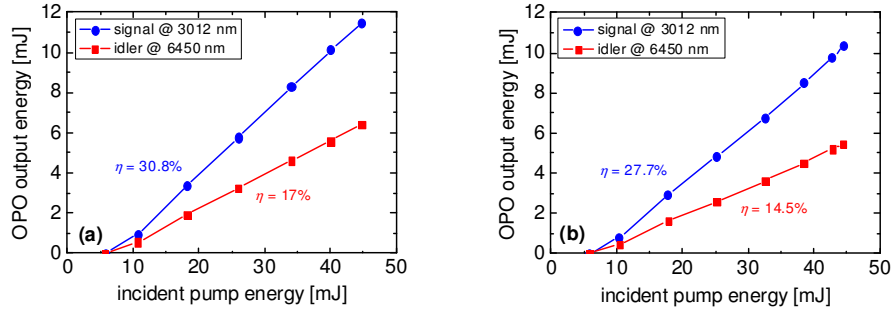


Figure 42: Latest RISTRA ZGP OPO results at 100 Hz (a) and 200 Hz (b). The pump pulse duration was 30 ns (a) and 33 ns (b), and the pump spot diameter was 3.8 mm in both cases. The relative humidity was 33% (a) and 36% (b).

To further increase the output power, in the latest experiments the intracavity half-wave plate was exchanged and the Ho^{3+} :LLF MOPA system was optimized to produce shorter pulse widths of ~ 30 ns. With maximum of 44.8 mJ incident on the ZGP crystal the idler output energy of the RISTRA OPO reached 6.4 mJ at 100 Hz, see Fig. 42a. This measurement was done without flushing the box around the OPO. If one compares with Fig. 38 the difference is a slightly better slope efficiency of 17% for the idler and 30.8% for the signal. The relative humidity was lower in the latest experiment but the main factor was the shorter pump pulse. At 200 Hz and maximum pump energy of 44.5 mJ an idler output energy of 5.45 mJ was obtained which gives an average power of 1.09 W at 6.45 μm , Fig. 42b. No saturation at maximum pump power is seen in the dependence in Fig. 42b.

The verification efforts within the MIRSURG project comprised design of a fiber delivery system to make the developed mid-IR OPO systems suitable for MIS and tissue ablation experiments which were successfully realized using the RISTRA type ZGP OPO pumped by the Ho:LLF laser. Visualization set-ups were made transportable in order to be able to perform “on site” experiments.

Design of an IR delivery system: The system was designed to meet a number of qualifications. It had to be usable at a large range of IR wavelengths, with various gas environments at the fiber entrance to reduce optical breakdown in the focus of the laser beam, and to accept fibers with universal SMA coupling in a reproducible manner. The design and construction are briefly described below.

At first the fiber coupler was designed to be connected with an articulated arm. In this case the Coherent Utrapulse CO_2 laser was used for initial tests. A 120 mm ZnSe lens was incorporated in the coupler to focus the incoming beam into the connected fiber. To be able to adjust the lens in x-y direction for beam alignment, a three point spring blade system was used (Fig. 43, left). In the distal end of the coupler a cylinder was implemented in a metal tube which can move 10 mm in Z direction for fine adjustment of the focal length. The metal cylinder can be easily translated and fixed by turning two rings against a notch that sticks out through an opening at the side. The metal cylinder accepts SMA terminated fibers. The metal tube has a luer-lock on the side to connect to a gas flush,

so the inside of the coupler can be filled with a special gas to reduce optical breakdown due to the high fluence at the focal point especially using ns pulses. Furthermore, it prevents particles formed during tissue ablation to enter and damage the tip of the fiber.

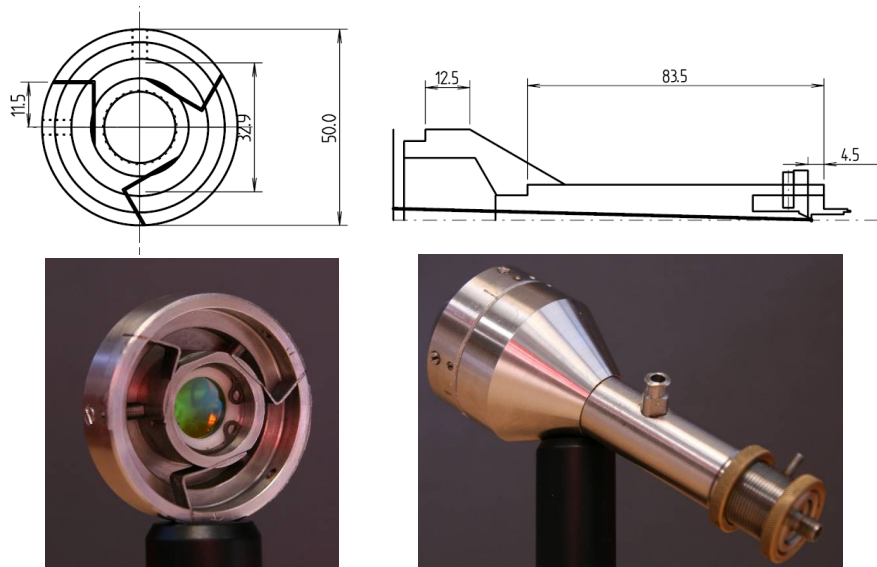


Figure 43: Proximal end of coupler with lens holder (left) and coupler with flush functionality (right).



Figure 44: Open design fiber coupler.

As this system was designed already for end-stage use with gas flush functionality (Fig. 43, right), it proved to be impractical for bench testing. The alignment with laboratory lasers was challenging and difficult to control. A new coupling system was designed from off-the-shelf components which enables easy alignment (Fig. 44). Due to the open structure the beam can be observed throughout the optical system and the entrance of the fiber can be checked for irregularities and indication of degradation or damage. This new design does not have integrated flushing capabilities. This shortage can be overcome by positioning a tube with nozzle to create a gas flow at the proximal end to prevent optical breakdown for both hollow waveguides and solid core fibers, and at the distal end, to prevent particles entering the hollow waveguide.

Infrared fibers: Fibers suitable for the IR range (2-20 μm) stay far behind the characteristics, like transmission and strength, of silica fibers used at shorter wavelengths (0.3 to 2 μm). In general, potential IR fiber materials can be divided in few categories: (i) glasses, such as heavy metal fluoride – HMFG (e.g. ZBLAN), germanate, and chalcogenide, (ii) crystals (polycrystalline, e.g. AgBrCl, or single crystal, e.g. sapphire), and (iii) hollow waveguides. The focus was on fibers capable to transmit 6.45 μm radiation and made of material that can be used in a clinical environment. Based on

literature study, personal contacts with leading scientists in IR fiber development and companies producing IR fiber optics, the following sources for fibers were selected, first for use in a feasibility study and later for the 6.45 μm wavelength (Table 7):

Table 7: IR fibers obtained for the project.

Source	Website	Type	Material	Brand	λ range
Polymicro Technologies	www.polymicro.com	hollow			3, 10 μm
Omniguide	www.omni-guide.com	hollow		Omniguide	10 μm
CeramOptec	www.ceramoptec.com	solid	AgClBr	OptranMIR	4 - 13 μm

All fibers were measured and their transmission losses were calculated. The transmission results of hollow waveguides are more promising in first instance. However, bending losses are substantial and make them less attractive. The transmission through the band-gap hollow-waveguide (HWG) is significantly lower compared to the other fibers and also suffers from bending losses. As they are designed specifically for CO₂ laser applications, the transmission at 6.45 μm is expected to be lower.

Therefore, the silver halide fiber seems most promising for clinical applications, while these fibers have low bending losses and there is no risk of damaging the distal end due to pollution of the open end by particles, which is a substantial risk using hollow waveguides.

Transmission measurements were performed at 6.45 μm with the silver halide fiber and the HWG. The pulse width of the OPO system used was ~ 30 ns and the energy around 4.5 mJ per pulse. This resulted in a transmission of $\sim 50\%$ for both the fiber and the HWG, as shown in Table 8.

Table 8: IR fibers transmission comparison at 10.6 and 6.45 μm .

Fiber type	Wavelength [μm]	Core diameter [μm]	Fiber length [mm]	Transmission [%]
Hollow waveguide <i>Polimicro</i>	10.6	500	1000	73.6
	6.45			50
Silver halide fiber <i>Ceramoptec</i>	10.6	850		69.7
	6.45			48

There was some uncertainty about the damage threshold of the solid core fibers at high peak powers due to the short pulse width. However, after testing the fiber with the pump laser for the OPO (~ 30 ns at 2 μm), it showed that the damage threshold was well above a fluence of 1 J/cm².

Tissue ablation experiments: First tissue ablation experiments were performed using the macro-pulse CSP SPOPO. The output characteristics of this flashlamp pumped system for this experiment were: average power of 25 mW at 6.4 μm , corresponding to macro-pulse energy of 1 mJ at 25 Hz, each macro-pulse consisting of ~ 200 picosecond pulses at 100 MHz, i.e. about 2 μs long. The beam was only loosely focused on porcine liver tissue to a spot diameter of ~ 2 mm resulting in a fluence of ~ 0.1 J/cm² for the macro-pulse. The exposure time during these experiments was ~ 100 s. Figure 45a shows the thermal imaging result of the experiments. The white spot in the blue area (tissue sample) shows the ablation spot. The red posts in the figure show the ends of the tissue holder. The photograph in Fig. 45b shows the liver tissue ablation result after 100 s.

The lack of ablation is ascribed to the large beam waist at the tissue surface. Calculations indicate that first expanding the SPOPO idler beam to a diameter of ~ 2 cm and then focusing it with the same lens will produce a spot diameter of ~ 0.3 mm with fluence in excess of 4 J/cm², more than sufficient to reach the ablation threshold (~ 1 J/cm²).

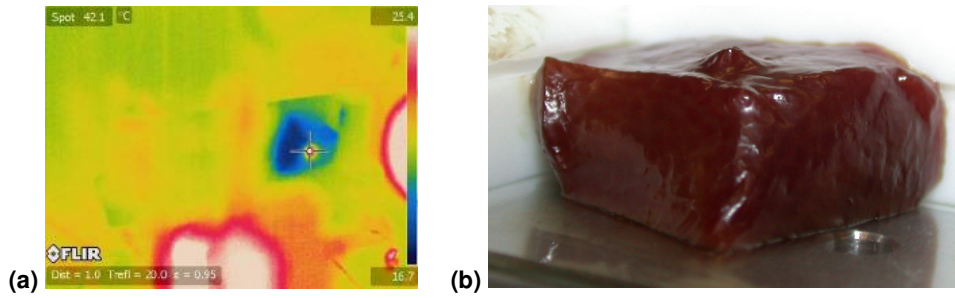


Figure 45: Thermal camera imaging of porcine liver tissue ablation (a) and the result of 100 s long ablation (b).

Next tissue ablation experiments were performed with the Ho-laser pumped OPO system which delivers ~ 30 ns pulses at energy level of >5 mJ per pulse at $6.45 \mu\text{m}$, which was sufficient to ablate tissue efficiently. The visualisation set-ups were used to analyse the ablation and coagulation effects on biological tissue and tissue phantoms. The set-up for these experiments is shown in Fig. 46. The output beam is indicated by the red arrow and was focussed on the tissue by a 10 cm CaF_2 lens, shown at the starting point of the red arrow. This resulted in a spot size diameter of $\sim 530 \mu\text{m}$. Tissue samples were positioned in the white holder situated at the end of the red arrow. A mechanical shutter was used to create discrete pulse trains of 50, 100, 200 and 400 pulses at 100 Hz, and three different macro-pulse energy levels were used: 2, 3.2 and 4.7 mJ.

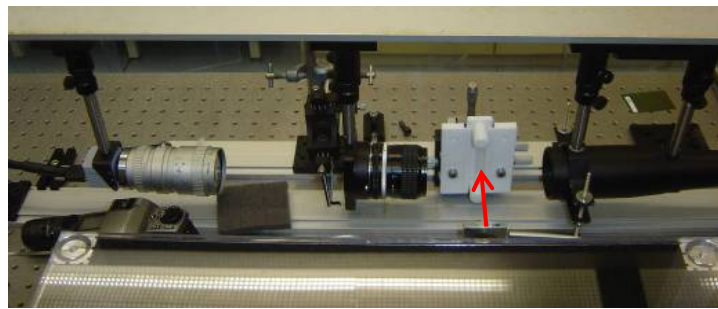


Figure 46: Schlieren experimental set-up used at ISL.

Albumin enriched gel was used to mimic additional protein content in the tissue. In this way it was possible to examine the effect of the selected wavelength on the amide groups. The ablation craters that were created were marginally shallower but significantly wider than in the normal gel (Fig. 47). This could be explained by the higher absorption by the amide bonds creating more forceful explosive vapour formation which induces more mechanical damage (wider crater) at the surface.

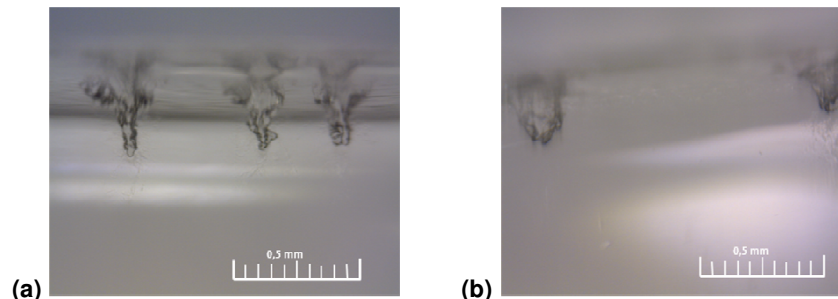


Figure 47: Ablation crater in normal (a) and albumin enriched (b) polyacrylamide gel for 50 pulses at 4.7 mJ/per pulse.

Additional experiments were conducted in biological tissues: porcine liver and bovine muscle. Examples of the craters created are presented in Fig. 48.

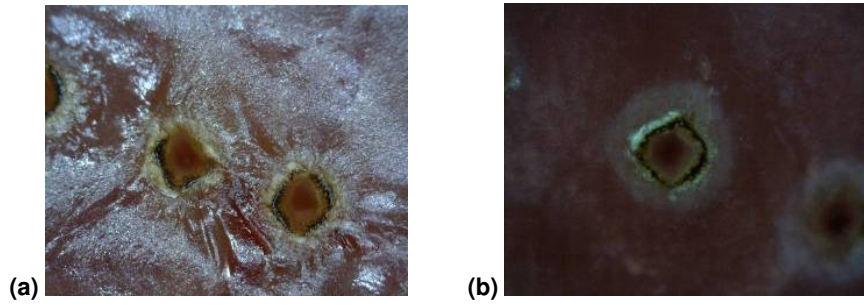


Figure 48: Ablation crater in porcine liver (a) and bovine muscle tissue (b) for 200 pulses at 4.7 mJ/per pulse.

It is clearly seen that the tissue is ablated very efficiently and there is only a small zone of thermal damage visible by the coagulation effect seen inside the crater. A small zone of carbonisation at the entrance reflects the heat accumulation in the outer rim of the beam spot that was below ablation threshold. It is seen from Fig. 49 that bovine muscle tissue is ablated more efficiently; this could be caused by the different tissue structure. Liver tissue is softer than muscular tissue. Therefore some of the energy will be lost due to the resonance of tissue surface on the impact of the laser pulse.

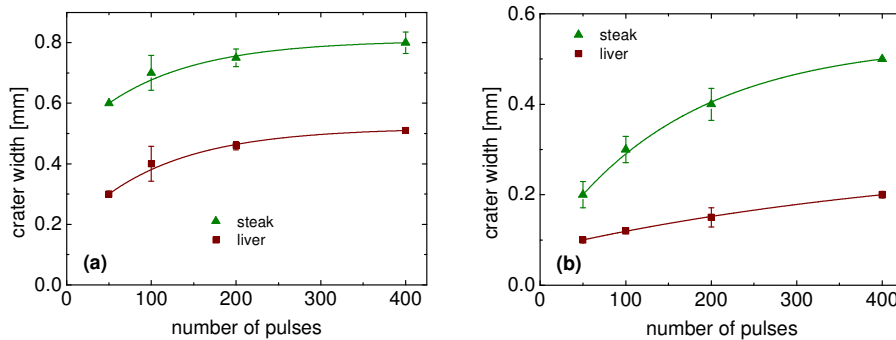


Figure 49: Crater (a) and coagulation (b) width analysis for biological tissue as a function of accumulated pulse energy.

Comparison of tissue ablation with surgical reference lasers: To compare the ablation characteristics of the developed within the MIRSURG project 6.45 μm OPO source with current surgical mid-IR lasers, additional experiments have been performed with reference lasers using the Coherent Ultrapulse CO₂ laser at 10.6 μm and the Biolase Waterlase MD Er:YSGG laser at 2.79 μm . Strictly speaking comparison by variation of only one parameter is impossible. While the repetition rates were quite similar and the energy fluence could be adjusted by attenuation or the focal spot size, these systems exhibit not only very different wavelengths but also very different pulse durations: ~30 ns for the OPO at 6.45 μm , 50 μs for the CO₂ laser and 700 μs for the Er:YSGG laser.

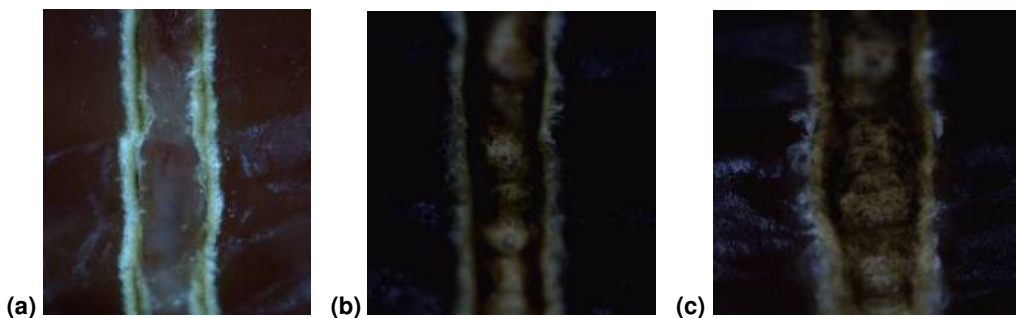


Figure 50: Porcine liver ablation run with the 6.45 μm OPO pulses of 4.7 mJ at 100 Hz (a), with Er-laser at 5 mJ and 75 Hz (b), and with CO₂ laser at 6 mJ and 100 Hz (c).

The CO₂ laser, operating at 100 Hz was focused to a spot size of ~600 μm. The Er-laser operating at 75 Hz (it was unfortunately unstable at 100 Hz, the repetition rate chosen for the OPO) was directed to the tissue by its own waveguide and focused by a microlens to a spot size of ~550 μm. However, due to the very short focal length of the lens used (3-5 mm), the confocal parameter is also very short compared to the other set-ups. This makes it difficult to estimate precisely the fluence and in general results in lower ablation efficiency. The fluence during all laser experiments was kept at ~2 J/cm². Surgical dissection of tissue was mimicked by translating it on a linear actuator through the laser beam at a speed of ~1 mm/s. Images of ablated tissue areas are shown in Fig. 50.

There is relatively more coagulation and carbonisation visible on the ablation track of the CO₂ and the Er-laser. However, as already mentioned, it is impossible to ascribe the difference to a single parameter, e.g. the wavelength. It can be also speculated that the main effect is related to the different pulse duration, with thermal effects increasing with the pulse length. Therefore, additional research has to be performed in the future to exclude this pulse width variation. Also the spot and waist geometry were different and will contribute to variation in the tissue ablation effects. A good chance for a proper comparison is to use the OPO pump laser which operates at a wavelength ~2 μm with very similar temporal and spatial characteristics as the OPO idler output.

With these tissue ablation experiments the primary goal of the MIRSURG project has been achieved: a table top laser system (much smaller and cheaper than a FEL) that can effectively ablate biological tissues at a wavelength of 6.45 μm with a pulse length in the ns range. Although the average power targeted (>1 W) has been achieved at 200 Hz, the >5 mJ pulse energy available is more than sufficient for the tissue ablation itself and the optimum repetition rate that can be chosen (200 Hz, 100 Hz or less) will depend in real applications on the speed necessary to achieve the required effect within a reasonable time scale.

1.4 Potential Impact (including the socio-economic impact and the wider societal implications of the project so far) and the main dissemination activities and exploitation of results

The development of new innovation technologies with direct relevance to enhancing the competitiveness of European industry is one of the cornerstones of ICT research and development in FP7. In this respect, the project MIRSURG has been in line with many of the envisioned objectives. The ICT program aims at transition to a knowledge-based society by stimulating the transformation of the industry towards higher added value and sustainable growth. This aspect has been addressed in MIRSURG by a vertical approach utilizing the multidisciplinary character of the consortium through integration of material research and laser device technology with medical science and health. In each research area, strong impact on further advancement of that technological sector has been targeted, thus simultaneously enhancing the competitiveness of Europe in several key areas where intense international competition exists. The work program has been at the same time well focused and at the cutting-edge of photonics technology at the highest international level.

The project has been timely, because the development of novel mid-IR optical tools for minimal invasive human surgery was at early stages of investigation and so could have a major impact on health issues for the European citizen. MIRSURG has been undertaken in a timely manner ahead of international competitors, so that there could be a chance for this field to deliver major long-term benefits to the European citizen and industry. A concerted and focused research program has led to major progress and encouraging achievements.

The project has provided an important solution to a major requirement in human surgery and a new generation of optical sources at 6.45 μm has been the main result that offers major advantages of simplicity and practicality, improved functionality, reduced power consumption and cost, high efficiency, and table-top solid-state design (all important issues in terms of environmental and social issues) for clinical applications. Such a development could potentially revolutionize the field of minimally invasive human surgery. As replacements for the FEL, the developed laser systems also offer superior output characteristics such as well-defined and narrow spectral bandwidth which, through wavelength tuning, allow better identification of the fundamental mechanisms responsible for the effects of minimal collateral damage observed in tissue ablation experiments.

The developed laser sources will be valuable additions in the technologic advancement of minimal invasive surgery using, for example, navigated miniature robotic arms through small ports in the human body. Using the fiber delivery system developed, with a diameter <1 mm, any organs within the human body could be targeted. The system can be perfectly combined with the emerging optical diagnostics techniques such as Raman spectroscopy, which are also based on fiber optics. With high selectivity and specificity, it will be possible to ablate tissue with accuracy down to cellular level.

The project MIRSURG will have a strong impact on scientific and technological advancement of Europe in this field, since there are currently no coherent optical sources commercially available worldwide (USA, Japan, North America, elsewhere) that can offer comparative performance to devices developed in this project. The results, therefore, place Europe in a strong leadership position at the forefront of this field internationally, with large impact on its scientific and technological competitiveness at the global level. The project achievements offer a major opportunity for Europe to establish full scientific and technological dominance in key areas of photonics for the foreseeable future, which is a major strategic objective of ICT.

This project MIRSURG had a focused program, which was directly motivated and driven by a specific and important application in the field of minimal invasive human surgery. The development

of the advanced solid-state coherent sources within this project was an important step in realization of a particular class of non-invasive tools for preventive and therapeutic treatment based on photonic technologies. As such, the project will have major long-term societal impact in meeting the emerging challenges in the health (prevention and cure) of the European citizen.

The project achievements will also help consolidate leading market positions for European industry in photonic device technology and materials as well as applications of these systems. A strong element of the project has been the participation of industrial and innovative SME partners, who are interested in close interaction with the scientific and academic partners. The consortium included a total of 9 participants from 7 European countries, of which 4 are industrial partners, including 3 SMEs. One of the industrial partners (TRT) is a major global leader in the field of optoelectronics and photonics and one of the SMEs (LISA) is at the forefront of commercial laser technology at the international level specifically targeting human surgery. The other two SMEs also have a proven track record of successful commercialization of laser technology and OPO systems. The participation of such a strong industrial sector in the consortium is clearly indicative of the timeliness of the work program and considerable interest of European industry in the proposed technology. The novel technology that will be stimulated by the realization of the project MIRSURG is, therefore, of direct relevance to the European industry. The devices developed offer opportunities for commercial exploitation in the medium to long-term, given their practicability, versatility and spectral coverage where alternative sources with similar capabilities do not exist. With table-top all-solid-state design, high output efficiency, low power consumption and low cost/performance ratio, the developed systems are attractive technology for commercial uptake in an area that is continually in need of innovation and which continues to grow at a steady rate and where there is a major technological and commercial gap in the mid-IR spectral domain.

As a result of the realization of the project MIRSURG new knowledge in the area of photonics has been created, and revolutionary technologies and innovative devices for minimally invasive human surgery in the mid-IR have been developed. The integration of efforts between the scientific institutions and industrial partners in the consortium enabled timely transfer of RTD results into tangible economic and social benefits. The proposed sources could also have an impact on other areas in FP7 such as safety and security (e.g. mid-IR counter-measures, range-finding and LIDAR, IR imaging, detection of explosives, chemical, biological, nuclear and doping agents, free-space communications), environment (e.g. industrial and urban pollution monitoring, air quality control, gas leak detection and pipeline inspection, moisture measurement and quality control in food processing, determination of acid content in vegetable oil, monitoring alcohol and sugar content as well as carbonation in beverages, bio-diesel content in fuel mixtures), and nanotechnology, where ps pulses with small thermal release can be conveniently exploited in the field of nano-patterning for creation of waveguides and inscriptions in transparent media. A straightforward extension of the macro-pulse ps solid-state laser developed by one of the SME partners (Bright) toward shorter pulses and higher repetition rates (multi-kHz) could fulfil such an application requirement. All such applications offer important societal implications with regard to improving the quality of life for the European citizen.

The market potential for laser sources is also huge. With further advances in fiber technology and development of more viable delivery systems as well as diode-based solid-state laser systems, there is every reason to believe that the medical laser market in particular will continue its expansion. In this context, the mid-IR laser sources developed within MIRSURG will clearly contribute to exploiting such a large market, as well as directing the medical laser technology towards the more compact, efficient, and environmentally friendly diode-pumped solid-state laser. In terms of commercial opportunities, the gap in the market has been becoming more evident in recent years due to the absence of such viable solid-state technology. Therefore, the world market share in the specific

medical segment envisaged could approach 100% which will have a direct impact on the economic competitiveness and wealth creation in Europe in the near- and long-term.

Pulsed laser systems in the mid-IR have in general a great market potential for a variety of medical and, in particular, surgical applications. The high absorption of human tissue at these wavelengths allows a very well-defined and localized incision with low lateral damage. Very precise and smooth cutting of tissue is possible. The high optical beam quality achieved (M^2 factor) will allow focusing to very small beam diameters when using long focal lengths in non-contact operations. Thus, for any micro-surgical application in which no flexible endoscope is employed (e.g. in neurology or ENTO), such a laser system would be ideal. It will be a superior alternative to the commonly used CO₂ medical laser. Most equipment for beam propagation of the CO₂ laser such as mirrors or micro manipulators can be used for any mid-IR laser system. So, there already exists a large market (CO₂ laser market), where this new laser system can be commercially exploited. With the investigated fibers for the mid-IR, it will also be possible to use such a laser system for minimally invasive surgical applications where an endoscope is employed. The higher absorption of human tissue in the mid-IR leads to lower penetration depth and reduced damage of the surrounding tissue. Also, dental applications are potentially feasible with a pulsed laser system in the mid-IR.

The work program of MIRSURG, while challenging and presenting few risks, at the same time has offered strong elements of originality and timeliness. The strength of the project came from the unique combination of complementary expertise and know-how available within the consortium, strong industrial participation, a multidisciplinary and complementary approach, and timeliness due to scientific, technological and commercial gap. The joint research and development combined expertise from partners in different fields, reduced the overall financial burden and thus improved the output/input ratio, while the expected technological breakthroughs will possibly contribute to a reduction of brain drain to the USA and North America.

The impact of the project is strong because it has been carried out at the European level and the consortium partners all offered cutting-edge expertise in their respective fields at the highest international level. The partners also provided all the necessary ingredients, from source development expertise to applications and commercial development, to undertake the project in the most successful and timely manner, ensuring maximum impact and consolidation of scientific, technological, societal and economic development in Europe.

To date, we are not aware of any similar activity at European or national level aimed at achieving the main objectives as formulated in the MIRSURG project.

The dissemination policy of the MIRSURG project included promotion of the results inside and outside the consortium. The integration activities comprised exchange of know-how and mobility of personnel, joint studies and publications of the results, the establishment of shared database and a project website. The results achieved were and will be delivered to relevant industrial entities, research associations and specific user groups/networks involved in mid-IR laser and related technologies.

Publications in the leading journals and contributions to major international conferences, which are generally accompanied by exhibitions and international fairs, input to EU and National Policy Committees, directly through own website and personal advisory initiatives have been the main dissemination policy initiatives.

In all cases, suitable measures have been taken for reasonable protection of strategic information, which has been the responsibility of the Coordinator and Project Management. These included coordination of the publication activity, exchange of important information through personal meetings, exchange of technical know-how only during personal stays, and so on. Issues relating to

patents and in general to the IPR protection were addressed in the Consortium Agreement signed by all partners. The most important provisions were:

Knowledge was supposed to be property of the contractor generating it. The joint ownership of knowledge had to be avoided to the extent possible, except when there was no solution to separate it between two or more participants. In case of a joint ownership, the participants concerned had to conclude a specific agreement, as to the allocation among themselves and the terms of exercising such ownership of the results in accordance with the provisions of the Contract. The owner of the knowledge had to provide adequate and effective protection for knowledge that is capable of industrial or commercial application. The participants would publish information on the knowledge arising from the project only under the condition that this does not affect the protection of that knowledge.

Each participant enjoyed access rights to the results of the other participants originating from the project on a royalty-free basis as much as such access rights were required to carry out their own work under the project.

The pre-existing know-how (background) of the participants, which was excluded from access rights, and the conditions to use pre-existing know-how that was owned by a participant, were specified in the Consortium Agreement.

The participants will have disseminated the results of the project within a period of two years after the end of the project according to the Contract. The partners concluded the conditions for the commercial exploitation of the results in respect of the principle of the free trade of goods and competition rules within the EU in the Consortium Agreement.

The website of the MIRSURG project, created by the Project Management, served and will further serve to disseminate information about the project both to the consortium partners and to the interested (expert) public.

For the partners, the website primarily has served as a platform to facilitate communication between them. Most important documents could be found in the internal section, including minutes and presentations from the meetings, reporting material, and all deliverables. Public deliverables are available also in the public section.

A page entitled “external collaborators” has been added to the website, listing the companies or institutes in connection with some project partners that provided unique materials for the project without being part of the consortium.

The MIRSURG website played and will continue to play a key role in the dissemination of foreground, because it contains information on all the results generated. In this way, it provides full transparency concerning the efficiency (input/output) achieved within the project. The web pages relating to the generated results have been regularly updated. The last website update relevant to this report was from March 31st 2012. This includes Highlights, Press Releases, Publications in Journals, as well as Presentations at Conferences.

However, in order to protect the priority of the achievements within the project: (i) papers still under consideration were not exposed on the website, (ii) results which do not need patent protection were submitted for publication as soon as possible, (iii) the reporting material was based on data which is at least submitted and accepted for publication.

In all relevant publications the financial support from the EC has been acknowledged. This is normally not permitted in conference abstracts/summaries but in that case the EC support is acknowledged directly in the talk given or on the poster.

The project website will be maintained for further two years after the end of the project, and even updated, at least by adding any publications which continue to result from the project.

The training aspect (the education and skills development) has been integrated with the research activities of MIRSURG primarily through the involvement of PhD students and post-doctoral scientists in the research organizations who have been supported, fully or partly, by the grant. This aspect together with the specific dissemination policy is expected to increase the visibility of the novel technologies addressed in this project and to attract people into such newly emerging technologies. As for the educational aspects a total of 8 PhD theses (2xMBI, 2xBright, 1xISL, 1xKTH, 1xLISA, 1xICFO) were or are still being carried out fully or partially in the framework of the MIRSURG project.

The dissemination activities have been complemented with specialist seminars and general colloquia (unpublished) by consortium members at universities and other academic institutions, as well as technical and industrial forums outside the consortium itself or the relevant technical conferences, with the goal of achieving information and knowledge diffusion in the most effective, timely and widespread manner to a broader audience. Many of the consortium partners, being leaders in their own respective fields, have been often invited to present seminars and colloquia at various national and trans-nations forums, and these talks presented excellent opportunities for publicizing the MIRSURG project and disseminating the project results and related activities to much wider audience. In addition, to enhance the exposure of the technology further afield, the research results have been included in Summer Schools and conference Short Courses, which were attended by general undergraduate and PhD students and young researchers in industrial companies and SMEs.

While without special financial support it was impossible to organize a dedicated workshop, in the final stage, after the essential results had been obtained, there was active participation with 4 presentations by the consortium at SPIE Photonics West 2012 in San Francisco (CA). This combined symposium/industrial fair is unique since it comprises a symposium on “Lasers and Applications in Science and Engineering” and a Symposium on “Biomedical Optics” each consisting of many conferences and there are two related (LASE/BIOS) industrial exhibitions. During the sessions there were contacts / conversations with representatives of the medical community / industry as well as some of the original inventors of the MIS at 6.45 μm with FEL. Even stronger was the presence of MIRSURG at the Advanced Solid-State Photonics Congress in San Diego (CA), just after Photonics West 2012. There were a total of 7 presentations from MIRSURG partners (MBI, TRT, ICFO, ISL, KTH, UMC, Bright) in the first morning session “Mid-Infrared Parametric Sources” on January 30th de facto dominated by MIRSURG with 1 invited and 3 contributed talks. One can definitely state that the whole community learned about the MIS application and the EU Project MIRSURG from this session, the interest has been huge and there are great expectations that this new application field can boost the development of mid-IR coherent sources. Obviously new collaborations and activities will emerge from this for all the partners of MIRSURG.

Other important and effective initiatives relating to informing the general public about the project included exploitation of mass media. In addition, each consortium partner was encouraged to also inform about and include a link to the main consortium website administered by the coordinator.

In undertaking the dissemination activities described above, we took care that any information and material subject to know-how and IPR protection by the various consortium partners is not be disclosed and only such information that would be available through other alternative means of public disclosure is presented to the wider audience.

Commercial exploitation of the research results will be particularly effective, since at least one of the industrial partners (LISA) offers extensive know-how in the transfer of laser technology to the field of human surgery, with extensive global exposure, valuable knowledge of the market, and direct

access to potential clients. This provided an excellent route for direct and rapid technology transfer to the European industrial sector during the project.

It can be expected, that the impact resulting from the knowledge gained in the MIRSURG project will exceed the specific application area envisaged in the project itself. This is related to the possible exploitation of additional or intermediate results achieved within the project. Best examples for this are the unique picosecond macro-pulse laser system developed by the SME Bright, the 2- μm solid state lasers developed by ISL and the SME LISA, or the first stages of the OPOs and SPOPOs developed by the partners KTH and ICFO, respectively. The latter could be used not only as 2 μm sources, but in non-degenerate versions as 3- μm coherent sources with a number of additional advantages over the existing Er-lasers. These will all contribute to the added value of the generated results.

Within each work package, the MIRSURG project has targeted concepts which ensure the conservation of natural resources. For instance, within the laser development efforts at LISA devoted to Ho-based sources, the following aspects have been considered:

- minimizing the system components and usage of multifunctional elements, e.g. volume Bragg gratings (VBGs) for both wavelength stabilization and output coupling
- easy system integration/implementation thanks to laser diode stacks with embedded microlenses
- non-cascaded schemes increasing the overall efficiency: instead of using diode pumped Tm-based lasers as pump source, direct diode-pumping was implemented regarding Ho:YAG laser development

These mentioned aspects necessarily lead to compact, energy efficient, non-cascaded schemes which again significantly reduce the resources. Thus, the concept of the MIRSURG project has been ecologically beneficial. In addition, the scientific knowledge is expected to keep the industrial partners' leadership and would create new jobs.

Concerning TRT (major industrial partner), the MIRSURG project has enabled to study all the key parameters suited to the fabrication of Orientation-Patterned gallium arsenide (OP-GaAs) crystals for mid-IR generation with an unprecedented thickness over a large range of grating period (which is the parameter controlling the wavelength values). The experimental results obtained demonstrate that further exploitation of OP-GaAs as a versatile wavelength converting material is fully justified. Some of the latest samples made before the end of the project illustrate this opportunity: keeping the main wavelength target of the project, i.e. 6.45 μm , dedicated crystals have been fabricated to the benefit of one of the partners. Thanks to the availability from this partner of a pump source around 3 μm rather than 2 μm , an extended tunability in the mid-IR can be expected.

As with other custom-oriented R&D activities aimed at specific applications, Bright (SME) heavily invested in the MIRSURG project its expertise in diode-pumped short pulse lasers and amplifiers to achieve, with the other scientific and industrial partners, the very specific goal of this EU project. At the same time, as main pay-back, Bright has developed novel technological know-how and skills that strengthen and expand its business in the industrial and high-tech laser market.

Indeed, there is already a proof of this in the fact that, notwithstanding the critical 2009 global market turn-off, the company's gross income has increased from 2 to 3 M€ in the period 2008-2011, in part owing to the acquisition of new high-end customers requiring very specific products for aerospace and remote-sensing applications that were designed exploiting some of the laser technologies developed for MIRSURG.

Specifically, unique picosecond and sub-nanosecond laser designs have been developed by Bright within the MIRSURG project, and now these are already being exploited for a novel class of high-

energy diode-pumped Q-switched lasers recently introduced by Bright on the market. Of particular relevance for laser performance optimization are the solid-state bulk amplifier stages developed for the project and offered by the company to expand its product line, increasing flexibility and performance to the benefit of customers' needs.

Inspired by the excellent performance of the seed laser installed in MIRSURG picosecond system, lately the company also started the development of even more compact and long-term reliable picosecond laser solutions based on a novel fiber-laser product. Some of these results are presently considered for patent applications.

The results of the involvement of Bright and LISA in the MIRSURG project have also been occasionally relevant in terms of publications, which give an edge in terms of return R&D image of the companies. The most relevant achievements concerning the laser developments have been published in large diffusion ISI journals, in a book chapter monographs, and in peer-reviewed international conference proceedings.

As a further most valuable, positive fall-out of the participation in MIRSURG, with clear socio-economic implications, two PhD engineering students, who had their partial training in Bright on technologies specifically developed for MIRSURG, have been hired after completion of their studies, and a third post-doc student, working at the Laser Source Laboratory of Pavia University, is currently supported by a grant paid by the company and will soon join in and work along the fiber-laser project. There exist also similar plans in the company LISA, in relation to future exploitation of foreground.

The final note concerning Bright and LISA is on the excellent relationships with other project partners that let them foresee future collaborations, for example with ICFO, ISL, and MBI (but, possibly, also with the other industrial partners), for expanding the company's offer of wavelength flexible sources in the nanosecond and picosecond time regimes.

Concerning the SME LISA, also direct applications for the developed diode-pumped Ho:YAG laser exist. They depend on the operation mode of the laser. In cw operation there are several application fields. In surgery, the Ho:YAG laser could be used as a cutting tool which provides clean cuts and excellent haemostasis. More aspects will be outlined in the exploitation plan.

The research on 2 μm Tm-lasers led ISL to refine numerical calculations for thermal lensing and birefringence. Based on the verification during the project, this know-how is now used for different ongoing research activities in solid-state lasers at ISL. The results obtained in the successful operation of the high-energy OPO confirmed various ideas, which now allowed ISL to obtain record results at different wavelengths in the mid-IR.


The identification of CSP as the most promising material for 1 μm pumped mid-IR OPOs tunable up to 6.5 μm and its characterization at MBI, which revealed a nonlinear coefficient far above the expectations, had a positive effect on its further development and sponsoring of its research which was very important since novel materials require normally a period of the order of a decade to get mature for the market. Thus, the superior properties CSP could be exploited within the MIRSURG project not only by MBI in their ns OPO design, but also in SPOPOs, both by Euroscan and ICFO using different pump sources, although this nonlinear crystal was discovered after the start of the project. The successful realization at Euroscan and ICFO of compact, high-energy, single-stage picosecond SPOPOs based on CSP with the specified characteristics in the mid-IR, pumped directly at 1064 nm, offers significant potential not only for practical medical surgery applications but in addition for material processing and nonlinear spectroscopy. For Euroscan products this means increased competitiveness and opening new markets for their existing SPOPO technology. A possible more effective exploitation route will be technology transfer and collaboration with Radiantis, a spin-

off company created by the ICFO partner in 2005, and involvement of the Bright partner for an all-solid-state compact and reliable pump laser system design. This could provide a unique opportunity for the development of the macro-pulse format mid-IR SPOPO as a commercial medical instrument. The compact ns OPOs developed at MBI obviously cannot reach the energy levels near 6.45 μm achievable with 2 μm pump sources due to fundamental quantum efficiency limit, however, they are much simpler in design and rely on commercial pump lasers, hence, could find medical applications whenever lower power density is sufficient, i.e. in ophthalmic surgical procedures.

Large-energy and narrow-band OPOs employing large aperture structured ferroelectrics are important not only for specific goals of this project but also for developing custom-wavelength sources for Raman and fluorescence spectroscopy and remote sensing. One of spin-off companies from the KTH group (BOPO AB) is developing narrowband OPO systems for UV resonant Raman spectroscopy applications. The technologies developed within this project will be very suitable for use in such devices. As the cascaded large energy ns OPOs are relevant for range of remote sensing and defence applications, relevant patent applications are under consideration for specific solutions allowing efficient energy transfer from 1 μm to the mid-IR. In particular, the European Space Agency recently expressed specific interest in large-aperture periodically poled crystals for their portfolio of technologies for future missions. This interest resulted in a tender for increasing the readiness level for the technology where KTH group participates as a subcontractor.

The role of UMC in the MIRSURG project has been to investigate the potential of the developed by the other partners, mid-IR coherent sources for new surgical applications. The OPO system of ISL finally tested presents a unique tunable wavelength in combination with an energy/power level which has never been available except for FEL facilities. This enables research possibilities not easily accessible before especially on molecular bonds of biological tissues in laboratory settings. There are new developments in e.g. regenerative medicine where biological tissues are grown ex-vivo in laboratory settings. For precise cutting of such tissues the mid-IR 6.45 μm source can be applied. However, the advantages of such novel coherent sources compared to other medical laser systems used that are already commercially available have yet to be verified at comparable pulse durations. Another unique approach can be the combination with the pump laser near 2 μm so that the hybrid laser system can have dual wavelength characteristics for both coagulation and precise tissue cutting. The mid-IR OPO source is also easily tunable around 6.45 μm which makes it useful for spectroscopic research of molecules.

1.5 Address of the project public website, if applicable as well as relevant contact details.

	<p><i>Project coordinator name:</i> Dr. Valentin Petrov <i>Project coordinator organization:</i> Max-Born-Institute for Nonlinear Optics and Ultrafast Spectroscopy 12489 Berlin, Germany petrov@mbi-berlin.de</p> <p>www.mirsurg.eu</p>
---	---

List of beneficiaries and contact details:

#		Short name	Full Name	Contact person	e-mail
1		MBI	Forschungsverbund Berlin e.V.: Max-Born-Institut	Valentin Petrov	petrov@mbi-berlin.de
2		TRT	Thales Research and Technology	Eric Lallier Arnaud Grisard	eric.lallier@thalesgroup.com arnaud.grisard@thalesgroup.com
3		ICFO	Institut de Ciències Fotòniques	Majid Ebrahim-Zadeh	Majid.Ebrahim@icfo.es
4		LISA	LISA Laser Products OHG	Peter Fuhrberg	pfuhrberg@lisalaser.de
5		ISL	Institut Franco-Allemand de Recherche de Saint-Louis	Marc Eichhorn Christelle Kieleck	eichorn_m@isl.tm.fr kieleck@isl.tm.fr
6		Bright	Bright Solutions S.R.L.	Antonio Agnesi Giuliano Piccinno	antoniangelo.agnesi@unipv.it g.piccinno@brightsolutions.it
7		KTH	Kungliga Tekniska Hogskolan	Valdas Pasikevicius	vp@laserphysics.kth.se
8		Euroscan	Euroscan Instruments S.A.	Andre Peremans	andre.peremans@fundp.ac.be
9		UMC	Universitair Medisch Centrum Utrecht	Rudolf Verdaasdonk Stefan Been	r.verdaasdonk@umc.nl s.l.been@umcutrecht.nl

2. Use and dissemination of foreground

Section A (public)

The MIRSURG website has been the main instrument for dissemination of knowledge (foreground). The website contains full text of the materials from the following tables including all Press Releases, Publications in Journals (full text for those already appeared or for which a galley proof is available), Presentations at Conferences (Abstracts or Summaries of Past Conferences only), as well as a list of seminars/lectures/courses and unpublished reports.

There were 11 Printed Press Releases, 19 Online Press Releases, and one other (TV Videotext) announcing the Start of the project MIRSURG. On the website, one can find all links to these media in general and can read the press releases themselves. This information is summarized in the following tables. In April 2012, after the Final Review Meeting, a brief communication was submitted to the Photonics Newsletter (Photonics & Organic Electronics) of the Information Society and Media Unit of the EC. Also in April 2012, a final press release with a final project factsheet has been organized through the Public Relations Department of the Forschungsverbund Berlin e.V., to inform the public about the outcome of MIRSURG and the achieved results.

List of Printed Press Releases announcing the Start of the Project MIRSURG:

File Nr	Printed Press Releases	Title	Issue /Page	Date
DEL511	<u>The Parliament Magazine</u>	The Max-Born-Institute for Nonlinear Optics and Ultrafast Spectroscopy in Berlin coordinates an European consortium working on novel lasers for neurosurgery	issue 272, page 16	21 July 2008
DEL512	<u>Verbundjournal</u>	Präzisere Gehirn Operationen MBI-Forscher leiten ein EU-Projekt zur Entwicklung eines neuartigen Lasers für die Neurochirurgie	issue 75, page 11	15 September 2008
DEL513	<u>Health Technologies</u>	Neuer Laser für Gehirn-Operationen	issue 5, page 7	September 2008
DEL514	<u>Photonik</u>	MIR-Festkörperlaser für Gehirn-Operationen	issue 5, page 8	16 October 2008
DEL515	<u>TSB MEDICAL NEWS</u>	Präzisere Gehirn-Operationen per Laserstrahl Forscher des Max-Born-Instituts für Nichtlineare Optik und Kurzzeitspektroskopie leiten ein EU-Projekt zur Entwicklung eines routineteuglichen Lasers für Gehirnoperationen	newsletter 5, page 4	31 October 2008
DEL516	<u>Laser-Technik-Journal</u>	<u>Präzisere Gehirn-Operationen mit dem Laserstrahl</u>	issue 5, page 5	November 2008
DEL517	<u>Krankenhaus Technik + Management</u>	Gehirnoperationen mit Licht	issue 11, page 8	November 2008
DEL518	<u>MEDITEC International</u>	Neurochirurgischer Laser	issue 2, page 31	November 2008
DEL519	<u>The Parliament Magazine's RESEARCH REVIEW</u>	The Max-Born-Institute for Nonlinear Optics and Ultrafast Spectroscopy in Berlin coordinates an European consortium working on novel lasers for neurosurgery	issue 7, page 67	November 2008
DEL5110	<u>Medizin&Technik</u>	Mit dem Strahl bis ins Gehirn	issue 6, page 92	01 November 2008
DEL5111	<u>LASER MAGAZIN</u>	Präzisere Gehirn-Operationen per Laserstrahl	issue 6, page 49	01 December 2008

List of Online Press Releases announcing the Start of the Project MIRSURG:

File Nr.	Online: Webpage	Title	Direct Link	Date
DELO511	Innovationsreport http://www.innovationreport.de/	Präzisere Gehirn-Operationen per Laserstrahl MBI-Forscher leiten ein EU-Projekt zur Entwicklung eines neuartigen Lasers für die Neurochirurgie	http://www.innovationsreport.de/html/berichte/medizintechnik/praezisere_gehirn_operationen_per_laserstrahl_117870.html	10 September 2008
DELO512	pressefeiber http://www.pressefeiber.at/	Präzise Gehirn-Operation mit Licht	http://www.pressefeiber.at/index.php?option=com_content&view=article&id=4109:Pr%C3%A4zise%20Gehirn-Operation%20mit%20Licht&catid=52:medizinwellness&Itemid=73	15 September 2008
DELO513	Informationsdienst Wissenschaft http://idw-online.de/pages/de/	Präzisere Gehirn-Operationen per Laserstrahl Forscher des Max-Born-Institut für Nichtlineare Optik und Kurzzeitspektroskopie (MBI) wollen im Rahmen eines EU-Projekt einen routineteuglichen Laser für Gehirnoperationen entwickeln	http://idw-online.de/pages/de/news277986	15 September 2008
DELO514	iconcast http://www.iconocast.com/	Präzisere Gehirn-Operationen per Laserstrahl	http://www.iconocast.com/EB00000000000030/W5/News9.htm	15 September 2008
DELO515	FOBI – Fortbildung Online http://www.fortbildung-online.de/	Präzisere Gehirn-Operationen per Laserstrahl Forscher des Max-Born-Institut für Nichtlineare Optik und Kurzzeitspektroskopie (MBI) wollen im Rahmen eines EU-Projekt einen routineteuglichen Laser für Gehirnoperationen entwickeln	http://www.fortbildung-online.de/id_101822.html	15 September 2008
DELO516	presetext austria http://www.presetext.at/	Präzise Gehirn-Operation mit Licht Wissenschaftler arbeiten an Entwicklung eines routineteuglichen Lasers	http://www.presetext.at/pte.mc?pte=080915030	15 September 2008
DELO517	interconnections http://www.interconnections.de/	Präzisere Gehirn-Operationen per Laserstrahl	http://www.interconnections.de/id_101822.html	15 September 2008
DELO518	wallstreet:online http://www.wallstreet-online.de/	Präzise Gehirn-Operation mit Licht	http://www.wallstreet-online.de/nachrichten/nachricht/2537591.html	15 September 2008
DELO519	msn nachrichten http://nachrichten.at.msn.com/	Präzise Gehirn-Operation mit Licht Wissenschaftler arbeiten an Entwicklung eines routineteuglichen Lasers	http://nachrichten.at.msn.com/wissenschaft/article.aspx?cp-documentid=9600430	15 September 2008
DELO5110	Fachpresse: Das schweizerische Informationsportal... http://www.fachpresse.com/	Präzise Gehirn-Operation mit Licht Wissenschaftler arbeiten an Entwicklung eines routineteuglichen Lasers	http://www.fachpresse.com/news/artikel/praezise-gehirn-operation-mit-licht.html	15 September 2008
DELO5111	DAS JOURNAL DIE ONLINE ZEITUNG http://www.dasjournal.net/	Präzise Gehirn-Operation mit Licht Wissenschaftler arbeiten an Entwicklung eines routineteuglichen Lasers	http://www.dasjournal.net/pdf.php?a=11507	15 September 2008
DELO5112	UNI-PROTOKOLLE http://www.uni-protokolle.de/	Präzisere Gehirn-Operationen per Laserstrahl	http://www.uni-protokolle.de/nachrichten/text/163111/	15 September 2008

DELO5113	<u>AlphaGalileo</u> http://www.alphagalileo.org/	Präzisere Gehirn-Operationen per Laserstrahl	http://www.alphagalileo.org/index.cfm?fuseaction=readrelease&releaseid=532180&ez_search=1	15 September 2008
DELO5114	<u>scinexx - Das Wissensmagazin</u> http://www.scinexx.de/ http://www.g-o.de/	Gehirn-OPs per Laserstrahl Forscher entwickeln routineteauglichen Laser für minimalinvasive Eingriffe	http://www.scinexx.de/wissen-aktuell-8839-2008-09-18.html http://www.g-o.de/wissen-aktuell-8839-2008-09-18.html	18 September 2008
DELO5115	<u>Photonik</u> http://www.photonik.de/	MIR-Festkörperlaser für Gehirn-Operationen	http://www.photonik.de/index.php?id=nachrichten&L=1&artid=3013&tp=na	16 October 2008
DELO5116	<u>OTA-ONLINE</u> http://www.ota-online.info/	Präzise Gehirn-Operation mit Licht Forscher des Max-Born-Instituts (MBI) wollen im Rahmen des EU-Projekts MIRSURG einen Laser entwickeln, der minimalinvasive Operationen am Gehirn ermöglicht	http://www.ota-online.info/index.php?area=1&p=news&newsid=59	26 October 2008
DELO5117	<u>MESSE BERLIN</u> http://www1.messeberlin.de/vip8_1/website/Internet/Internet/www.messeberlin/deutsch/index.html	More Precise Laser Surgery by Laser Beam	http://www1.messeberlin.de/vip8_1/website/MesseBerlin/htdocs/www.laseroptics/en/Press/Newsletter/index.jsp#top	December 2008
DELO5118	World of Photonics Portal http://world-of-photonics.net/de/laser/start	Präzisere Gehirn-Operationen per Laserstrahl	http://www.world-of-photonics.net/link/de/21137929/~/layer/15539653-news	December 2008
DELO5119	<u>TSB Adlershof</u> http://www.tsb-adlershof.de/	Präzisere Gehirn-Operationen per Laserstrahl MBI-Forscher leiten ein EU-Projekt zur Entwicklung eines neuartigen Lasers für die Neurochirurgie	http://www.tsb-adlershof.de/infocenter/news/pr%C3%A4zisere-gehirn-operationen-laserstrahl	December 2008

VOX Film und Fernsehen	Bald neuer Laser für Gehirn-OPs? Videotext-page 610	09. November 2008
------------------------	--	-------------------

In May 2010, in order to promote the project an article about MIRSURG was submitted to the EOS website on the occasion of the launching of the new EOS brochure “How optics and photonics address Europe’s challenges of the 21st century”. The printed version of this brochure appeared later and can be downloaded now from the MIRSURG webpage as a PDF file. Both the brochure and the web gallery at www.myeos.org are widely promoted in the European optics and photonics community.

The further use and dissemination of foreground (including socio-economic impact and target groups for the results of the research) after the end of the project shall strictly follow the initial plan from Annex I and the guidelines as outlined in the previous section 1.4. As already mentioned, the project website will be maintained for at least further two years after the end of the project, and even updated, at least by adding any publications which continue to result from the project.

Section A (public)

The precise information collected in the following tables can be summarised as follows: Up to the date of the final report 85 papers were published in scientific peer-reviewed journals or are in press (electronic copy or galley proof exists). Nine of them are Invited/Review papers or Book Chapters.

Results obtained within the MIRSURG project were reported at 52 International Scientific Conferences, in 17 different countries. The total number of conference presentations was 113, 29 of them were Invited/Plenary Talks or Postdeadline papers. Materials based on project results are in black colour in the corresponding tables and materials having only general relation and using only partial support from MIRSURG are in gray colour. The latter were not used for preparation of the periodic activity reports. Invited/Review Papers and Book Chapters as well as Invited/Plenary and Postdeadline Talks are outlined in red colour. All materials can be downloaded from the website and in the case of conferences there is a link to the event, too. Some of the journals have open access: at present this holds for the electronic OSA journals *Optics Express* and *Optical Materials Express*.

A total of 19 seminars/lectures/talks or short courses (unpublished) were given at different events in 8 countries. Links to these events, where they exist, can be found on the website.

In the following 3 cumulative tables chronological numbering of the journal (J..), conference (C..), and unpublished (U..) presentations is used.

Table A1: Scientific publications in peer reviewed journals relating to the foreground of the project: black – directly related and used in the reports, gray – indirectly related

No/Date	Journal	Title	Authors	Partners involved
J1 Sep 08	Proc. SPIE, Vol. 7115, pp. 71150O/1-10, 2008	"Tandem PPKTP and ZGP OPO for mid-infrared generation"	Markus Henriksson, Lars Sjöqvist, Gustav Strömqvist, Valdas Pasiskevicius, Fredrik Laurell	KTH
J2 Nov 08	Optics Letters, Vol. 33, pp. 2650-2652, 2008	"Efficient, high-repetition-rate, femtosecond optical parametric oscillator tunable in the red"	Adolfo Esteban-Martin, Omid Kokabee, Majid Ebrahim-Zadeh	ICFO
J3 Dec 08	Optics Letters, Vol. 33, pp. 2955-2957, 2008	"High-power, continuous-wave, second-harmonic generation at 532 nm in periodically-poled KTiOPO ₄ "	Goutam Kumar Samanta, Suddapalli Chaitanya Kumar, Manoj Mathew, Carlota Canalias, Valdas Pasiskevicius, Fredrik Laurell, Majid Ebrahim-Zadeh	ICFO, KTH
J4 Feb 09	Proc. SPIE, Vol. 7197, pp. 719702/1-14, 2009	"Tunable, high-power, solid-state sources for the blue and ultraviolet"	Goutam Kumar Samanta, Adolfo Esteban-Martin, Masood Ghotbi,	ICFO

	Invited Paper		Majid Ebrahim-Zadeh	
J5 Feb 09	Proc. SPIE, Vol. 7197, pp. 71970M/1-8, 2009	"The nonlinear coefficient d_{36} of CdSiP_2 "	Valentin Petrov, Frank Noack, Ivaylo Tunchev, Peter Schunemann, Kevin Zawilski	MBI
J6 Feb 09	Optical Materials, Vol. 31, pp. 590-597, 2009	"Orthorhombic nonlinear crystals of $\text{Ag}_x\text{Ga}_x\text{Ge}_{1-x}\text{Se}_2$ for the mid-infrared spectral range"	Valeriy Badikov, Konstantin Mitin, Frank Noack, Vladimir Panyutin, Valentin Petrov, Alexander Seryogin, Galina Shevyrdyaeva	MBI
J7 Feb 09	Optics Letters, Vol. 34, pp. 428-430, 2009	"High-harmonic-repetition-rate, 1 GHz femtosecond optical parametric oscillator pumped by a 76 MHz Ti:sapphire laser"	Adolfo Esteban-Martin, Omid Kokabee, Konstantinos Moutzouris, Majid Ebrahim-Zadeh	ICFO
J8 May 09	Optics Communications, Vol. 282, pp. 2070-2073, 2009	"Compact sub-100-fs Nd:silicate laser"	Antonio Agnesi, Paolo Dallochio, Federico Pirzio, Giancarlo Reali	Bright
J9 May 09	Optics Letters, Vol. 34, pp. 1561-1563, 2009	"Stable, 9.6 W, continuous-wave single-frequency, fiber-based green source at 532 nm"	Goutam Kumar Samanta, Suddapalli Chaitanya Kumar, Majid Ebrahim-Zadeh	ICFO
J10 May 09	Optics Express, Vol. 17, pp. 9171-9176, 2009	"Low-threshold femtosecond Nd:glass laser"	Antonio Agnesi, Federico Pirzio, Giancarlo Reali	Bright
J11 Aug 09	Optics Express, Vol. 17, pp. 13441-13446, 2009	"Nd:YAG pumped nanosecond optical parametric oscillator based on LiInSe_2 with tunability extending from 4.7 to 8.7 μm "	Georgi Marchev, Aleksey Tyazhev, Vitaliy Vedenyapin, Dmitri Kolker, Alexander Yeliseyev, Sergei Lobanov, Ludmila Isaenko, Jean-Jacques Zondy, Valentin Petrov	MBI
J12 Aug 09	Optics Letters, Vol. 34, pp. 2255-2257, 2009	"Continuous-wave optical parametric oscillator pumped by a fiber laser green source at 532 nm"	Goutam Kumar Samanta, Suddapalli Chaitanya Kumar, Ritwick Das, Majid Ebrahim-Zadeh	ICFO
J13 Aug 09	Optics Express, Vol. 17, pp. 13711-13726, 2009	"High-power, single-frequency, continuous-wave second-harmonic-generation of ytterbium fiber laser in PPKTP and MgO:sPPLT "	Suddapalli Chaitanya Kumar, Goutam Kumar Samanta, Majid Ebrahim-Zadeh	ICFO
J14 Aug 09	Optics Express, Vol. 17, pp. 15635-15640, 2009	"Extended-cavity, tunable, GHz-repetition-rate femtosecond optical parametric oscillator pumped at 76 MHz"	Omid Kokabee, Adolfo Esteban-Martin, Majid Ebrahim-Zadeh	ICFO
J15 Sep 09	Proc. SPIE, Vol. 7487, pp. 74870F/1-9, 2009	"Broadly tunable LiInSe_2 optical parametric oscillator pumped by a Nd:YAG laser"	Georgi Marchev, Aleksey Tyazhev, Vitaliy Vedenyapin, Dmitri Kolker,	MBI

			Alexander Yelissev, Sergei Lobanov, Ludmila Isaenko, Jean-Jacques Zondy, Valentin Petrov	
J16 Sep 09	Optics Express, Vol. 17, pp. 17582-17589, 2009	"Mode spectrum of multi-longitudinal mode pumped near-degenerate OPOs with volume Bragg grating output couplers"	Markus Henriksson, Lars Sjöqvist, Valdas Pasiskevicius, Fredrik Laurell	KTH
J17 Oct 09	Optics Letters, Vol. 34, pp. 2399-2401, 2009	"Noncritical singly resonant optical parametric oscillator operation near 6.2 μm based on a CdSiP ₂ crystal pumped at 1064 nm"	Valentin Petrov, Peter G. Schunemann, Kevin T. Zawilski, Thomas M. Pollak	MBI
J18 Oct 09	IEEE Photon. Technol. Letters, Vol. 21, pp. 1417-1419, 2009	"Efficient frequency doubling of a low-power femtosecond Er-fiber laser in BiB ₃ O ₆ "	Kentaro Miyata, Fabian Rotemund, Valentin Petrov	MBI
J19 Oct 09	Optics Letters, Vol. 34, pp. 3053-3055, 2009	"Noncritical singly resonant synchronously pumped OPO for generation of picosecond pulses in the mid-infrared near 6.4 μm "	Andre Peremans, Dan Lis, Francesca Cecchet, Peter G. Schunemann, Kevin T. Zawilski, Valentin Petrov	Euroscan, MBI
J20 Nov 09	Proc. SPIE, Vol. 7501, pp. 750102/1-10, 2009 Invited Paper	"Femtosecond optical parametric generators and amplifiers for the near infrared based on BiB ₃ O ₆ "	Valentin Petrov, Alexander Gaydardzhiev, Masood Ghotbi, Ivaylo Nikolov, Ivan Buchvarov, Pancho Tzankov, Frank Noack	MBI
J21 Nov 09	Applied Physics Letters, Vol. 95, pp. 191103/1-3, 2009	"Periodically poled KTiOAsO ₄ for highly efficient midinfrared optical parametric devices"	Andrius Zukauskas, Nicky Thilmann, Valdas Pasiskevicius, Fredrik Laurell, Carlota Canalias	KTH
J22 Jan 10	Laser & Photonics Reviews, Vol. 4, pp. 53-98, 2010 Invited Review Paper	"Femtosecond nonlinear frequency conversion based on BiB ₃ O ₆ "	Valentin Petrov, Masood Ghotbi, Omid Kokabee, Adolfo Esteban-Martin, Frank Noack, Alexander Gaydardzhiev, Ivaylo Nikolov, Pancho Tzankov, Ivan Buchvarov, Kentaro Miyata, Andrzej Majchrowski, Ivan V. Kityk, Fabian Rotemund, Edward Michalski, Majid Ebrahim-Zadeh	MBI, ICFO
J23 Feb 10	Proc. SPIE, Vol. 7582, pp. 75820E/1-11, 2010	"LiInSe ₂ nanosecond optical parametric oscillator tunable from 4.7 to 8.7 μm "	Aleksey Tyazhev, Georgi Marchev, Vitaliy Vedenyapin, Dmitri Kolker, Alexander Yelissev, Sergei Lobanov, Ludmila Isaenko, Jean-Jacque Zondy, Valentin Petrov	MBI

J24 Feb 10	Proc. SPIE, Vol. 7582, pp. 75820G/1-8, 2010	"Synchronously pumped at 1064 nm OPO based on CdSiP ₂ for generation of high power picosecond pulses in the mid-infrared near 6.4 μm"	Andre Peremans, Dan Lis, Francesca Cecchet, Peter G. Schunemann, Kevin T. Zawilski, Valentin Petrov	Euroscan, MBI
J25 Feb 10	Advances in Solid-State Lasers: Development and Applications, ed. by M. Grishin, SCIYO, 2010, sciyo.com Chapter 11, pp. 213-238	"High gain solid-state amplifiers for picosecond pulses"	Antonio Agnesi, Federico Pirzio, Giancarlo Reali	Bright
J26 Mar 10	Applied Physics B, Vol. 98, pp. 737-741, 2010	"Sub-nanosecond single-frequency 10-kHz diode-pumped MOPA laser"	Antonio Agnesi, Paolo Dallochio, Federico Pirzio, Giancarlo Reali	Bright
J27 Apr 10	Applied Physics B, Vol. 99, pp. 135-140, 2010	"Multi-wavelength diode-pumped Nd:LGGG picosecond laser"	Antonio Agnesi, Federico Pirzio, Giancarlo Reali, Andrea Arcangeli, Mauro Tonelli, Zhitai Jia, Xutang Tao	Bright
J28 Apr 10	Optics Letters, Vol. 35, pp. 1230-1232, 2010	"Subnanosecond, 1 kHz, temperature-tuned, noncritical mid-infrared optical parametric oscillator based on CdSiP ₂ crystal pumped at 1064 nm"	Valentin Petrov, Georgi Marchev, Peter G. Schunemann, Aleksey Tyazhev, Kevin T. Zawilski, Thomas M. Pollak	MBI
J29 May 10	Optics Express, Vol. 18, pp. 10098-10103, 2010	"80-fs Nd:silicate glass laser pumped by a single-mode 200-mW diode"	Antonio Agnesi, Alessandro Greborio, Federico Pirzio, Giancarlo Reali	Bright
J30 May 10	Optics Express, Vol. 18, pp. 10742-10749, 2010	"Cavity length resonances in a nanosecond singly-resonant optical parametric oscillator"	Markus Henriksson, Lars Sjöqvist, Valdas Pasiskevicius, Fredrik Laurell	KTH
J31 May 10	Proc. SPIE, Vol. 7721, pp. 77210C/1-15, 2010 Invited Paper	"High gain solid-state modules for picosecond pulses amplification"	Antonio Agnesi, Federico Pirzio, Giancarlo Reali	Bright
J32 May 10	OSA Handbook of Optics, Vol. IV, Optical Properties of Materials, Nonlinear Optics, Quantum Optics, McGraw-Hill, USA, 2010 Chapter 17, pp. 1-33	"Continuous-wave optical parametric oscillators"	Majid Ebrahim-Zadeh	ICFO
J33 Sep 10	Applied Physics B, Vol. 100, pp. 759-764, 2010	"Picosecond Nd:BaY ₂ F ₈ laser discretely tunable around 1 μm"	Antonio Agnesi, Federico Pirzio, Giancarlo Reali, Alessandra Toncelli, Mauro Tonelli	Bright

J34 Sep 10	J. Opt. Soc. Am. B, Vol. 27, pp. 1902-1927, 2010 Review Paper	"Optical, thermal, electrical, damage, and phase-matching properties of lithium selenoindate"	Valentin Petrov, Jean-Jacques Zondy, Olivier Bidault, Ludmila Isaenko, Vitaliy Vedenyapin, Alexander Yelisseyev, Weidong Chen, Aleksey Tyazhev, Sergei Lobanov, Georgi Marchev, Dmitri Kolker	MBI
J35 Oct 10	Optics Letters, Vol. 35, pp. 3210-3212, 2010	"Efficient, high-power, ytterbium-fiber-laser-pumped picosecond optical parametric oscillator"	Omid Kokabee, Adolfo Esteban-Martin, Majid Ebrahim-Zadeh	ICFO
J36 Oct 10	Proc. SPIE, Vol. 7836, pp. 783609/1-6, 2010	"High-pulse energy Q-switched Tm ³⁺ :YAG laser for nonlinear frequency conversion to the mid-IR"	Georg Stöppler, Christelle Kieleck, Marc Eichhorn	ISL
J37 Nov 10	Appl. Phys. Express Vol. 3, pp. 112702/1-3, 2010	"99 fs Nd:glass laser mode-locked with carbon nanotube saturable absorber mirror"	Antonio Agnesi, Alessandro Greborio, Federico Pirzio, Giancarlo Reali, Sun Young Choi, Fabian Rotermund, Uwe Griebner, Valentin Petrov	Bright, MBI
J38 Dec 10	J. Opt. Soc. Am. B, Vol. 27, pp. 2739-2742, 2010	"Diode-pumped Nd:BaY ₂ F ₈ picosecond laser mode-locked with carbon nanotube saturable absorbers"	Antonio Agnesi, Luca Carrà, Federico Pirzio, Giancarlo Reali, Alessandra Toncelli, Mauro Tonelli, Sun Young Choi, Fabian Rotermund, Uwe Griebner, Valentin Petrov	Bright, MBI
J39 Dec 10	Optics Letters, Vol. 35, pp. 4142-4144, 2010	"Optical parametric generation in CdSiP ₂ "	Olivier Chalus, Peter G. Schunemann, Kevin T. Zawilski, Jens Biegert, Majid Ebrahim-Zadeh	ICFO
J40 Jan 11	Applied Physics B, Vol. 102, pp. 31-35, 2011	"Optimally-output-coupled, 17.5 W, fiber-laser-pumped continuous-wave optical parametric oscillator"	Suddapalli Chaitanya Kumar, Ritwick Das, Goutam Kumar Samanta, Majid Ebrahim-Zadeh	ICFO
J41 Jan 11	Optics Communications, Vol. 284, pp. 398-404, 2011	"Optimal performances of a mode-locking technique: Theoretical and experimental investigations of the frequency-doubling nonlinear mirror"	Alaa A. Mani, Dan Lis, Yves Caudano, Paul A. Thiry, Andre Peremans	Euroscan
J42 Jan 11	Phys. Stat. Sol. RRL, Vol. 5, pp. 31-33, 2011	"Phase-matching properties of BaGa ₄ S ₇ and BaGa ₄ Se ₇ : Wide-bandgap nonlinear crystals for the mid-infrared"	Valeriy Badikov, Dmitrii Badikov, Galina Shevyrdyaeva, Aleksey Tyazhev, Georgi Marchev, Vladimir Panyutin, Valentin Petrov, Albert Kwasniewski	MBI

J43 Feb 11	Proc. SPIE, Vol. 7917, pp. 79171S/1-8, 2011	"Effect of post-growth annealing on the optical properties of LiGaS ₂ nonlinear crystals"	Alexander Yelisseyev, Marina Starikova, Ludmila Isaenko, Sergei Lobanov, Valentin Petrov	MBI
J44 Feb 11	Proc. SPIE, Vol. 7917, pp. 79171L/1-8, 2011	"New mixed LiGa _{0.5} In _{0.5} Se ₂ nonlinear crystal for the mid-IR"	Vitaliy Vedenyapin, Ludmila Isaenko, Alexander Yelisseyev, Sergei Lobanov, Aleksey Tyazhev, Georgi Marchev, Valentin Petrov	MBI
J45 Feb 11	Proc. SPIE, Vol. 7917, pp. 79171G/1-10, 2011	"Some properties of the mixed GaS _{0.4} Se _{0.6} nonlinear crystal in comparison to GaSe"	Georgi Marchev, Aleksey Tyazhev, Vladimir Panyutin, Valentin Petrov, Frank Noack, Kentaro Miyata, Michael Griepentrog	MBI
J46 Feb 11	Proc. SPIE, Vol. 7917, pp. 79170L/1-6, 2011	"CdSiP ₂ optical parametric generator"	Olivier Chalus, Peter G. Schunemann, Kevin T. Zawilski, Jens Biegert, Majid Ebrahim-Zadeh	ICFO
J47 Feb 11	Optics Express, Vol. 19, pp. 4121-4128, 2011	"Ultra-broadband optical parametric generation in periodically poled stoichiometric LiTaO ₃ "	Martin Levenius, Valdas Pasiskevicius, Fredrik Laurell, Katia Gallo	KTH
J48 Mar 11	Optics Letters, Vol. 36, pp. 948-950, 2011	"Efficient diode-pumped laser operation of Tm:Lu ₂ O ₃ around 2 μm"	Philipp Koopmann, Samir Lamrini, Karsten Scholle, Peter Fuhrberg, Klaus Petermann, Günter Huber	LISA
J49 Apr 11	Laser Physics, Vol. 21, pp. 774-781, 2011	"GaS _{0.4} Se _{0.6} : relevant properties and potential for 1064 nm pumped mid-IR OPOs and OPGs operating above 5 μm"	Valentin Petrov, Vladimir L. Panyutin, Aleksey Tyazhev, Georgi Marchev, Alexander I. Zagumennyi, Fabian Rotermund, Frank Noack, Kentaro Miyata, Liudmila D. Iskhakova, Abdelmounaime F. Zerrouk	MBI
J50 Apr 11	Optics Letters, Vol. 36, pp. 1068-1070, 2011	"Interferometric output coupling of ring optical oscillators"	Suddapalli Chaitanya Kumar, Adolfo Esteban-Martin, Majid Ebrahim-Zadeh	ICFO
J51 Apr 11	Optics Express, Vol. 19, pp. 7833-7838, 2011	"Single-walled carbon nanotube saturable absorber assisted high-power mode-locking of a Ti:sapphire laser"	In Hyung Baek, Sun Young Choi, Hwang Woon Lee, Won Bae Cho, Valentin Petrov, Antonio Agnesi, Valdas Pasiskevicius, Dong-II Yeom, Kihong Kim, Fabian Rotermund	MBI, Bright
J52	Optics Letters,	"Picosecond mid-infrared optical parametric amplifier"	Kentaro Miyata, Georgi Marchev,	MBI

May 11	Vol. 36, pp. 1785-1787, 2011	based on the wide-bandgap GaS _{0.4} Se _{0.6} pumped by a Nd:YAG laser system at 1064 nm"	Aleksey Tyazhev, Vladimir Panyutin, Valentin Petrov	
J53 May 11	Optical Materials Express, Vol. 1, pp. 185-191, 2011	"Template-growth of periodically domain-structured KTiOPO ₄ "	Alexandra Peña, Bertrand Ménaert, Benoît Boulanger, Fredrik Laurell, Carlota Canalias, Valdas Pasiskevicius, Patricia Segonds, Corinne Félix, Jérôme Debray, Sébastien Pairis	KTH
J54 May 11	Optics Letters, Vol. 36, pp. 1671-1673, 2011	"Broadband, rapidly tunable Ti:sapphire-pumped BiB ₃ O ₆ femtosecond optical parametric oscillator"	Adolfo Esteban-Martin, Venkata Ramaiah-Badarla, Valentin Petrov, Majid Ebrahim-Zadeh	ICFO, MBI
J55 May 11	Optics Express, Vol. 19, pp. 11152-11169, 2011	"High-efficiency, multocrystal, single-pass, continuous-wave second harmonic generation"	Suddapalli Chaitanya Kumar, Goutam Kumar Samanta, Kavita Devi, Majid Ebrahim-Zadeh	ICFO
J56 June 11	Optical Materials Express, Vol. 1, pp. 201-206, 2011	"5 mm thick periodically poled Rb-doped KTP for high energy optical parametric frequency conversion"	Andrius Zukauskas, Nicky Thilmann, Valdas Pasiskevicius, Fredrik Laurell, Carlota Canalias	KTH
J57 June 11	Optical Materials Express, Vol. 1, pp. 316-320, 2011	"BaGa ₄ S ₇ : wide-bandgap phase-matchable nonlinear crystal for the mid-infrared"	Valeriy Badikov, Dmitrii Badikov, Galina Shevyrdyaeva, Aleksey Tyazhev, Georgi Marchev, Vladimir Panyutin, Franck Noack, Valentin Petrov, Albert Kwasniewski	MBI
J58 June 11	J. Applied Physics, Vol. 109, pp. 116104/1-2, 2011	"Sellmeier and thermo-optic dispersion formulas for CdSiP ₂ "	Kiyoshi Kato, Nobuhiro Umemura, Valentin Petrov	MBI
J59 June 11	Proc. SPIE, Vol. 8092, pp. 80921R/1-7, 2011	"Soft tissue ablation by picosecond synchronously-pumped CdSiP ₂ -based optical parametric oscillator tuned to 6.45 μm"	Nordine Hendaoui, Alaa A. Mani, Ernest Kakudji, Andre Peremans, Christophe Silien, Vincent Bruyninckx, Adolfo Esteban, Majid Ebrahim-Zadeh, Stefan Been, Rudolf M. Verdaasdonk, Peter G. Schunemann, Kevin T. Zawilski, Valentin Petrov	Euroscan, UMC, ICFO, MBI
J60 July 11	Optics Letters, Vol. 36, pp. 2578-2580, 2011	"High-power, continuous-wave, mid-infrared optical parametric oscillator based on MgO:sPPLT"	Suddapalli Chaitanya Kumar, Majid Ebrahim-Zadeh	ICFO
J61 Aug 11	Optics Letters, Vol. 36, pp. 3236-3238, 2011	"Compact, 1.5 mJ, 450 MHz, CdSiP ₂ picosecond optical parametric oscillator near 6.3 μm"	Suddapalli Chaitanya Kumar, Antonio Agnesi, Paolo Dallochio,	ICFO, Bright

			Federico Pirzio, Giancarlo Reali, Kevin T. Zawilski, Peter G. Schunemann, Majid Ebrahim-Zadeh	
J62 Aug 11	Optics Communications, Vol. 284, pp. 4049-4051, 2011	"Efficient femtosecond Yb:YAG laser pumped by a single-mode laser diode"	Antonio Agnesi, Alessandro Greborio, Federico Pirzio, Giancarlo Reali	Bright
J63 Aug 11	Optics Letters, Vol. 36, pp. 3033-3035, 2011	"Dual-wavelength, two-crystal, continuous-wave optical parametric oscillator"	Goutam Kumar Samanta, Majid Ebrahim-Zadeh	ICFO
J64 Oct 11	Optical Materials Express, Vol. 1, pp. 1292-1300, 2011	"Nonlinear, dispersive, and phase-matching properties of the new chalcopyrite CdSiP ₂ "	Vincent Kemlin, Benoit Boulanger, Valentin Petrov, Patricia Segonds, Bertrand Ménaert, Peter G. Schunemann, Kevin T. Zawilski	MBI
J65 Oct 11	Optical Materials Express, Vol. 1, pp. 1286-1291, 2011	"PbIn ₆ Te ₁₀ : new nonlinear crystal for three-wave interactions with transmission extending from 1.7 to 25 μm"	Samvel Avanesov, Valeriy Badikov, Aleksey Tyazhev, Dmitrii Badikov, Vladimir Panyutin, Georgi Marchev, Galina Shevyrdyaeva, Konstantin Mitin, Frank Noack, Polina Vinogradova, Nadezhda Schebetova, Valentin Petrov, Albert Kwasniewski	MBI
J66 Oct 11	Optics Express, Vol. 19, pp. 20316-20321, 2011	"50-mJ macro-pulses at 1064 nm from a diode-pumped picosecond laser system"	Antonio Agnesi, Luca Carrà, Paolo Dallochio, Federico Pirzio, Giancarlo Reali, Stefano Lodo, Giuliano Piccinno	Bright
J67 Nov 11	Optical Materials Express, Vol. 1, pp. 1447-1456, 2011	"Multi-watt laser operation and laser parameters of Ho-doped Lu ₂ O ₃ at 2.12 μm"	Philipp Koopmann, Samir Lamrini, Karsten Scholle, Michael Schäfer, Peter Fuhrberg, Günter Huber	LISA
J68 Nov 11	Rev. Sci. Instrum., Vol. 82, pp. 115107/1-7, 2011	"A laser system for the parametric amplification of electromagnetic fields in a microwave cavity"	Antonio Agnesi, Caterina Braggio, Giovanni Carugno, Federico Della Valle, Giuseppe Galeazzi, Giuseppe Messineo, Federico Pirzio, Giancarlo Reali, Giuseppe Ruoso	Bright
J69 Nov 11	Applied Physics B, Vol. 105, pp. 239-244, 2011	"A narrowband optical parametric oscillator tunable over 6.8 THz through degeneracy with a transversely-chirped volume Bragg grating"	Nicky Thilmann, Bjorn Jacobsson, Carlota Canalias, Valdas Pasiskevicius, Fredrik Laurell	KTH

J70 Dec 11	Optics Express, Vol. 19, pp. 26660-26665, 2011	"High-power, fiber-laser-pumped, picosecond optical parametric oscillator based on MgO:sPPLT"	Suddapalli Chaitanya Kumar, Majid Ebrahim-Zadeh	ICFO
J71 Jan 12	Applied Optics, Vol. 51, pp. 15-20, 2012	"Single-frequency, high-power, continuous-wave fiber-laser-pumped Ti:sapphire laser"	Suddapalli Chaitanya Kumar, Goutam Kumar Samanta, Kavita Devi, Stefano Sanguinetti, Majid Ebrahim-Zadeh	ICFO
J72 Jan 12	Optical Materials, Vol. 34, pp. 513-523, 2012 Invited Review	"Quasi-phase matched nonlinear media: Progress towards nonlinear optical engineering"	Valdas Pasiskevicius, Gustav Strömqvist, Fredrik Laurell, Carlota Canalias	KTH
J73 Jan 12	Optical Materials, Vol. 34, pp. 536-554, 2012 Invited Review	"Parametric down-conversion devices: the coverage of the mid-infrared spectral range by solid-state laser sources"	Valentin Petrov	MBI
J74 Jan 12	IEEE J. Sel. Top. Quantum Electron., Vol. 18, pp. 74-80, 2012	"Femtosecond Nd:glass lasers pumped by single-mode laser diodes and mode locked with carbon nanotube or semiconductor saturable absorber mirrors"	Antonio Agnesi, Alessandro Greborio, Federico Pirzio, Elena Ugolotti, Giancarlo Reali, Sun Young Choi, Fabian Rotermund, Uwe Griebner, Valentin Petrov	Bright, MBI
J75 Feb 12	Optics Communications, Vol. 285, pp. 315-321, 2012	"Spectroscopy and efficient laser emission of Yb ³⁺ :LuAG single crystal grown by μ -PD"	Stefano Veronesi, Ying Z. Zhang, Mauro Tonelli, Antonio Agnesi, Alessandro Greborio, Federico Pirzio, Giancarlo Reali	Bright
J76 Feb 12	Optics and Lasers in Engineering, Vol. 50, pp. 215-219, 2012	"High-power, continuous-wave Ti:sapphire laser pumped by fiber-laser green source at 532 nm"	Goutam Kumar Samanta, Suddapalli Chaitanya Kumar, Kavita Devi, Majid Ebrahim-Zadeh	ICFO
J77 Feb 2012	Applied Physics B, Vol. 106, p. 315-319, 2012	"Efficient high-power Ho:YAG laser directly in-band pumped by a GaSb-based laser diode stack at 1.9 μ m"	Samir Lamrini, Philipp Koopmann, Michael Schäfer, Karsten Scholle, Peter Fuhrberg	LISA
J78 Feb 12	Optics Letters, Vol. 37, pp. 515-517, 2012	"Directly diode-pumped high-energy Ho:YAG oscillator"	Samir Lamrini, Philipp Koopmann, Michael Schäfer, Karsten Scholle, Peter Fuhrberg	LISA
J79 Feb 12	Optics Letters, Vol. 37, pp. 740-742, 2012	"Optical parametric generation in CdSiP ₂ at 6.125 μ m pumped by 8 ns long pulses at 1064 nm"	Georgi Marchev, Aleksey Tyazhev, Valentin Petrov, Peter G. Schunemann, Kevin T. Zawilski, Georg Stöppler, Marc Eichhorn	MBI, ISL

J80 Feb 12	Optics Express, Vol. 20, pp. 4509-4517, 2012	"Tunable mid-infrared ZnGeP ₂ RISTRA OPO pumped by periodically-poled Rb:KTP optical parametric master-oscillator power amplifier"	Georg Stöppler, Marc Eichhorn Georg Stoeppler, Nicky Thilmann, Valdas Pasiskevicius, Andrius Zukauskas, Carlota Canalias, Marc Eichhorn	ISL, KTH
J81 Mar 12	Optics Communications, Vol. 285, pp. 742-745, 2012	"Femtosecond single-mode diode-pumped Cr:LiSAF laser mode-locked with single-walled carbon nanotubes"	Antonio Agnesi, Federico Pirzio, Elena Ugolotti, Sun Young Choi, Dong-II Yeom, Fabian Rotermund	Bright
J82	J. Crystal Growth, 2012	"Bulk PPKTP by crystal growth from high temperature solution"	Alexandra Pena, Bertrand Menaert, Benoit Boulanger, Fredrik Laurell, Carlota Canalias, Valdas Pasiskevicius, Luc Ortega, Patricia Segonds, Jérôme Debray, Corinne Felix	KTH
J83	Proc. SPIE, Vol. 8240, pp. 824013/1-7, 2012	"Comparison of linear and RISTRA cavities for a 1064 nm pumped CdSiP ₂ OPO"	Georgi Marchev, Aleksey Tyazhev, Georg Stöppler, Marc Eichhorn, Peter Schunemann, Valentin Petrov	MBI, ISL
J84	Proc. SPIE, Vol. 8240, pp. 824012/1-5, 2012	"Sub-nanosecond, 1-kHz, low-threshold, non-critical OPO based on periodically-poled KTP crystal pumped at 1064 nm"	Georgi Marchev, Valentin Petrov, Aleksey Tyazhev, Valdas Pasiskevicius, Nicky Thilmann, Fredrik Laurell, Ivan Buchvarov	MBI, KTH
J85	Proc. SPIE, Vol. 8240, pp. 824024/1-8, 2012	"High-energy, 450 MHz, CdSiP ₂ picosecond optical parametric oscillator near 6.3 μm for biomedical applications"	Suddapalli Chaitanya Kumar, Antonio Agnesi, Paolo Dallochio, Federico Pirzio, Giancarlo Reali, Kevin T. Zawilski, Peter G. Schunemann, Majid Ebrahim-Zadeh	ICFO, Bright

Table A2: Conferences relating to the foreground of the project:
black – directly related, gray – indirectly related

Date	Conference (Country)	No	Contribution		Partners involved
			Title	Authors	
30 th June - 4 th July 2008	17th International Laser Physics Workshop (LPHYS'08), Trondheim (Norway)	C1	"Narrow bandwidth high power IR OPOs with volume Bragg gratings" <i>invited paper</i> 4.8.2	M. Henriksson, L. Sjöqvist, V. Pasiskevicius, F. Laurell	KTH
		C2	"Optical parametric oscillators: technology and applications" <i>invited paper</i> 4.9.2	M. Ebrahim-Zadeh	ICFO
31 st Aug - 5 th Sep 2008	3rd EPS-QEOD Europhoton Conference on Solid State, Fiber and Waveguided Light Sources, Paris (France)	C3	"20-50 kHz high efficiency mid-infrared OP-GaAs OPO pumped by a 2 μ m holmium laser" paper WEoD.3	C. Kieleck, M. Eichhorn, A. Hirth, D. Faye, E. Lallier	ISL
		C4	"High-energy picosecond tunable solid-state laser system with GHz repetition rate" paper TUoB.5	A. Agnesi, L. Carrá, S. Lodo, F. Pirzio, G. Reali, D. Scarpa, A. Tomaselli, C. Vacchi	Bright
		C5	"QPM-GaAs for mid-infrared applications" <i>invited paper</i> WEoD.1	E. Lallier, D. Faye, A. Grisard, B. Gérard	TRT
15 th Sep - 18 th Sep 2008	SPIE Europe Remote Sensing, Cardiff (UK)	C6	"Tandem PPKTP and ZGP OPO for mid- infrared generation" paper [7115-23]	M. Henriksson, L. Sjöqvist, G. Strömqvist, V. Pasiskevicius, F. Laurell	KTH
8 th Dec - 11 th Dec 2008	Photonics Global Conference 2008, Singapore	C7	"Advances in ultrafast and continuous-wave optical parametric oscillators" <i>invited paper</i>	M. Ebrahim-Zadeh	ICFO
24 th Jan - 29 th Jan 2009	Photonics West'09: Lasers and applications in science and engineering, SPIE Conference 7197: "Nonlinear Frequency Generation and Conversion: Materials, Devices, and Applications VIII" San Jose, CA (USA)	C8	"The nonlinear coefficient d_{36} of CdSiP ₂ " paper [7197-21]	V. Petrov, F. Noack, I. Tunchev, P. Schunemann, K. Zawilski	MBI
		C9	"Tunable, high-power, solid-state sources for the blue and ultraviolet" <i>invited paper</i> [7197-01]	M. Ebrahim-Zadeh	ICFO

1 st Feb - 4 th Feb 2009	Advanced Solid-State Photonics , Denver, CO (USA)	C10	"CdSiP ₂ : a new nonlinear optical crystal for 1- and 1.5-micron-pumped mid-IR generation" paper TuC4	P. G. Schunemann, K. T. Zawilski, T. M. Pollak, V. Petrov, D. E. Zelmon	MBI
		C11	"Optical parametric oscillators for the visible and ultraviolet" invited paper TuC1	M. Ebrahim-Zadeh	ICFO
31 st May - 5 th June 2009	Conference on Lasers and Electro-Optics CLEO'09, Baltimore, MD (USA)	C12	"1.27 W, tunable, continuous-wave, single- frequency, solid-state blue source" paper CThZ6	G. K. Samanta, M. Ebrahim-Zadeh	ICFO
		C13	"Stable, high-power, continuous-wave, single- frequency source at 532 nm using periodically- poled MgO:sPPLT" paper CThZ3	S. Chaitanya Kumar, G. K. Samanta, M. Ebrahim-Zadeh	ICFO
		C14	"Internally frequency-doubled PPLN femtosecond optical parametric oscillator tunable in the visible" paper CThS4	A. Esteban-Martin, O. Kokabee, M. Ebrahim-Zadeh	ICFO
		C15	"1-GHz femtosecond optical parametric oscillator pumped by a 76-MHz Ti:sapphire laser" paper CWC5	O. Kokabee, A. Esteban-Martin, K. Moutzouris, M. Ebrahim-Zadeh	ICFO
		C16	"Efficient frequency doubling of a femtosecond Er-fiber laser using BiB ₃ O ₆ " paper CTuR6	K. Miyata, F. Rotermund, V. Petrov	MBI
		C17	"Q-switched Tm ³⁺ :YAG rod laser with crystalline fiber geometry" paper CWH2	M. Eichhorn, C. Kieleck, A. Hirth	ISL
		C18	"GaS _x Se _{1-x} compounds for nonlinear optics" paper CWJ1	V. L. Panyutin, A. I. Zagumennyi, A. F. Zerrouk, F. Noack, V. Petrov	MBI
		C19	"Femtosecond nonlinear frequency conversion using BiB ₃ O ₆ crystals from 250 nm in the UV to 3000 nm in the near-IR" invited paper CThV1	V. Petrov	MBI
8 th June - 12 th June 2009	Middle Infrared Coherent Sources MICS'2009, Trouville (France)	C20	"Near-degenerate volume Bragg grating PPKTP OPOs in tandem OPO mid-IR sources" paper PO8	M. Henriksson, L. Sjöqvist, V. Pasiskevicius, F. Laurell	KTH
		C21	"Generation of 16.6 W of tunable mid-infrared	S. Chaitanya Kumar, R. Das, G. K.	ICFO

			radion with an Yb-fiber-laser-pumped, continuous-wave optical parametric oscillator" paper MO10	Samanta, M. Ebrahim-Zadeh	
		C22	"Quasi phase matched gallium arsenide for mid-infrared applications" invited paper MO6	E. Lallier, D. Faye, A. Grisard, B. Gerard	TRT
		C23	"Materials and devices for direct nonlinear frequency conversion to the mid-IR above 4 μm with near 1 μm pumping" invited paper MO4	V. Petrov	MBI
14 th June - 19 th June 2009	Conference on Lasers and Electro-Optics – CLEO Europe 2009, Munich (Germany)	C24	"Sub-nanosecond passively Q-switched multi-kHz MOPA laser system" paper CA5.3 TUE	A. Agnesi, P. Dallochio, C. Di Marco, F. Pirzio, G. Reali	Bright
		C25	"1.2 W, tunable, continuous-wave, single-frequency, solid-state blue source" paper CD.P.34 TUE	G. K. Samanta, M. Ebrahim-Zadeh	ICFO
		C26	"Stable, high-power, continuous-wave, single-frequency optical parametric oscillator pumped by a frequency-doubled fiber laser" paper CD.P.20 TUE	G. K. Samanta, S. Chaitanya Kumar, R. Das, M. Ebrahim-Zadeh	ICFO
		C27	"32% efficient, 9.6 W, continuous-wave, Yb-fiber-laser-pumped single-pass second-harmonic-generation in MgO:sPPLT" paper CD7.3 THU	R. Das, S. Chaitanya Kumar, G. K. Samanta, M. Ebrahim-Zadeh	ICFO
		C28	"Extended-cavity GHz-repetition-rate femtosecond optical parametric oscillator pumped at 76 MHz" paper CD10.3 FRI	O. Kokabee, A. Esteban-Martin, K. Mouzouris, M. Ebrahim-Zadeh	ICFO
		C29	"16.6 W, continuous-wave, Yb-fiber-laser-pumped, singly-resonant optical parametric oscillator based on MgO:PPLN" paper CD7.2 THU	S. Chaitanya Kumar, R. Das, G. K. Samanta, M. Ebrahim-Zadeh	ICFO
12 th July - 17 th July 2009	Advances in Optical Sciences: OSA Optics & Photonics Congress 2009, Nonlinear Optics (NLO), Honolulu, HI (USA)	C30	"Non-critical singly resonant OPO operation near 6.2 μm based on a CdSiP ₂ crystal pumped at 1064 nm" invited paper NThA2	P. G. Schunemann, K. T. Zawilski, T. M. Pollak, V. Petrov	MBI

13 th July - 17 th July 2009	18 th International Laser Physics Workshop (LPHYS'09), Barcelona (Spain)	C31	"Progress in optical parametric oscillators" <i>invited paper</i> 5.5.3	M. Ebrahim-Zadeh	ICFO
19 th July - 24 th July 2009	24 th International Conference on Photochemistry, Toledo (Spain)	C32	"Novel light sources for ultrafast science and technology" <i>invited paper</i> IL11	M. Ebrahim-Zadeh	ICFO
9 th Aug - 14 th Aug 2009	The 17 th American Conference on Crystal Growth and Epitaxy, Lake Geneva, WI (USA)	C33	"Mid-infrared frequency conversion in CdSiP ₂ " paper TUE 14:15 Maple Lawn C	P. G. Schunemann, K. T. Zawilski, L. A. Pomeranz, T. M. Pollak, L. P. Gonzales, V. Petrov	MBI
26 th Aug - 28 th Aug 2009	Northern Optics 2009, Vilnius (Lithuania)	C34	"Tandem optical parametric oscillator mid- infrared laser source" paper O-10, Technical Digest, p. 46	M. Henriksson, L. Sjöqvist, V. Pasiskevicius, F. Laurell	KTH
31 st Aug - 3 rd Sep 2009	SPIE Europe Security + Defence, Berlin (Germany)	C35	"Broadly tunable LiInSe ₂ optical parametric oscillator pumped by a Nd:YAG laser" paper [7487-14]	G. Marchev, A. Tyazhev, V. Vedenyapin, D. B. Kolker, A. Yelisseyev, S. Lobanov, L.I. Isaenko, J. Zondy, V. Petrov	MBI
7 th Sep - 9 th Sep 2009	Colloque sur les Lasers et l'Optique Quantique COLOQ'11, Mouans-Sartoux (France)	C36	"L'arséniure de gallium : un matériau optique non linéaire pour le moyen infrarouge" <i>invited lecture</i> WED 11:00	E. Lallier, D. Faye, A. Grisard, B. Gerard	TRT
14 th Sep - 18 th Sep 2009	Conference on Ultrafast and Nonlinear Optics UFNO'2009, Burgas (Bulgaria)	C37	"Femtosecond optical parametric generators and amplifiers for the near infrared based on BiB ₃ O ₆ " <i>invited paper</i> UFL-I1	V. Petrov	MBI
26 th Sep - 1 st Oct 2009	17 th International Conference on Advanced Laser Technologies ALT'09, Antalya (Turkey)	C38	"GaS _{0.4} Se _{0.6} : relevant properties and potential for 1064 nm pumped mid-IR OPOs and OPGs operating above 5 μm" <i>invited paper</i> THU 9:00	V. Petrov, V. L. Panyutin, A. Tyazhev, G. Marchev, A. I. Zagumennyi, F. Rotermund, F. Noack	MBI
		C39	"New frontiers in tunable laser technology: optical parametric oscillators spanning the ultraviolet to mid-infrared" <i>invited paper</i> WED 18:20	M. Ebrahim-Zadeh	ICFO
		C40	"16.6 W, near- and mid-infrared optical parametric oscillator pumped by an Yb fiber laser" paper Poster Session: Laser Systems	S. Chaitanya Kumar, R. Das, G. K. Samantha, M. Ebrahim-Zadeh	ICFO

		C41	"Continuous-wave, single-frequency optical parametric oscillator pumped by a frequency-doubled fiber laser" paper Poster Session: Laser Systems	G. K. Samanta, S. Chaitanya Kumar, R. Das, M. Ebrahim-Zadeh	ICFO
27 th Sep - 30 th Sep 2009	1 st EOS Topical Meeting on Lasers 2009, Capri (Italy)	C42	"Fiber-based-SHG-pumped, high-power, single-frequency continuous-wave optical parametric oscillator" paper Mo 16:30 [2159]	G. K. Samanta, S. Chaitanya Kumar, R. Das, M. Ebrahim-Zadeh	ICFO
		C43	"Optimally-output-coupled, 17.5 W, Yb-fiber-laser-pumped continuous-wave optical parametric oscillator" postdeadline paper We 11:30 [2382]	S. Chaitanya Kumar, R. Das, G. K. Samanta, M. Ebrahim-Zadeh	ICFO
		C44	"Narrowband and tunable optical parametric oscillator near and at degeneracy using a transversely chirped Bragg grating" paper Mo 16:15 [2304]	B. Jacobsson, N. Thilmann, V. Pasiskevicius, F. Laurell	KTH
		C45	"Quasi phase matched gallium arsenide for mid-infrared applications" invited paper Mo 11:45 [2328]	E. Lallier, D. Faye, A. Grisard, B. Gerard	TRT
23 rd Jan - 28 th Jan 2010	Photonics West'10: Biomedical optics, SPIE Conference 7562: "Optical Interactions with Tissues and Cells XXI", San Francisco, CA (USA)	C46	"New method to visualize subsurface absolute temperature distributions and dynamics during laser-tissue interactions using thermocameras" paper [7562-30]	S. Been, T. de Boorder, J. Klaessens, R. Verdaasdonk	UMC
23 rd Jan - 28 th Jan 2010	Photonics West'10: Lasers and applications in science and engineering, SPIE Conference 7582: "Nonlinear Frequency Generation and Conversion: Materials, Devices, and Applications IX", San Francisco, CA (USA)	C47	"LiInSe ₂ nanosecond optical parametric oscillator tunable from 4.7 to 8.7 μm" paper [7582-13]	A. Tyazhev, G. Marchev, V. Vedenyapin, D. B. Kolker, A. P. Yelisseyev, S. Lobanov, L. I. Isaenko, J.-J. Zondy, V. Petrov	MBI
		C48	"Synchronously pumped at 1064 nm OPO based on CdSiP ₂ for generation of high-power picosecond pulses in the mid-infrared near 6.4 μm" paper [7582-15]	A. Peremans, D. Lis, F. Cechet, P. G. Schunemann, K. T. Zawilski, V. Petrov	Euroscan, MBI
31 st Jan - 3 rd Feb 2010	Advanced Solid-State Photonics, San Diego, CA (USA)	C49	"High-power Ho:YAG laser in-band pumped by laser diodes at 1.9 μm and wavelength stabilized by a volume Bragg grating" paper AMB13	S. Lamrini, P. Koopmann, K. Scholle, P. Fuhrberg, M. Hofmann	LISA

		C50	"Periodically poled KTiOAsO ₄ for mid-infrared light generation" paper AMC6	A. Zukauskas, N. Thilmann, V. Pasiskevicius, F. Laurell, C. Canalias	KTH
		C51	"Cavity length resonances in a singly resonant optical parametric oscillator with a volume Bragg grating" paper AMB21	M. Henriksson, L. Sjöqvist, V. Pasiskevicius, F. Laurell	KTH
4 th Mar - 6 th Mar 2010	IONS Spring Meeting 2007, IONS-7 Europe, Galway (Ireland)	C52	"Fiber-laser-pumped high-power, high-repetition-rate, ultrafast optical parametric oscillators in near to mid-infrared" paper Thu 11:45	O. Kokabee, A. Esteban-Martin, M. Ebrahim-Zadeh	ICFO
19 th Mar - 20 th Mar 2010	International Workshop on Solid State Lasers: "Solid State Lasers. 50 years after", Tarragona (Spain)	C53	"Parametric down-conversion devices: the coverage of the mid-infrared spectral range by solid-state laser sources" invited lecture FRI 17:00	V. Petrov	MBI
22 nd Mar - 24 th Mar 2010	Laser Optics Berlin, Berlin (Germany)	C54	"Table-top all-diode-pumped MOPA laser for generation of high-energy, high-frequency picosecond pulse trains" paper Mo 11:10	A. Agnesi, F. Pirzio, G. Reali, G. Piccinno	Bright
12 th Apr - 16 th Apr 2010	Photonics Europe, Brussels (Belgium)	C55	"High gain solid-state amplifier modules for picosecond pulses amplification" invited paper [7721-11]	A. Agnesi, F. Pirzio, G. Reali	Bright
16 th Apr - 18 th Apr 2010	American Society for Laser Medicine and Surgery 30th Annual Conference, Phoenix, AZ (USA)	C56	"Comparison of laser interaction mechanisms produced by varying pulse shape and pulse duration in ablative fractional treatment settings" paper #23 [Lasers in Surgery and Medicine, Vol. 42, Issue S22 (Supplement), pp 9 -10, 2010]	R. Choye, V. Lemberg, R. Verdaasdonk, C. Jadczyk	UMC
16 th May - 21 st May 2010	Conference on Lasers and Electro-Optics CLEO'10, San Jose, CA (USA)	C57	"Efficient, high-power, 16-GHz, picosecond optical parametric oscillator pumped by an 81-MHz fiber laser" paper CThP2	O. Kokabee, A. Esteban-Martin, M. Ebrahim-Zadeh	ICFO
		C58	"High-power, broadband, continuous-wave, mid-infrared optical parametric oscillator based on MgO:PPLN" paper CThH6	S. Chaitanya Kumar, R. Das, G. K. Samanta, M. Ebrahim-Zadeh	ICFO

		C59	"Stable, 17.5 W, optimally-output-coupled, Yb-fiber-pumped mid-infrared optical parametric oscillator" paper CThP6	S. Chaitanya Kumar, R. Das, G. K. Samanta, M. Ebrahim-Zadeh	ICFO
		C60	"High-power, fiber-laser-pumped picosecond optical parametric oscillator for the near- to mid-infrared" paper CThY1	O. Kokabee, A. Esteban-Martin, M. Ebrahim-Zadeh	ICFO
		C61	"Generation of tunable, ultrashort pulses in the near-IR with an OPA system based on BIBO" paper CFN5	M. Ghotbi, V. Petrov, F. Noack	MBI
		C62	"Sub-nanosecond, 1-kHz, temperature-tuned, non-critical mid-IR OPO based on CdSiP ₂ crystal pumped at 1064 nm" paper CThH3	V. Petrov, G. Marchev, P. G. Schunemann, A. Tyazhev, K. T. Zawilski, T. M. Pollak	MBI
		C63	"High power diode pumped 2 μm laser operation of Tm:Lu ₂ O ₃ " paper CMDD1	P. Koopmann, S. Lamrini, K. Scholle, P. Fuhrberg, K. Petermann, G. Huber	LISA
		C64	"Optical parametric oscillators: a new generation" invited paper CThP1	M. Ebrahim-Zadeh	ICFO
20 th May - 21 th May 2010	Applied Optoelectronics Conference, Vologda (Russia)	C65	"Artificial materials for nonlinear optics" plenary lecture P8	E. Lallier	TRT
28 th June – 2 nd July 2010	14th International Conference on Laser Optics LO-2010, St. Petersburg (Russia)	C66	"Wide tunable nanosecond OPO based on new nonlinear crystals" invited paper ThR1-21	G. Marchev, A. Tyazhev, V. Vedenyapin, D. Kolker, A. Yelisseyev, S. Lobanov, L. Isaenko, Je.-Ja. Zondy, V. Petrov	MBI
		C67	"Monocrystals for nonlinear frequency conversion to the mid-IR above 4 μm" invited paper WeW1-17	L. Isaenko, V. Petrov, A. Yelisseyev, V. Vedenyapin	MBI
23 rd Aug - 27 th Aug 2010	International Conference on Coherent and Nonlinear Optics (ICONO) and Lasers, Applications, and Technologies (LAT) Conference, ICONO/LAT 2010, Kazan (Russia)	C68	"Wide tunable nanosecond OPO based on LiInSe ₂ " paper IME2	A. Tyazhev, G. Marchev, V. Petrov, V. Vedenyapin, A. Yelisseyev, S. Lobanov, L. Isaenko, D. Kolker, J.-J. Zondy	MBI

29 th Aug - 3 rd Sep 2010	4th EPS-QEOD EUROPHOTON CONFERENCE on Solid-State, Fibre, and Waveguide Coherent Light Sources, Hamburg (Germany)	C69	"High peak power sub-nanosecond MOPA laser system" paper WeB5	A. Agnesi, P. Dallocchio, S. Dell'Acqua, F. Pirzio, G. Reali	Bright
		C70	"Compact femtosecond Nd:glass lasers pumped by a low-power single-mode laser diode" paper ThC2	A. Agnesi, A. Greborio, F. Pirzio, G. Reali, E. Ugolotti	Bright
		C71	"Compact high-power Ho:YAG MOPA in-band pumped by laser diode stacks at 1.9 μm " paper WeC5	S. Lamrini, P. Koopmann, K. Scholle, P. Fuhrberg, M. Hofmann	LISA
20 th Sep - 23 rd Sep 2010	SPIE Europe Security + Defence, Toulouse (France)	C72	"High-pulse energy Q-switched Tm ³⁺ :YAG laser for nonlinear frequency conversion to the mid-IR" paper [7836-08]	G. Stöppler, C. Kieleck, M. Eichhorn	ISL
11 th Dec - 15 th Dec 2010	PHOTONICS 2010: 10th International Conference on Fiber Optics & Photonics, IIT Guwahati, Assam (India)	C73	"Advances in continuous-wave optical parametric oscillators" invited paper	M. Ebrahim-Zadeh, G. K. Samanta, S. Chaitanya Kumar	ICFO
20 th Jan- 21 st Jan 2011	3rd Dutch Bio-Medical Engineering Conference 2011, Egmond aan Zee (The Netherlands)	C74	"Mid-infrared solid-state laser systems for minimally invasive surgery" paper 134	S. Been, H. J. Noordmans, R. M. Verdaasdonk	UMC
22 nd Jan - 27 th Jan 2011	Photonics West'11: Biomedical optics, SPIE Conference 7897: "Optical Interactions with Tissue and Cells XXII", San Francisco, CA (USA)	C75	"Comparison of thermal and mechanical effects in tissue depending on laser parameters of Er:Cr:YSGG and Er:YAG lasers using high-speed thermal optical thermography" paper [7897-02]	R. M. Verdaasdonk, V. G. Lemberg	UMC
		C76	"Subsurface temperature imaging techniques during infrared laser-tissue interactions" paper [7897-32]	R. M. Verdaasdonk, S. Been, J. H. Klaessens	UMC
22 nd Jan - 27 th Jan 2011	Photonics West'11: Biomedical optics, SPIE Conference 7883A: "Photonics in Dermatology and Plastic Surgery", San Francisco, CA (USA)	C77	"The effect of pulse shape and duration in ablative fractional CO ₂ laser treatment studied with high-speed thermal imaging: implications for clinical use" paper [7883A-20]	R. M. Verdaasdonk, V. G. Lemberg, C. Jadczyk, R. Choye	UMC

22 nd Jan - 27 th Jan 2011	Photonics West'11: Lasers and applications in science and engineering, SPIE Conference 7917: "Nonlinear Frequency Generation and Conversion: Materials, Devices, and Applications X", San Francisco, CA (USA)	C78	"Effect of post-growth annealing on the optical properties of LiGaS ₂ nonlinear crystals" paper [7917-64]	A. Yelisseyev, M. Starikova, L. Isaenko, S. Lobanov, V. Petrov	MBI
		C79	"New mixed LiGa _{0.5} In _{0.5} Se ₂ nonlinear crystal for the mid-IR" paper [7917-56]	V. Vedenyapin, L. Isaenko, A. Yelisseyev, S. Lobanov, A. Tyazhev, G. Marchev, V. Petrov	MBI
		C80	"Some properties of the mixed GaS _{0.4} Se _{0.6} nonlinear crystal in comparison to GaSe" paper [7917-51]	G. Marchev, A. Tyazhev, V. Panyutin, V. Petrov, F. Noack, K. Miyata, M. Griepentrog	MBI
		C81	"CdSiP ₂ picosecond optical parametric generator" paper [7917-20]	O. Chalus, P. G. Schunemann, K. T. Zawilski, J. Biegert, M. Ebrahim-Zadeh	ICFO
10 th Feb - 11 th Feb 2011	Optical Society of Korea Winter Annual Meeting 2011, Seoul (Korea)	C82	"Mode-locking of Nd-doped glass lasers based on carbon nanotube saturable absorber" paper FP-IV9	S. Y. Choi, A. Agnesi, V. Petrov, F. Rotermund	Bright, MBI
13 th Feb - 16 th Feb 2011	Advanced Solid-State Photonics, Istanbul (Turkey)	C83	"Femtosecond Nd:glass lasers mode-locked with carbon nanotube saturable absorber mirror" paper AWA18	A. Agnesi, A. Greborio, F. Pirzio, G. Reali, E. Ugolotti, S. Y. Choi, F. Rotermund, U. Griebner, V. Petrov	Bright, MBI
		C84	"Long wavelength laser operation of Tm:Sc ₂ O ₃ at 2116 nm and beyond" paper ATuA5	P. Koopmann, S. Lamrini, K. Scholle, P. Fuhrberg, K. Petermann, G. Huber	LISA
		C85	"Diode-pumped Tm:Lu ₂ O ₃ thin disk laser" paper ATuB14	M. Schellhorn, P. Koopmann, K. Scholle, P. Fuhrberg, K. Petermann, G. Huber	ISL, LISA
16 th Feb - 18 th Feb 2011	Advances in Optical Materials, Istanbul (Turkey)	C86	"Phase-matching properties of BaGa ₄ S ₇ and BaGa ₄ Se ₇ : wide-bandgap nonlinear crystals for the mid-infrared" paper JWB4	V. Badikov, D. Badikov, G. Shevyrdyaeva, A. Tyazhev, G. Marchev, V. Panyutin, V. Petrov, A. Kwasniewski	MBI
		C87	"Optical, thermal, electrical, damage, and phase-matching properties of lithium selenoindate" invited paper AIFA3	J.-J. Zondy, V. Petrov, L. Isaenko, A. Yelisseyev, O. Bidault	MBI
		C88	"5 mm thick periodically poled Rb:KTiOPO ₄ for high power optical frequency conversion" paper JWB1	A. Zukauskas, N. Thilmann, V. Pasiskevicius, F. Laurell, C. Canalias	KTH

1 st May - 6 th May 2011	Conference on Lasers and Electro-Optics CLEO'11, Baltimore, MD (USA)	C89	"Optical parametric generation of mid-infrared picosecond pulses beyond 6 μm in CdSiP_2 " paper CTuD1	O. Chalus, A. Esteban-Martin, P. G. Schunemann, K. T. Zawilski, J. Biegert, M. Ebrahim-Zadeh	ICFO
		C90	"Picosecond mid-IR optical parametric amplifier based on $\text{GaS}_{0.4}\text{Se}_{0.6}$ pumped by a Nd:YAG laser system at 1064 nm " paper CTuD2	K. Miyata, G. Marchev, A. Tyazhev, V. Panyutin, V. Petrov	MBI
		C91	" BaGa_4S_7 : Wide-bandgap phase-matchable nonlinear crystal for the mid-infrared" paper CTuL4	V. Badikov, D. Badikov, G. Shevyrdyaeva, A. Tyazhev, G. Marchev, V. Panyutin, V. Petrov	MBI
		C92	"High fidelity large aperture periodically poled Rb:KTiOPO_4 for high energy frequency conversion" paper CTuE6	A. Zukauskas, N. Thilmann, V. Pasiskevicius, F. Laurell, C. Canalias	KTH
22 nd May - 26 th May 2011	Conference on Lasers and Electro-Optics – CLEO Europe 2011, Munich (Germany)	C93	"Mid-IR optical parametric oscillator based on LiGaS_2 " paper CD.P.15	A. Tyazhev, V. Vedenyapin, G. Marchev, A. Yelisseyev, L. Isaenko, M. Starikova, S. Lobanov, V. Petrov	MBI
		C94	"Mid-infrared optical parametric generation in CdSiP_2 " paper CD.P.20	O. Chalus, P. G. Schunemann, K. T. Zawilski, J. Biegert, M. Ebrahim-Zadeh	ICFO
		C95	"Optical parametric oscillators spanning the ultraviolet to mid-infrared" invited paper CA12.3	M. Ebrahim-Zadeh	ICFO
		C96	"Efficient laser operation of $\text{Ho:Lu}_2\text{O}_3$ at room temperature" paper CA1.6	S. Lamrini, P. Koopmann, M. Schäfer, K. Scholle, P. Fuhrberg, K. Petermann, G. Huber	LISA
24 th May - 26 th May 2011	European Conferences on Biomedical Optics, SPIE Conference 8092: "Medical Laser Applications and Laser-Tissue Interactions V", Munich, (Germany)	C97	"Soft tissue ablation by picosecond synchronously-pumped CdSiP_2 -based optical parametric oscillator tuned to 6.45 μm " paper [8092-56]	N. Hendaoui, E. Kakoudgi, M. Aladin, C. Silien, A. G. Peremans, V. Bruyninckx, A. Esteban-Martin, M. Ebrahim-Zadeh, S. Been, R. M. Verdaasdonk, P. G. Schunemann, K. T. Zawilski, V. P. Petrov	Euroscan, UMC, ICFO, MBI
17 th July - 22 nd July 2011	Nonlinear Optics (NLO) 2011, Kauai, HI (USA)	C98	"New nonlinear crystal for three-wave interactions with transmission extending from 1.7 to 25 μm " paper NMA2	V. Badikov, D. Badikov, G. Shevyrdyaeva, A. Tyazhev, G. Marchev, V. Panyutin, F. Noack, V. Petrov, A. Kwasniewski	MBI

13 th Aug - 20 th Aug 2011	XXX URSI General Assembly and Scientific Symposium, Istanbul (Turkey)	C99	"Advances in quasi phase-matched optical frequency converters" <i>invited paper</i>	V. Pasiskevicius, C. Canalias, K. Gallo, F. Laurell	KTH
3 rd Sep - 8 th Sep 2011	19th International Conference on Advanced Laser Technologies ALT'11, Golden Sands (Bulgaria)	C100	"Advances in frequency converters with structured ferroelectrics" <i>invited paper</i> I-1-NL	V. Pasiskevicius, C. Canalias, K. Gallo, F. Laurell	KTH
25 th Sep - 28 th Sep 2011	2nd EOS Topical Meeting on Lasers (ETML'11), Capri (Italy)	C101	"Mode-locked ytterbium-doped fiber laser operating in the positive dispersion regime tunable over the range 1045-1065 nm" paper [4488]	A. Agnesi, L. Carrà, C. Di Marco, R. Piccoli	Bright
		C102	"Femtosecond single-mode diode-pumped Cr:LiSAF laser mode-locked with single-walled carbon nanotubes" paper [4489]	A. Agnesi, F. Pirzio, E. Ugolotti, S. Y. Choi, F. Rotermund	Bright
21 st Jan - 26 th Jan 2011	Photonics West'12: Biomedical optics, SPIE Conference 8221: "Optical Interactions with Tissue and Cells XXIII", San Francisco, CA (USA)	C103	"Effect of microsecond pulse length and tip shape on explosive bubble formation of 2.78 μm Er,Cr:YSGG and 2.94 μm Er:YAG laser" paper [8221-12]	R. M. Verdaasdonk, M. Verleng, A. van der Veen, V. Lemberg, P. Pham, W. Landgraf, D. Boutoussov	UMC
21 st Jan - 26 th Jan 2012	Photonics West'12: Lasers and applications in science and engineering, SPIE Conference 8240: "Nonlinear Frequency Generation and Conversion: Materials, Devices, and Applications XI", San Francisco, CA (USA)	C104	"Sub-nanosecond 1-kHz low-threshold non- critical OPO based on periodically poled KTP crystal pumped at 1064 nm" paper [8240-12]	G. Marchev, V. Petrov, A. Tyazhev, V. Pasiskevicius, N. Thilmann, F. Laurell, I. Buchvarov	MBI, KTH
		C105	"Comparison of linear and RISTRA cavities for a 1064-nm pumped CdSiP ₂ OPO" paper [8240-13]	G. Marchev, A. Tyazhev, G. Stöppler, M. Eichhorn, P. G. Schunemann, V. Petrov	MBI, ISL
		C106	"High-energy 450-MHz CdSiP ₂ picosecond optical parametric oscillator near 6.3 microns for biomedical applications" paper [8240-24]	S. Chaitanya Kumar, A. Agnesi, P. Dallocchio, F. Pirzio, G. C. Reali, K. T. Zawilski, P. G. Schunemann, M. Ebrahim-Zadeh	ICFO, Bright
29 th Jan - 1 st Feb 2012	Advanced Solid-State Photonics, San Diego, CA (USA)	C107	"Quasi-phase-matched gallium arsenide for mid infrared frequency conversion" <i>invited paper</i> AM1A.1	E. Lallier, A. Grisard, B. Gerard, A. Hildenbrand, C. Kieleck, M. Eichhorn	TRT, ISL
		C108	"Mid-infrared optical parametric generation in CdSiP ₂ crystal pumped by 8-ns long pulses at 1064 nm"	G. Marchev, A. Tyazhev, V. Petrov, P. G. Schunemann, K. Zawilski, G. Stoepler, M. Eichhorn	MBI, ISL

			paper AM1A.3	
		C109	"ZGP RISTRA OPO operating at 6.45 μm and application in surgery" paper AM1A.5	G. Stoeppler, M. Eichhorn, M. Schellhorn, S. L. Been, R. M. Verdaasdonk ISL, UMC
		C110	"Compact, high-energy, picosecond optical parametric oscillator at 450 MHz near 6 micron" paper AM1A.4	S. Chaitanya Kumar, A. Agnesi, P. Dallochio, F. Pirzio, G. Reali, K. Zawilski, P. G. Schunemann, M. Ebrahim-Zadeh ICFO, Bright
		C111	"Compact, high-efficient $\text{Tm}^{3+}:\text{LiLuF}_4$ thin-disk laser" paper AW5A.1	G. Stoeppler, D. Parisi, M. Tonelli, M. Eichhorn ISL
		C112	"Quadratic cascading effects in broadband optical parametric generation" paper AT2A.3	M. Levenius, M. Conforti, F. Baronio, V. Pasiskevicius, F. Laurell, K. Gallo KTH
1 st Feb - 3 rd Feb 2012	Advances in Optical Materials, San Diego, CA (USA)	C113	"Holmium-doped lutetia: A novel diode pumped laser at 2124 nm" paper IW5D.4	P. Koopmann, S. Lamrini, K. Scholle, C. Kränkel, P. Fuhrberg, G. Huber LISA

Table A3: Seminars, lectures, talks, short courses and other unpublished reports relating to the foreground of the project:

Date	No	Type	Place	Title	Author/Speaker/ Participant	Partners responsible / involved
01.09 2008	U1	lecture	Summer School of the 3rd EPS-QEOD Europhoton Conference on Solid-State, Fiber and Waveguided Light Sources, Paris (France), 31st August – 5th September 2008	"Optical parametric device technology and applications"	M. Ebrahim-Zadeh	ICFO
02.10 2008	U2	lecture	Conference "Quelques Remarquables Applications du Laser en Médecine" at OPTO Paris (France), 30th September - 2nd October 2008	"Q-switched Tm:YAG lasers for non-linear mid-infrared generation in laser surgery"	M. Eichhorn, C. Kieleck, A. Hirth	ISL
16.03 2009	U3	short course	Doctoral School of Photonics Oostduinkerke (Belgium), 16 th - 18 th March 2009	"Wavelength conversion with nonlinear optics"	M. Ebrahim-Zadeh	ICFO
02.06 2009	U4	short course	Conference on Lasers and Electro-Optics CLEO Baltimore, MD (USA), 31 st May - 5 th June, 2009	"Practical optical parametric oscillators"	M. Ebrahim-Zadeh	ICFO
14.06 2009	U5	short course	Conference on Lasers and Electro-Optics – CLEO Europe 2009 Munich (Germany), 14 th June - 19 th June, 2009	"Optical parametric oscillators"	M. Ebrahim-Zadeh	ICFO
23.07 2009	U6	talk	8th Euro American Workshop on Information Optics (WIO'09) Paris (France), 20 th - 24 th July, 2009	"Advances in laser wavelength conversion technology"	M. Ebrahim-Zadeh	ICFO
06.11 2009	U7	seminar	Helsinki University of Technology Helsinki (Finland)	"Nonlinear optics: A powerful tool for manipulation of laser light"	M. Ebrahim-Zadeh	ICFO
17.11 2009	U8	talk	Sweden-Japan MIR THz collaboration network Stockholm (Sweden), 17 th November, 2009	"Development of mid-infrared coherent sources and functional materials"	V. Pasiskevicius	KTH
08.02 2010	U9	seminar	Gwangju Institute of Technology (GIST), Gwangju (Korea)	"Functional components for midinfrared coherent sources"	V. Pasiskevicius	KTH

10.02 2010	U10	seminar	Ajou University, Suwon (Korea)	"Functional components for midinfrared coherent sources"	V. Pasiskevicius	KTH
14.05 2010	U11	seminar	Spectra Physics Friday Seminar, Santa Clara, CA (USA), 14 th May, 2010	"Materials and OPOs for direct nonlinear frequency conversion to the mid-IR above 4 μm with near 1 μm pumping"	V. Petrov	MBI
18.05 2010	U12	short course	Conference on Lasers and Electro-Optics CLEO San Jose, CA (USA), 16 th – 21 st May, 2010	"Practical optical parametric oscillators"	M. Ebrahim-Zadeh	KTH
25.05 2010	U13	talk	Workshop "Applications Médicales" at ISL, Saint-Louis (France), 25 th May, 2010	"Laser development for minimally invasive surgery at ISL: European MIRSURG Project"	G. Stöppler, C. Kieleck, M. Eichhorn	ISL
15.06 2010	U14	seminar	Institute of Applied Physics University of Bonn, Bonn (Germany)	"Laser light conversion and manipulation with nonlinear optics"	M. Ebrahim-Zadeh	ICFO
23.09 2010	U15	lecture	Institute of Photonic Sciences, Barcelona (Spain), LaserFest	"The laser: From Maiman to modern times"	M. Ebrahim-Zadeh	ICFO
13.10 2010	U16	seminar	Max-Planck Institute for Quantum Optics, Garching (Germany)	"Acquiescent light"	M. Ebrahim-Zadeh	ICFO
22.05 2011	U17	short course	Conference on Lasers and Electro-Optics – CLEO Europe 2011 Munich (Germany), 22 nd May - 26 th May, 2011	"Optical parametric oscillators"	M. Ebrahim-Zadeh	ICFO
22.06 2011	U18	invited talk	10th Euro-American Workshop on Information Optics (WIO'11) Benicassim (Spain), 19 th - 24 th June, 2011	"Optical parametric oscillators: New advances"	M. Ebrahim-Zadeh	ICFO
16.11 2011	U19	colloquium	IFSW Institut für Strahlwerkzeuge Universität Stuttgart, Stuttgart (Germany)	"Untersuchungen an Mid-IR OPO's für die minimalinvasive Chirurgie"	G. Stöppler	ISL